NTIS $8.75

Lockheed

HUNTSVILLE RESEARCH & ENGINEERING CEN

LOCKHEED MISSILES & SPACE COMPANY, INC.

A SUBSIDIARY OF LOCKHEED AIRCRAFT CORPORATION

HUNTSVILLE, ALABAMA

LOCKHEED MISSILES & SPACE COMPANY INC.
HUNTSVILLE RESEARCH & ENGINEERING CENTER
HUNTSVILLE RESEARCH PARK
4800 BRADFORD DRIVE, HUNTSVILLE, ALABAMA

EVALUATION OF ABSORPTION CYCLE FOR SPACE STATION ENVIRONMENTAL CONTROL SYSTEM APPLICATION

FINAL REPORT

November 1972

Contract NAS8-25986

Prepared for National Aeronautics and Space Administration
Marshall Space Flight Center, Alabama 35812

by

W. H. Sims
M. J. O'Neill
H. C. Reid
P. M. Bisenius

APPROVED: Juan K. Lovin

Juan K. Lovin, Supervisor
Thermal Environment Section

J. S. Farrior

J. S. Farrior
Resident Director

FOREWORD

This report represents the results of work performed by Lockheed's Huntsville Research & Engineering Center for the NASA-Marshall Space Flight Center, Alabama, under Exhibit A of Contract NAS8-25986.

Dr. Lynn D. Russell, Director of Engineering, University of Tennessee in Chattanooga, served as a consultant on the study. Drs. Russell, R.L. McNeely and T.M. Carney conducted a research subcontract to Lockheed-Huntsville, entitled "Systematic Investigations to Synthesize New Refrigerant-Absorbent Fluid Combinations."

The NASA Contract Officer's Representative (COR) for the study was Mr. Robert L. Middleton, NASA-MSFC, S&E-ASTN-PLB.

SUMMARY

Since June 1970, Lockheed-Huntsville has been conducting a study for NASA-MSFC to evaluate an absorption cycle refrigeration system to provide environmental control for the space station. During the first phase of this study, which ended in March 1971, extensive analytical and experimental efforts led to the following developments:

- A fluid combination (R-22/DME-TEG) was found which was suitable for use in the space station system;
- Parametric cycle analyses verified that total system weight and radiator area requirements would be compatible with the space station mission constraints;
- Subscale testing verified that gravity-independent vapor absorption and generation were feasible.

The results of the first phase are completely documented in Ref. 1.

During the second phase of the study, further analytical and experimental development efforts were pursued. A zero-gravity liquid/vapor separator was analyzed, designed, fabricated, and tested. The results of the separator testing verified the capability of this component to function adequately, but further instrumentation and control devices are needed in the current experimental assembly to allow stable separation to occur over long time periods. The complete discussion of the separator study is presented in Section 2.

A detailed parametric design analysis was conducted for the vapor generator. The results of the analysis were used to design a light-weight, efficient generator for the absorption refrigeration system. The results of the analysis and the prototype design of the generator are presented in Section 3.

A detailed parametric design analysis was conducted for the absorber. The results of the analysis were used to design a light-weight, efficient absorber for the absorption refrigeration system. The results of the analysis and the prototype design of the absorber are presented in Section 4.

Based upon the results of the generator and absorber analyses, the cycle performance optimization analysis was revised. The results of the revised analysis showed improvement in performance over previous results. They are presented in Section 5.

The test assembly was relocated from Lockheed-Palo Alto to Lockheed-Huntsville. Significant modifications were made in the test system that resulted in much better performance than was achieved in the first phase of the study. Further testing was conducted, which is described in Section 6.

Under a subcontract, personnel at the University of Tennessee at Chattanooga conducted a study of alternate fluid combinations. Several new refrigerant-absorbent pairs were analyzed and tested. Although some of these fluid pairs represent workable alternatives to R-22/DME-TEG, none showed a definite superiority for the space station application. The results of this fluid study are presented in Section 7.

A comparison was made between the absorption system, the vapor compression system, and the conventional pumped fluid radiator system for space station environmental control. The results of the comparison verify the superiority of the absorption system. They are presented in Section 8.

The basic conclusion of the study to date is that absorption cycle refrigeration is feasible for providing space station environmental control, and that the absorption system is superior to available alternative environmental control systems in several ways. Specific conclusions and recommendations for continued development are presented in Section 9.

CONTENTS

CONTENTS (Continued)

LIST OF ILLUSTRATIONS

LIST OF ILLUSTRATIONS (continued)

NOMENCLATURE

Symbol	Description
A	area
C	screen constant
c_p	specific heat at constant pressure
D	diameter
DME-TEG	dimethyl ether of tetraethylene glycol
f	friction factor
g	gravitational acceleration at earth's surface ($32\ ft/sec^2$)
h	specific enthalpy
$\bar{h}$	mean heat transfer coefficient
k	thermal conductivity
L	length
LBP	liquid breakthrough pressure differential
M	molecular weight
$\dot{m}$	mass flow rate
P	pressure
Pr	Prandtl number
Q	heat rate
R	radius
R-22	Refrigerant No. 22
Re	Reynolds number

Symbol	Description
S.S.	stainless steel
T	temperature
t	thickness
V	velocity
VBP	vapor breakthrough pressure differential
W	work rate (power)
X	mole fraction
x	position coordinate

Subscripts

A	absorbent
Carnot	pertaining to reversed Carnot cycle
cond	condenser
D	diameter
evap	evaporator
eq	equilibrium
G, g, GEN	generator
HI	high pressure portion of cycle
L	liquid
LO	low pressure portion of cycle
R	refrigerant
rad	radiator
sink	effective black body sink
ss	stainless steel
T, t	total

Symbol	Description
V	vapor
w	wall
Greek	
β	coefficient of performance
Δ	differential
ϵ	emissivity
η	mass transfer efficiency
μ	viscosity
ρ	density
σ	Stefan-Boltzmann constant
τ	shear stress

Section 1
INTRODUCTION

To provide environmental control for the space station, energy must be transferred from the vehicle to its environment by radiation. Since the radiator area required to radiate a unit of energy decreases with increasing radiator temperature, it is desirable to operate space radiators at elevated temperatures, especially when available radiator area is limited. To transfer energy from a low temperature ($40^{\circ}F$) environmental control heat exchanger to a high temperature radiator requires an active refrigeration system. Of the two primary types, the absorption cycle system offers several advantages over the vapor compression cycle system. The absorption cycle refrigeration system is more advantageous in that it (1) requires less shaft power since thermal energy is used as the primary input; (2) is nearly vibration-free since no vapor compressor is required; and (3) requires less maintenance since the troublesome vapor compressor is absent. In addition, in the space station application, a thermal control function can be provided by removing waste heat from thermal power sources for input thermal energy. Because of these potential advantages, Lockheed-Huntsville has been evaluating the absorption cycle for space station environmental control applications since 1970 under a contract with NASA-MSFC.

The primary problem areas involved in developing an absorption system for the space station are:

- Finding safe, thermodynamically acceptable fluids for the system;
- Developing components capable of efficient performance in free-fall environment;
- Minimizing total system weight to a flight-acceptable level;
- Optimizing radiator area so that available vehicle skin area can be used for the radiator surface, thereby precluding the need for heavy deployed radiators.

The analytical and experimental efforts that Lockheed has expended to provide solutions in each of these problem areas are the subject of this report.

Section 2
SEPARATOR ANALYSIS, DESIGN AND FABRICATION

One of the essential components of the space station absorption cycle environmental control system is the liquid/vapor separator, which performs the task of diverting the weak solution liquid into the recuperator and the refrigerant vapor into the condenser. It is important that the separation process be efficient, since liquid carryover into the condenser degrades overall system performance. In a normal terrestrial absorption refrigeration system, liquid/vapor separation is effected easily by the use of gravitational forces. However, in the free-fall environment of a space vehicle, a gravity-independent separator is required. During the current study, a subscale gravity-independent liquid/vapor separator was analyzed, designed, fabricated, and tested. The details of the analysis and design of the separator are presented in Appendix A of this document. The results of the separator tests are presented in Section 6.4.

A schematic of the subscale gravity-independent separator is presented in Fig. 2-1. The separator utilizes vortex motion in the liquid phase, as well as hydrophilic and hydrophobic screens, to perform the phase separation process. The separator was purposely overdesigned such that the vortex motion should provide satisfactory separation even without the screens, and such that the screen combination should provide satisfactory separation even without the vortex motion. To further increase the confidence level of satisfactory performance, five hydrophilic screen materials and five hydrophobic screen materials were selected for fabrication; therefore, there were 36 different modes of operation available with various screen combinations.

The construction materials were chosen to prevent attack by the DME-TEG. The separator housing was made of stainless steel, and only stainless steel and teflon were used for screen materials, the former being hydrophilic

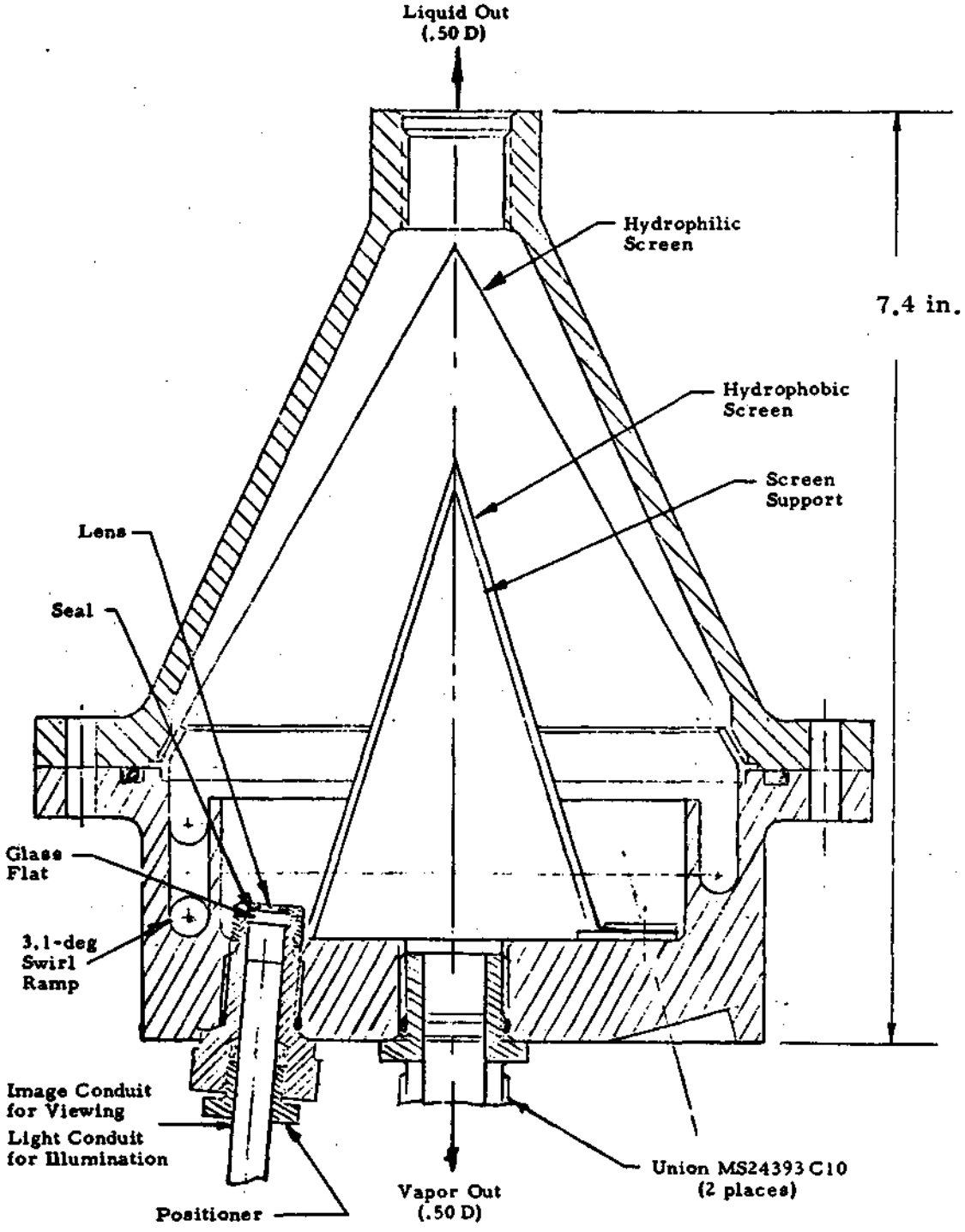

Fig. 2-1 - Subscale Gravity-Independent Separator Design

and the latter hydrophobic. The flow within the separator was monitored visually with a fiber optics system (Fig. 2-1).

The entire separator assembly was designed by Lockheed-Huntsville. The final hardware was supplied by NASA-MSFC as government-furnished equipment.

Section 3
GENERATOR ANALYSIS AND DESIGN

In the absorption cycle space station environmental control system, the heat input occurs at the vapor generator. The heat input raises the temperature of the fluid, thereby lowering the equilibrium concentration of refrigerant in the absorbent. Therefore, refrigerant vapor is released from solution and made available for producing the refrigeration effect in the condenser/evaporator portion of the absorption cycle. In commercial terrestrial absorption systems, the generator generally utilizes natural gas combustion for heat input, and often the generation process is heavily dependent upon gravity. In a space application for the absorption system, a gravity-independent generator is essential. During the current study, a full-scale prototype generator was parametrically analyzed, and the results of the analysis were used to design a light-weight, efficient generator for the space station environmental control system.

The analysis of the generator was necessarily complex because of the two-phase, two-component flow in conjunction with simultaneous heat transfer, mass transfer, momentum transfer, and phase change. The mathematical model was selected as a smooth-wall cylindrical tube, with the wall temperature held constant at $30^{\circ}F$ above the required exit temperature of the generator. The heat required to maintain this wall temperature was assumed to be available from unspecified waste heat sources. Preliminary calculations revealed that the generator performance would be best for high Reynolds number flow conditions. At high Reynolds numbers, the two-phase flow regime would be homogenous, bubbly flow. Therefore, the model assumed homogeneous, bubbly flow within the generator, and thermodynamic and transport properties were evaluated accordingly. Because of the complexity of the analysis, an analytical solution was impractical; therefore, a numerical

approach to the problem was used. The generator tube was divided into multiple small control volumes, or nodes, and the flow conditions at the exit of each node were determined by simultaneously solving the energy equation, momentum equation, continuity equations, and thermodynamic equations of state for the node. By using this technique, the temperature, pressure, quality, liquid concentration, enthalpy and velocity distributions were determined along the generator. A computer program was coded to provide such a solution for any set of input parameters. Input parameters included inlet flow conditions, tube diameter, mass transfer efficiency and number of tubes. A parametric analysis of the generator was conducted, using this computer program.

A detailed discussion of the mathematical model and analytical treatment of the generator is presented in Appendix B of this document. Results of the parametric analysis are also presented in Appendix B.

From the results of the parametric analysis, the full-scale prototype generator design shown in Fig. 3-1 was selected as optimum. The weight and volume of this generator are minimal, and the pressure drop through it is small. The design is quite simple, and will yield the desired flow conditions at the exit. The flow conditions of Fig. 3-1 correspond to the space station optimized system for a generator temperature of 350°F, as discussed in Section 5.

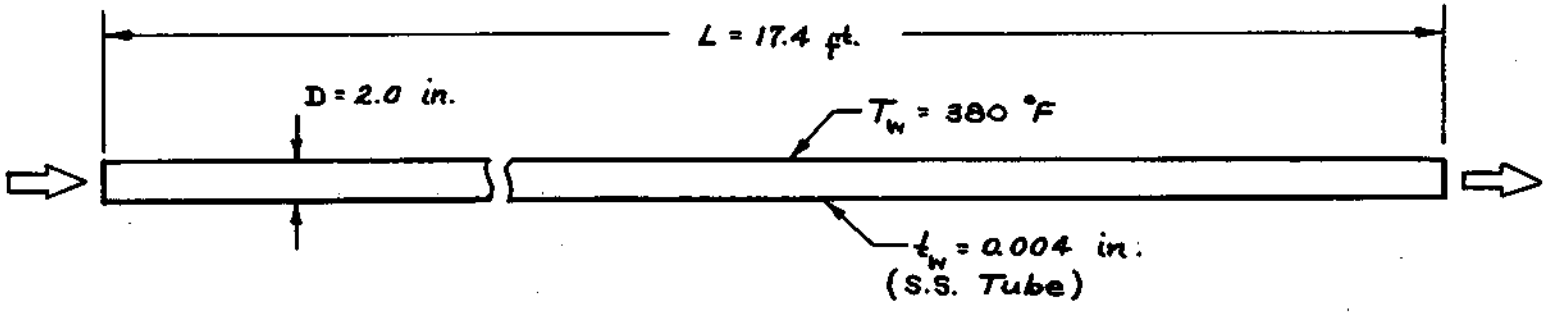

Inlet Conditions

- P = 381.2 psia
- T = 324.2 °F
- X_R = 0.4093 moles refrigerant / moles solution

Exit Conditions

- P = 380.9 psia
- T = 350.0 °F
- X_R = 0.3599 moles refrigerant / moles solution

Total Generator Weight = 17.2 lb_m (tube) + 9.8 lb_m (fluid inside)
= 27 lb_m

Figure 3-1 - Full Scale Prototype Gravity-Independent Generator Design

Section 4
ABSORBER ANALYSIS AND DESIGN

In the absorption cycle space station environmental control system, the refrigerant vapor returning from the evaporator is recombined with the weak solution liquid in the absorber. The space station absorber is basically a radiator which dumps the heats of vaporization and mixing from the fluid combination to allow the vapor to be completely absorbed by the liquid. The efficiency of the absorption process must be essentially 100% to avoid cavitation difficulties in the pump directly downstream of the absorber. Earth-bound absorbers often rely heavily upon gravitational forces to effect or augment the absorption process. In the space station system, however, a gravity-independent absorber is essential. During the current study, a full-scale prototype absorber was parametrically analyzed, and the results of the analysis were used to design a light-weight, efficient absorber for the space station environmental control system.

The analysis of the absorber was quite similar to the analysis of the generator discussed in Section 3. The mathematical model and analytical treatment of the absorber are discussed in Appendix C of this document. Results of the parametric analysis of the absorber are also presented in Appendix C.

From the results of the parametric analysis, the full-scale prototype absorber design shown in Fig. 4-1 was selected as optimum. The absorber weight (including tubes and fluid) is small, and the pressure drop is minimal. The design is quite simple, and will yield the desired flow conditions at the exit. The flow conditions of Fig. 4-1 correspond to the space station optimized system for a generator temperature of 350^{o}F, as discussed in Section 5.

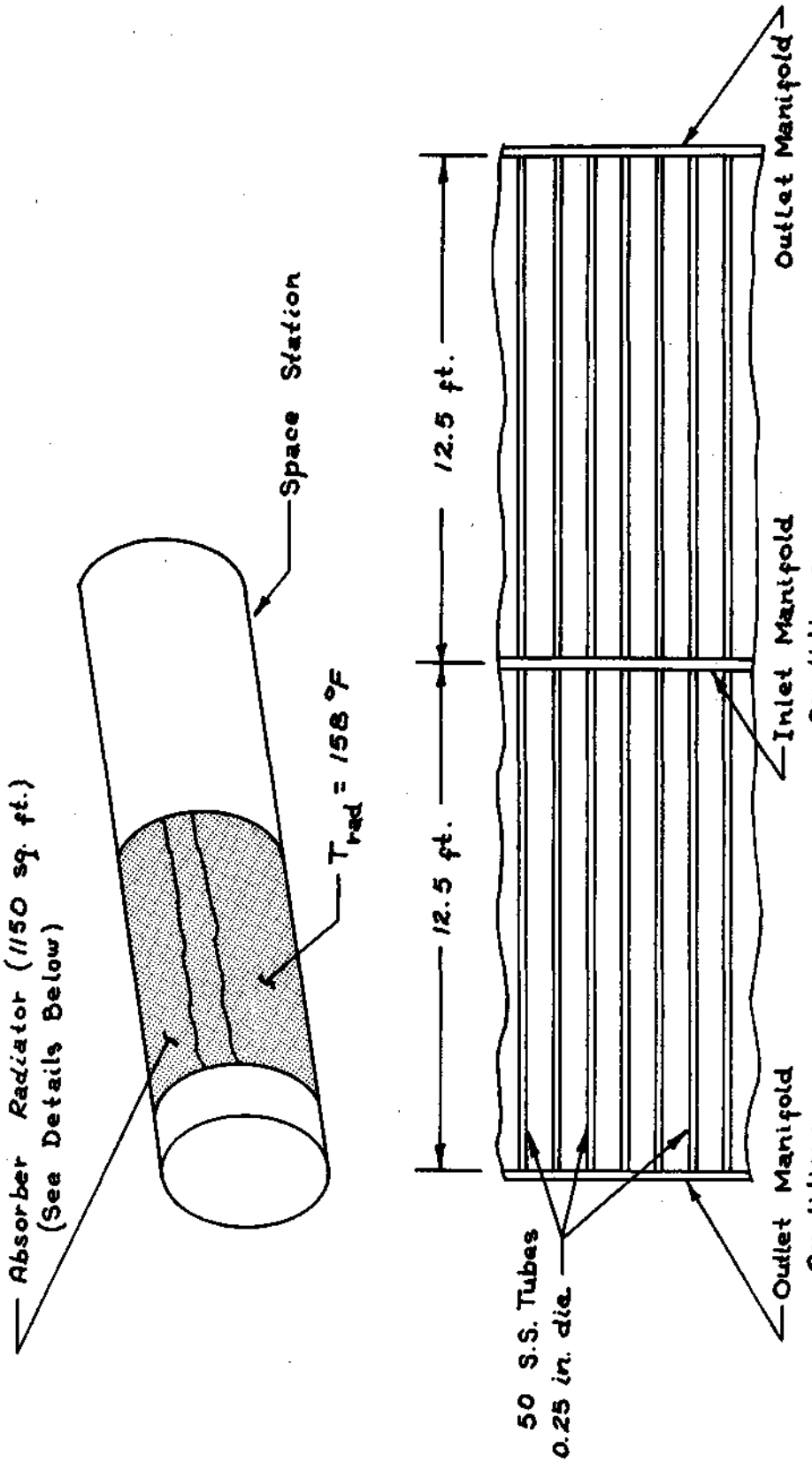

Total Absorber Weight (including fluid inside) = 115 lb_m

Figure 4-1 - Full Scale Prototype Gravity-Independent Absorber Design

Section 5
REVISED CYCLE PERFORMANCE ANALYSIS

During the first phase of the study, computer programs were written to analyze the space station absorption system and to determine the total system weight and radiator area for different operating temperatures, pressures, and flow rates. One program was automated to find the minimum possible weight of the system for a given generator temperature; another to find the minimum possible radiator area of the system for a given generator temperature. During the current study, certain revisions were made to these computer programs to make them more accurate, based upon the results of the most up-to-date analytical and empirical efforts. The major revisions are listed below.

- Based upon the results of the fluids study conducted by UTC, improved P-T-X data fitting techniques were used for the R-22/DME-TEG fluid combination.
- Based upon the results of the generator and absorber design analyses, more realistic weight equations were used for these components, and more realistic mass transfer efficiencies were utilized.
- Based upon updated space station constraint data, better values of radiator area density and incident heat flux were used.
- A hydraulic motor for weak solution power recovery was added to the analytical model with its associated weight penalty and pump power reduction.
- A realistic electrical power penalty was added to the program weight calculations.

With the modifications, the weight-optimized program and the area-optimized program were used to determine the total system weight and area as functions of generator temperature. The results of these analyses are presented in Fig. 5-1.

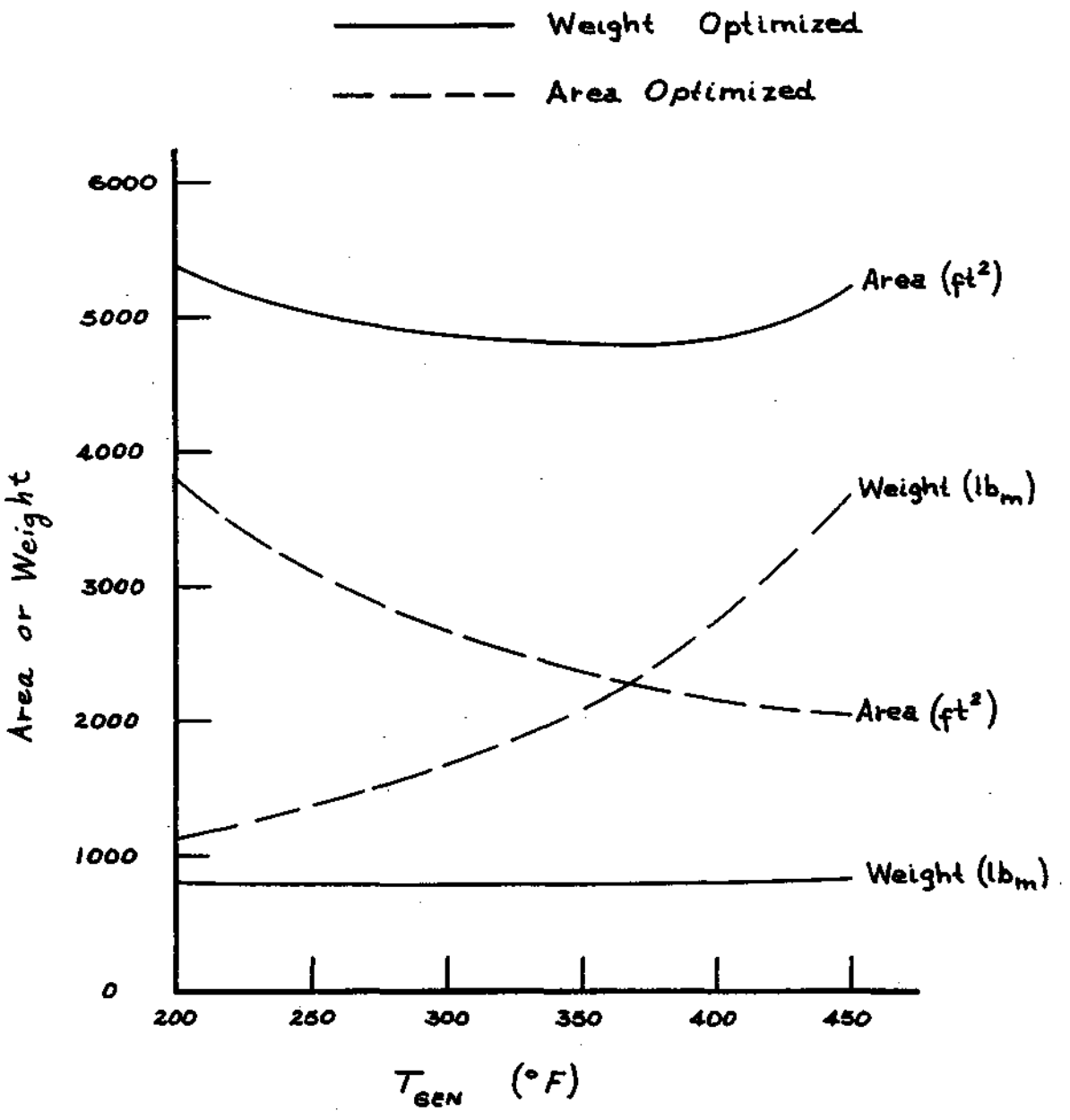

Figure 5-1 Optimized System Weight and Radiator Area Dependence on Generator Temperature

Although the curves in Fig. 5-1 represent the minimum weight and radiator area required for the space station absorption system for different generator temperatures, the optimum space station system does not correspond either to the area-optimized or to the weight-optimized system. To understand this point, it must be recalled that the space station will have about 2500 ft^2 of available integral radiatior area; i.e., available vehicle hull area into which radiator tubes can be integrated. The importance of this integral radiator area limitation rests upon the fact that the weight penalty for an integral radiator is about 0.1 lb_m/ft^2, while the weight penalty for a deployed radiator with its required supporting structures is about 2.0 lb_m/ft^2. Therefore, the optimum space station system will be the one which weighs the least and requires 2500 ft^2 of radiator area or less. This set of combined weight and area constraints does not correspond to either the area-optimized or the weight-optimized system. Therefore, an additional analysis was conducted to find the optimum space station system. A generator temperature of 350°F was selected, since the R-22/DME-TEG fluid combination is considered safe and stable below this temperature. Safety and stability are not well-defined above this temperature. (A recommended effort for determining the actual chemical stability of the fluid combination is included in Section 9.)

Because of the importance of this optimized space station system, the detailed results of this analysis are presented in Fig. 5-2, including heat rates, weights, temperatures, pressures, flow rates, etc. For this set of cycle conditions, the total system weight is only 1618 lb_m. A comparison between this absorption cycle system and the two most competitive alternatives, the vapor compression system and the conventional pumped fluid radiator system, is presented in Section 8. As expected, the absorption system is superior in total system weight to either of the alternatives and it offers other significant advantages over the vapor compression system, including lower power requirements, less vibration, less maintenance, and waste heat removal.

Component	Energy Input	Weight *	Radiator Area Required
• Evaporator	35.0 kw	75 lb_m	0 ft^2
• Condenser	-49.4	135	1350
• Subcooler	0	25	0
• Separator	0	25	0
• Absorber	-48.9	115	1150
• Generator	58.8	27	0
• Recuperator	0	630	0
• Pump	4.2	160	0
• Power Pack	- 0.4	283	0
• Hydraulic Motor	- 3.7	143	0
		Total 1618 lb_m	Total 2500 ft^2

* Weight includes fluid inside components

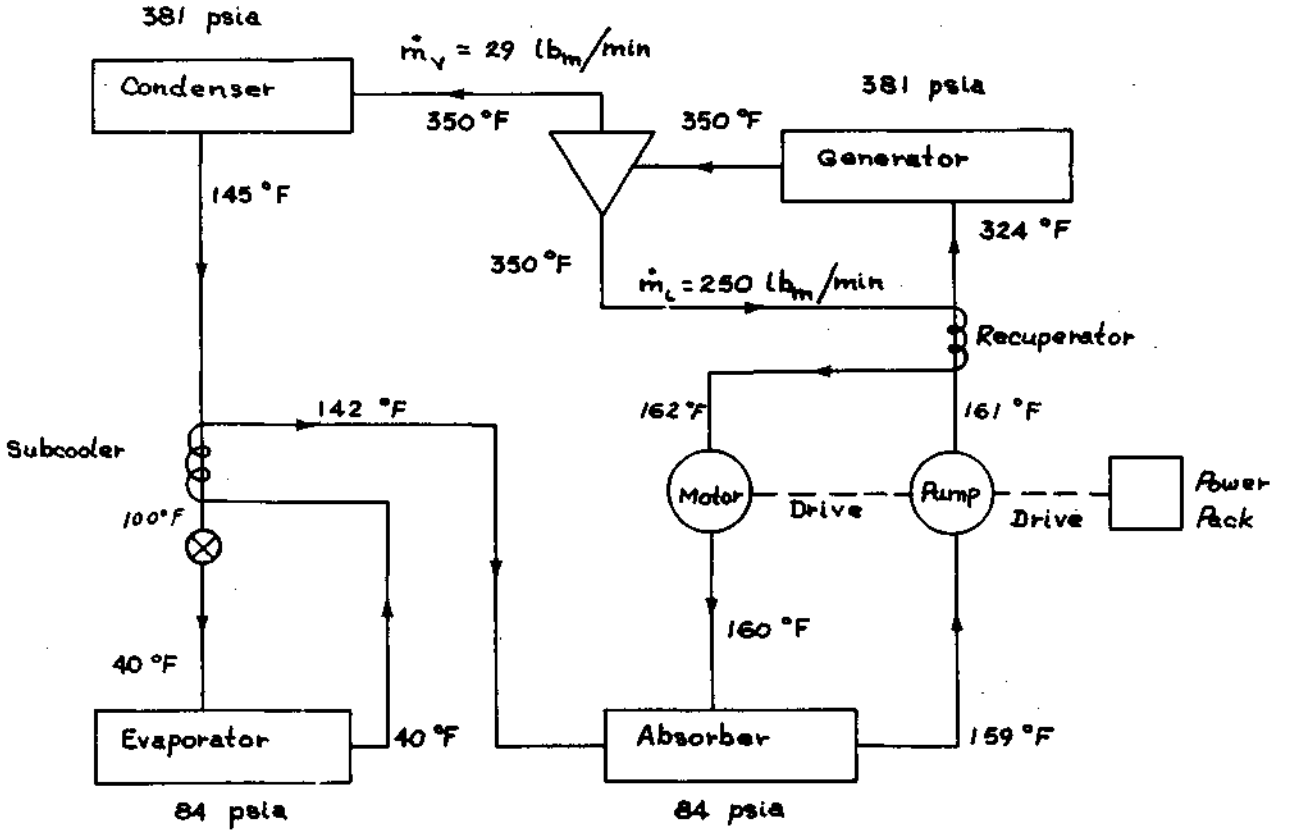

Figure 5-2 - Space Station Optimized System for T_G = 350 °F

Section 6
SUBSCALE TESTING OF THE ABSORPTION SYSTEM

During the first phase of this study, an experimental assembly was designed and fabricated at Lockheed-Palo Alto, the purpose of which was to verify the feasibility of vapor generation and absorption without the aid of gravity, and to substantiate analytical predictions. Although the original assembly successfully accomplished these objectives, flow oscillations and pump cavitation occurred during testing, making long-time period operation impossible. Therefore, several significant modifications were made to the test assembly when it was relocated at Lockheed-Huntsville under the second phase of the study. The revised test system is shown schematically in Fig. 6-1. The system modifications and test efforts are discussed in the following sections.

6.1 TEST SYSTEM MODIFICATIONS

Analysis of the original test system resulted in the identification of pump cavitation as the primary cause of flow instability. The cavitation was due to the excessive net positive suction head (NPSH) requirement of the original pump. The NPSH represents the maximum pressure drop which occurs when the fluid initially enters the pump. Since the fluid entering the pump in the test system is saturated (having just left the absorber), it is at its boiling point, and any pressure reduction will cause fluid within the pump to boil spontaneously. Therefore, the original pump was replaced with a regenerative turbine pump with an NPSH requirement of one foot of water. Lockheed selected the pump, which was supplied by NASA-MSFC as government-furnished equipment. To supply the NPSH requirement, the pump was located two feet below the surge tank (Fig. 6-1) so that the gravitational head pressure would exceed the NPSH requirement of the pump. The new pump worked perfectly in this configuration throughout the test program. Pressure control was obtained

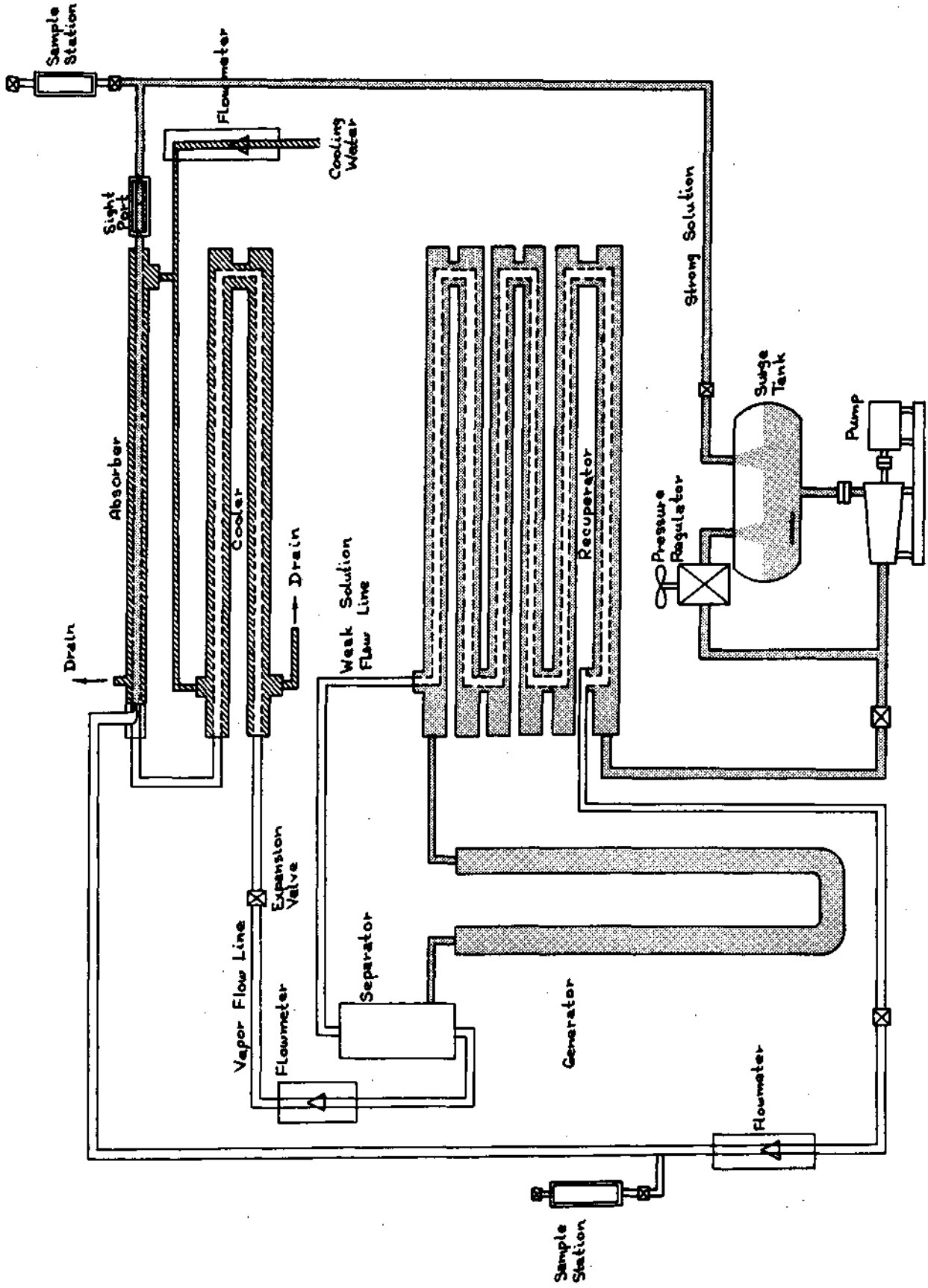

Figure 6-1 - Revised Test System Schematic

with the pressure regulator in the bypass line, as shown in Fig. 6-1. Flow rate control was obtained with the manual valve downstream of the pump. Any combination of flow rate and pressure rise was easily and accurately obtainable with this valve system.

In addition to supplying the required gravitational head pressure to the pump, the new surge tank added to the system during the current phase of the study also served several other important functions:

- The surge tank served as a mixing tank during charging of the system, thereby eliminating the need for the mixing vessel used previously.
- The large liquid volume within the surge tank eliminated the possibility of cavitation even during transient periods such as startup and shutdown.
- The large vapor volume offered expansion room in case of surges.

The surge tank was ASME coded for 400 psia and 400°F operation in accordance with LMSC safety regulations.

In addition to the modifications mentioned above, two other major modifications were made:

- The absorber design was modified to improve vapor absorption. This is discussed further in Section 6.3.
- The gravity-independent separator was installed in the test system for its performance verification. This is discussed further in Section 6.4.

6.2 NOMINAL CYCLE TESTING

During the first phase of this study, total system testing under steady-state conditions was limited to very short periods because of flow oscillations. With the test system modifications described in Section 6.1, the oscillation problem was eliminated and testing periods of several hours duration were

easily obtained. As in the previous phase of the study, the nominal cycle conditions chosen for experimental study corresponded to a generator temperature of 250°F. This temperature was chosen instead of a higher, more optimal value because the chemical stability and safety of the R-22/DME TEG fluids at elevated temperatures are not well known. The conditions around the cycle were chosen to correspond to the area-optimized cycle with flow rates scaled to 1/53 of full scale.

During the first few nominal cycle test runs, vapor bubbles were seen in the view port downstream of the absorber, indicating incomplete absorption. The problem was caused by insufficient turbulence within the absorber which allowed the vapor bubbles to accumulate at the top of the tube. To overcome this problem, the absorber design was altered by placing pins within the tube perpendicular to the flow to induce turbulence. Further discussion of the absorber modification and performance is given in Section 6.3. The new design eliminated the problem of incomplete absorption and for the remainder of the test program the absorber functioned properly.

Several nominal test runs were made to ensure repeatability. Figure 6-2 presents the results of a typical run, showing the theoretical design temperatures, pressures, concentrations, and flow rates around the cycle as well as the measured temperatures, pressures, concentrations, and flow rates. From Fig. 6-2, it is apparent that the agreement between predicted and measured performance is good. The few discrepancies were due in general to heat losses from the system and non-optimum controls in the test assembly. For example, T_{10} is at 190°F rather than 250°F because of heat losses from the vapor to ambient as the vapor moved from location 5 (where it was at 250°F) to location 10. Similarly, T_4 is at 220°F rather than 236°F because of heat losses to ambient from the recuperator. Also, T_2 and T_3 are somewhat lower than their design values because of control difficulties with the cooling water circuit which was used to absorb heat from the vapor cooler and absorber. All other temperatures and pressures are close to their design values. The flow rates are also very close to the design values. Better controls plus

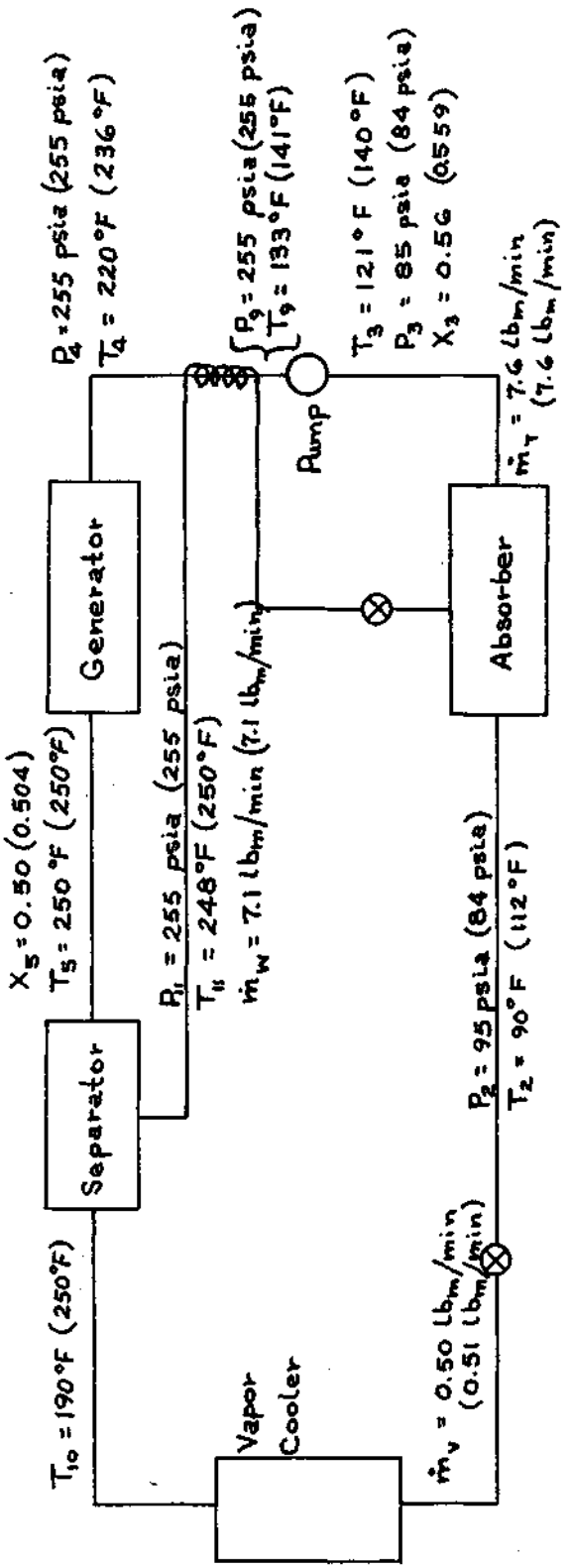

Notes: Theoretical values are in parentheses next to measured values.
The vapor cooler simulates the condenser, evaporator, and subcooler.

Fig. 6-2 - Nominal Cycle Test Results

smaller, better insulated components and plumbing would reduce the discrepancies between theory and measurement to completely acceptable values. More important than matching temperature, pressure, and flow rate values exactly, however, is that the system performed in a stable steady-state, steady-flow condition for several hours during each test run with complete absorption and stable vapor generation, without the aid of gravity in either the absorber or generator, and at conditions very close to theoretical design conditions. Also, initial system startup and final shutdown posed no significant difficulties, verifying system stability during these two most crucial transient periods of operation.

In summary, the nominal cycle testing verified the practicality of stable vapor generation and absorption without the aid of gravity and, in general, the thermodynamic states and flow rates around the cycle agreed well with prediction. Also, the modifications to the test system were successful in allowing stable system operation for long test periods.

6.3 ABSORBER ALTERATION AND PERFORMANCE

The original absorber was simply a tube surrounded by a coaxial cooling jacket, with the weak solution entering the tube through a jet with a screen over its exit and with the vapor entering the tube radially. Initial nominal cycle testing under steady-state, steady-flow conditions was accompanied by incomplete absorption which was apparent in the view port at the exit of the absorber. The lack of absorption was due to insufficient turbulence within the absorber, which allowed the vapor bubbles to accumulate at the top of the absorber tube. The Reynolds number was only 10^4 inside the absorber and this value was not large enough to provide homogeneous bubbly flow. A design modification was needed to correct the inadequate absorber performance.

Several different design alterations were tried. Nozzle modifications were unsuccessful in providing the needed turbulence. A twisted metal tape was placed within the absorber, but it also proved ineffective in inducing the

required turbulence. Finally, a smaller diameter tube was fitted with 3/16-inch dowel pins welded in place perpendicular to the flow direction. The pins were located at six-inch intervals along the smaller tube and each pin was rotated 45 deg. about the tube axis from the previous pin. This smaller tube was installed within the old absorber tube. The smaller tube provided higher fluid velocity and the pins provided alternate fluid acceleration and deceleration; the overall effect was enhanced mixing and turbulence over the entire length of the absorber. To support the smaller tube/pin assembly in obtaining highly turbulent flow, a new nozzle assembly was also fabricated and installed. The new nozzle was an 8-in. length of 1/4-in. copper tubing with a 0.030 in. hole in the outlet end, and with 40 additional 0.030-in. holes uniformly spaced along the length of the nozzle. This nozzle configuration ensured better initial liquid/vapor mixing than had been achieved with a single liquid jet.

The modified absorber was installed in the test assembly and operated under the nominal cycle design conditions described in Section 6.2. The complete absence of vapor at the viewport verified that complete absorption was achieved. The test system was run for several hours on several different occasions under steady-state, steady-flow conditions and complete absorption was achieved in every test.

6.4 GRAVITY-INDEPENDENT LIQUID/VAPOR SEPARATOR TESTING

During the current phase of the space station absorption cycle environmental control system study, a gravity-independent liquid/vapor separator was analyzed, designed, fabricated, and tested. The analysis, design and fabrication are discussed in Section 2 of this document. After the nominal cycle test program was completed, the gravity-independent separator was installed in the test assembly for experimental verification of its performance. To verify that the separation process was independent of gravity, the separator was tested in two different orientations: (1) the most favorable orientation with respect to the gravity vector; i.e., with liquid out the bottom and vapor out the top; (2) the least favorable orientation with respect to the gravity vector; i.e.,

with liquid out the top and vapor out the bottom. If the separator functioned satisfactorily in both orientations, the logical conclusion would be that it would function satisfactorily in a neutral gravity environment. The results of the testing in each orientation are discussed in the following two sections.

6.4.1 Separator Testing in Gravity-Aided Orientation

As described in Section 2, the gravity-independent liquid/vapor separator was designed to allow operation with or without a hydrophilic and/or a hydrophobic screen. For the initial separator test, the separator was fitted with a hydrophilic screen (No. 3, Table A-1) and a hydrophobic screen (No. 10, Table A-1), and the separator was mounted with the liquid outlet at the bottom and the vapor outlet at the top. The test assembly was brought to nominal cycle steady-state, steady-flow conditions while the normal gravity separator was being used. Then the two-phase flow was diverted from the normal separator to the gravity-independent separator. During this first test, successful separation was not achieved and the separator was dismantled for inspection. This inspection revealed that the adhesive used to mount the hydrophobic screen had failed under exposure to the DME-TEG, thereby leaving the hydrophobic screen almost totally unattached from its mounting fixture and in a totally unworkable condition. Therefore, the hydrophobic screen was removed from the separator and not replaced since all hydrophobic screens had been attached to their mounting fixtures with the same adhesive.

The separator was reassembled with only the hydrophilic screen fitted within. The test was repeated with the separator mounted in the gravity-aided orientation. The separator operated successfully, yielding the same liquid flow rate and vapor flow rate that had been observed using the normal separator. However, the separator required constant attention during the test to achieve this complete separation. This constant attention was required because of minor stable oscillations in the vapor flow rate from the generator. These small oscillations caused no problems where the normal separator was being used, since it had a relatively large volume, and the oscillations caused only

a slightly fluctuating liquid level. However, since the gravity-independent separator had been purposely minaturized to more accurately simulate the actual space station system, the small oscillations were large enough to empty or fill completely the small volume of the gravity-independent separator. Therefore, the valves at the entrance and exits of the separator were continually adjusted to maintain a stable liquid/vapor interface within the separator. A fiber optics system allowed this liquid/vapor interface to be monitored visually during the test.

After the test was completed, the separator was dismantled and the hydrophilic screen removed. The screen-free separator was then mounted in the gravity-aided orientation to determine if satisfactory separation could be achieved without the hydrophilic screen. The test was conducted and separation was again achieved. Constant attention was again required for the reasons described earlier. Since successful operation was achieved without screens, no further tests were conducted using alternate screens.

6.4.2 Separator Testing in Gravity-Impeded Orientation

After the separator test in the gravity-aided orientation was completed, the separator was installed in a gravity-impeded orientation; i.e., with the liquid outlet at the top and the vapor outlet at the bottom. In the initial test, severe difficulties were encountered in starting flow through the separator without completely filling it with either liquid or vapor. To overcome this flow initiation problem, the plumbing was rearranged so that the normal separator was upstream of the gravity-independent separator with valves to allow any desired flow rate of liquid and any desired flow rate of vapor to be introduced into the gravity-independent separator. Even with this plumbing arrangement, however, the same difficulties that occurred in the gravity-aided orientation were multiplied in the gravity-impeded orientation. Successful separation was achieved, but only for short periods of time, of the order of 10 sec. The problems were compounded by deterioration of the fiber optics system, apparently due to contact with DME-TEG. The separation difficulties were still

due primarily to the small stable fluctuations in vapor flow rate from the generator, which were large enough to cause great difficulty when coupled with the small volume of the separator.

Although operation in the gravity-impeded orientation was verified for only short time periods, long-term operation could be achieved by one or both of the following modifications:

- Replacing the current generator with an optimized, well-insulated, high Reynolds number generator to eliminate the small stable oscillations;
- Adding an automated control system to adjust the separator valves to maintain a stable liquid/vapor interface within the separator.

Neither of these modifications was feasible under the current scope of effort, but the separator concept is considered verified as a practical, workable device for effecting liquid/vapor flow separation in the space station environmental control system.

Section 7

ANALYSIS AND TESTING OF ALTERNATE FLUID COMBINATIONS

Under a subcontract, the University of Tennessee at Chattanooga conducted a study of several refrigerant-absorbent fluid combinations to determine their applicability to the space station environmental control system. The study included fluid pair analysis, selection, solubility measurements, and computer evaluation for space station applicability. The results identified several workable alternatives to the previously chosen R-22/DMETEG combination, but in general the superiority of the chosen fluid pair was verified. The complete results of the fluids study are presented in Appendix D.

Section 8

COMPARISON OF ABSORPTION CYCLE, COMPRESSION CYCLE, AND CONVENTIONAL PUMPED FLUID RADIATOR SYSTEMS FOR SPACE STATION ENVIRONMENTAL CONTROL

The primary benefit of active refrigeration systems for use in the space environment is the capability of such systems to utilize radiators at temperatures higher than the required environmental control heat exchanger temperature. Because of their high temperature operation, such radiators can be considerably smaller in area than their conventional low temperature counterparts. For an application like the space station, this reduction in radiator area may mean a tremendous savings in total vehicle weight, provided that the required radiator area can be integrated into the available vehicle skin. Weight savings is due to the fact that the weight penalty for an integral radiator is of the order of 0.1 lb_m/ft^2 while the weight penalty for a deployed radiator system with its supporting structures is of the order of 2.0 lb_m/ft^2.

The space station will have an available integral area of about 2500 ft^2 with an effective sink temperature of about 20°F for $\epsilon_{rad} = 0.9$ (Ref. 2). Therefore, to maintain the environmental control heat exchanger at 40°F, a conventional pumped fluid radiator must operate at a mean temperature of about 30°F. To dump the required 35 kW cooling load at this temperature, the conventional radiator area must be 17,200 ft^2, far in excess of the available 2500 ft^2. Therefore, a conventional pumped fluid radiator system would require a deployed radiator in addition to the integral radiator. A deployed radiator for the space station will have an effective sink temperature of about -78°F (Ref. 2). Therefore, a conventional pumped fluid radiator system would require 1755 ft^2 of deployed radiator area in addition to the 2500 ft^2 of integral radiator area. Thus, assuming radiator weight penalties of 0.1 lb_m/ft^2 for integral radiators and 2.0 lb_m/ft^2 for deployed radiators, the total radiator weight for the conventional system would be 3760 lb_m.

For a vapor compression refrigeration system, the radiator heat load can be calculated as:

$$Q_{rad} = Q_{cond} = Q_{evap} + W_{pump} ,$$

where

$$W_{pump} = \frac{Q_{evap}}{\beta_{actual}} .$$

From Ref. 3, the "actual typical values quoted" for coefficient of performance of electric-driven vapor compression systems are about 40% of β_{Carnot}. Thus,

$$W_{pump} = \frac{Q_{evap}}{0.4\,\beta_{Carnot}} = 2.5\,Q_{evap}\left(\frac{T_{rad} - T_{evap}}{T_{evap}}\right) .$$

Substituting this result into the first equation yields:

$$Q_{rad} = Q_{evap}\left(2.5\,\frac{T_{rad}}{T_{evap}} - 1.5\right) .$$

Also, the radiator heat load must meet the following constraint:

$$Q_{rad} = \sigma A \epsilon \left(T_{rad}^4 - T_{sink}^4\right) .$$

Combining the previous two equations yields:

$$\sigma A \epsilon \left(T_{rad}^4 - T_{sink}^4\right) = Q_{evap}\left(2.5\,\frac{T_{rad}}{T_{evap}} - 1.5\right) .$$

For

$\epsilon = 0.9$,

$A = 2500\ ft^2$,

$T_{sink} = 20^{\circ}F$,

$Q_{evap} = 35\ kW$,

and $T_{evap} = 40^{\circ}F$,

the above equation can be solved to yield:

$$T_{rad} = 91^{\circ}F.$$

Using this result, the pump power can be calculated to yield

$$W_{pump} = 8.925\ kW.$$

For the space station, the weight penalty for electrical power will be about 500 lb_m/kW (Ref. 2). Thus, a vapor compression system would require 4462 lb_m of power related equipment. In addition to this power weight, a vapor compression system would require the following:

- Evaporator — 75 lb_m (same as for absorption cycle)
- Condenser — 250 lb_m (2500 ft^2 x 0.1 lb_m/ft^2)
- Compressor — 25 lb_m (Ref.4).

Thus, the total vapor compression system weight would be about 4812 lb_m.

For an absorption cycle system optimized for the space station application, and with a generator temperature of 350°F, the total weight of the system will be 1618 lb_m. A weight breakdown is shown in Table 8-1. This

Component	Weight *	
• Evaporator	75	lb_m
• Condenser	135	"
• Subcooler	25	"
• Separator	25	"
• Absorber	115	"
• Generator	27	"
• Recuperator	630	"
• Pump	160	"
• Power Pack	283	"
• Hydraulic Motor	143	"
Total	1618	"

*Weight includes fluid inside components

Table 8-1 - Weight Breakdown for Space Station Optimized System with T_6 = 350 °F

system requires a radiator area of 2500 ft^2, which is equal to the available integral area of 2500 ft^2. Therefore, it becomes apparent that the total weight for the absorption cycle system for space station environmental control is less than for the vapor compression system and less than for the conventional pumped fluid radiator system. In addition to this weight superiority, the absorption cycle system offers the following advantages over the vapor compression system:

- Lower power requirement
- Less vibration (no vapor compressor)
- Less maintenance
- Waste heat removal.

In conclusion, the absorption cycle system for space station environmental control is superior to the vapor compression and conventional radiator systems in several ways, including total system weight.

Section 9
CONCLUSIONS AND RECOMMENDATIONS

9.1 CONCLUSIONS

The primary conclusion of the study to date is that the absorption cycle refrigeration system is feasible for providing space station environmental control. Specific conclusions which verify this primary conclusion are:

- The total system weight for an optimized absorption cycle environmental control system for the space station is less than the total system weight for either a vapor compression system or a conventional pumped fluid radiator system.
- Besides having weight superiority, the absorption system offers several other advantages over its competitors, including lower power requirement, less vibration, less maintenance, and waste heat removal.
- A zero-gravity liquid/vapor separator was analyzed, designed, fabricated, and successfully tested. The feasibility of developing a flight-type separator for the full-scale space station environmental control system is therefore verified.
- A full-scale prototype absorber was analyzed and designed. The weight of the required plumbing will be small compared to the integral radiator weight penalty, which itself will not be excessive.
- A full-scale prototype generator was analyzed and designed. The weight of the generator is small compared to the total system weight.
- Revised cycle optimization analyses verified the capability of the absorption system to utilize waste heat and available integral radiator area to provide space station environmental control.
- The improved test assembly, utilizing a new pump, surge tank, and absorber design functioned well for periods extending to several hours. No serious instabilities or oscillations were observed after these modifications were made. The system performed well for both on-design and off-design tests.

- Under a subcontract to Lockheed, the University of Tennessee at Chattanooga conducted a study to synthesize new fluid combinations for absorption refrigeration. Although several fluid combinations were found to be workable alternatives, the R-22/DME-TEG combination was found to be superior for the space station application, verifying its choice earlier in the study.

9.2 RECOMMENDATIONS

Based upon the results of the study to date, the following specific recommendations for further development efforts are made:

- Conduct detailed prototype design analyses of the condenser and evaporator components of the environmental control system.
- Conduct a study of the controls necessary to ensure proper system performance during all phases of the space station mission.
- Design and fabricate a condenser, evaporator, and precooler for the subscale test assembly.
- Replace the large recuperator in the test assembly with a compact heat exchanger.
- Add an isolated conditioned space to the test assembly to simulate the space station conditioned space.
- Replace the current generator in the experimental assembly with an optimized one based on the analytical studies already completed.
- Replace the current absorber in the experimental assembly with an optimized one based on the analytical studies already completed.
- Replace non-optimized valves and plumbing in the test assembly with improved counterparts.
- Add controls to the experimental assembly to permit long-term stable operation in totally zero-gravity mode.
- Consider increasing scale factor from 2 to 5 percent. This would provide 6000 Btu/hr cooling or $\frac{1}{2}$ ton of refrigeration.
- In all modifications to the test system, direct efforts toward miniaturization to simulate the space station system more realistically.

- From the results of the further analytical and empirical studies, improve total system analytical model and continually reoptimize cycle parameters.
- Conduct long-term chemical stability studies of R-22/DME-TEG at the temperatures, pressures, and concentrations to be used in the space station system.
- To improve the thermodynamic analyses of the system, determine experimentally the enthalpy and density of liquid and vapor mixtures of DME-TEG and R-22 as functions of pressure, temperature, and concentration. Also determine the composition of the saturated vapor as a function of temperature and pressure.
- In order to extend the usefulness of the absorption system being developed, review other space missions to determine other applications for the system. The planned moon base is one example of a mission for which the system could prove ideal with minor design modifications.

Section 10
REFERENCES

1. Hale, D. V. et al, "Evaluation of Absorption Cycle for Space Station Environmental Control System Application – Interim Report," LMSC-HREC D162909, Lockheed Missiles & Space Company, Inc., Huntsville, Ala., March 1971.

2. Copeland, R. J. et al, "Evaluation and Selection of Refrigeration Systems for Lunar Surface and Spacecraft Applications," Report T122RP04, Vought Missiles & Space Company, Dallas, Texas, 31 October 1971.

3. Whitlow, E. P., "Trends of Efficiencies in Absorption Refrigeration Machines," ASHRAE J., p.44, December 1966.

4. Blutt, J. R., and S. E. Sadek, "A Gravity Independent Vapor Absorption Refrigerator," NASA CR-836, Dynatech Corp., Cambridge, Mass., July 1967.

Appendix A

A.1 SURVEY OF CONCEPTS

Primary emphasis for this study was given to concepts which required no external power and contained no moving parts. Thus, concepts which utilized electrostatic means for separation, or required impellers or similar devices were not considered. This emphasis was in the interest of finding the simplest, maintenance free, and reliable separation concept. The three basic types of separators considered and the separation mechanism(s) employed in each are listed below.

Separator Type	Separation Mechanism
Vortex	Centrifugal force acting on fluids of widely different densities (liquid/vapor).
Hydrophobic/Hydrophilic	Screen materials with pores sized so that surface tension and contact angle control liquid or vapor passage.
Wick	Wicking material with pores sized to allow passage of vapor and which collects liquid (surface tension) for sucking out a separate outlet.

Figures A-1, A-2, A-4 and A-6 illustrate configurations based on these types of separators. Each of these concepts have been subjected to laboratory 1g tests. Additionally, the vortex (Fig. A-1) and Wedge hydrophobic/hydrophilic (Fig. A-2) separators have been tested in the near zero g environment (KC-135 flights). Particulars of these concepts are discussed in the following paragraphs.

Vortex Separator

The vortex separator shown in Fig. A-1 was developed by Martin-Marietta Corp. (Denver Division) for a zero gravity whole body shower system (Ref. A.1).

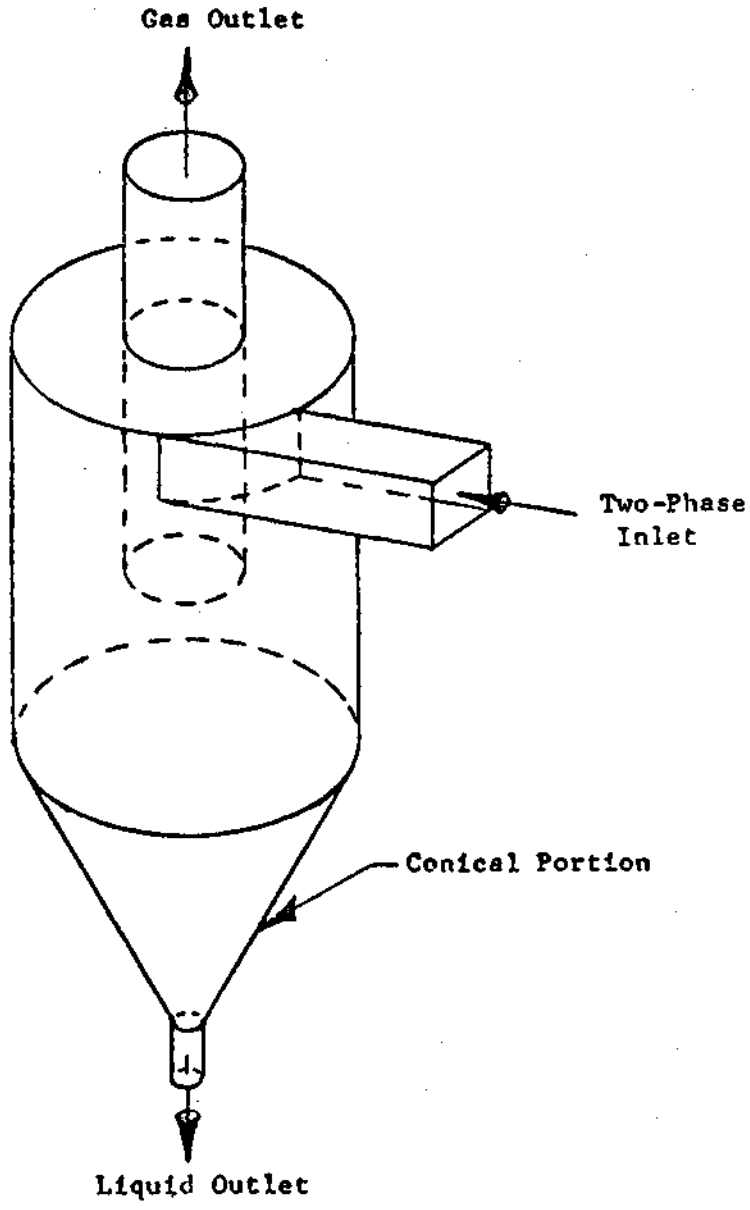

Fig. A-1 - Basic Vortex Separator Configuration (from Ref. A.1)

Basically, this separator was used for separation of air and water contaminated with urea, dissolved solids, particulate matter such as hair and skin, soap, and/or bacteria. Tests were conducted with variations of this concept in which the mixture inlet, water outlet and gas outlet configurations were changed to improve separation performance. Typical problems encountered involved difficulties in forcing water out of the liquid outlet port (negative pressure at cone apex), and in preventing water reentrainment in the gas outlet. These were solved satisfactorily with a vortex breaker plate at the outlet and a deflector cylinder at the inlet plus other minor inlet and outlet modifications. However, tests in zero gravity (KC-135 flights) still indicated problems in preventing water reentrainment in the gas, and in water removal rate (water build-up in the separator).

The essential conclusion reached from a review of the vortex separator is that this type separator may be adequate for the shower system but would be marginal or inadequate for the absorption cycle refrigeration system application because of the liquid reentrainment problem. However, the vortex separation principles may be very useful in combination with other separation methods.

Wedge Separator

This configuration (Fig.A-2) is one of several hydrophobic/hydrophilic separators evaluated in laboratory 1g tests and in zero gravity flight tests (KC-135) by Lockheed's Biotechnology Organization (Sunnyvale, Calif.). Other types included a parallel surface, and a wavy surface hydrophobic/hydrophilic membrane configuration, plus a cartridge type. The wedge configuration appeared to be representative of the better performance configurations and is used here for comparison with other concepts. This effort is described in detail in Ref.A.2.

A more accurate terminology for use of this concept for liquids other than water (hydro) would be lyophilic (liquid loving) and lyophobic (liquid hating). However, to avoid confusion the hydrophilic/hydrophobic terminology

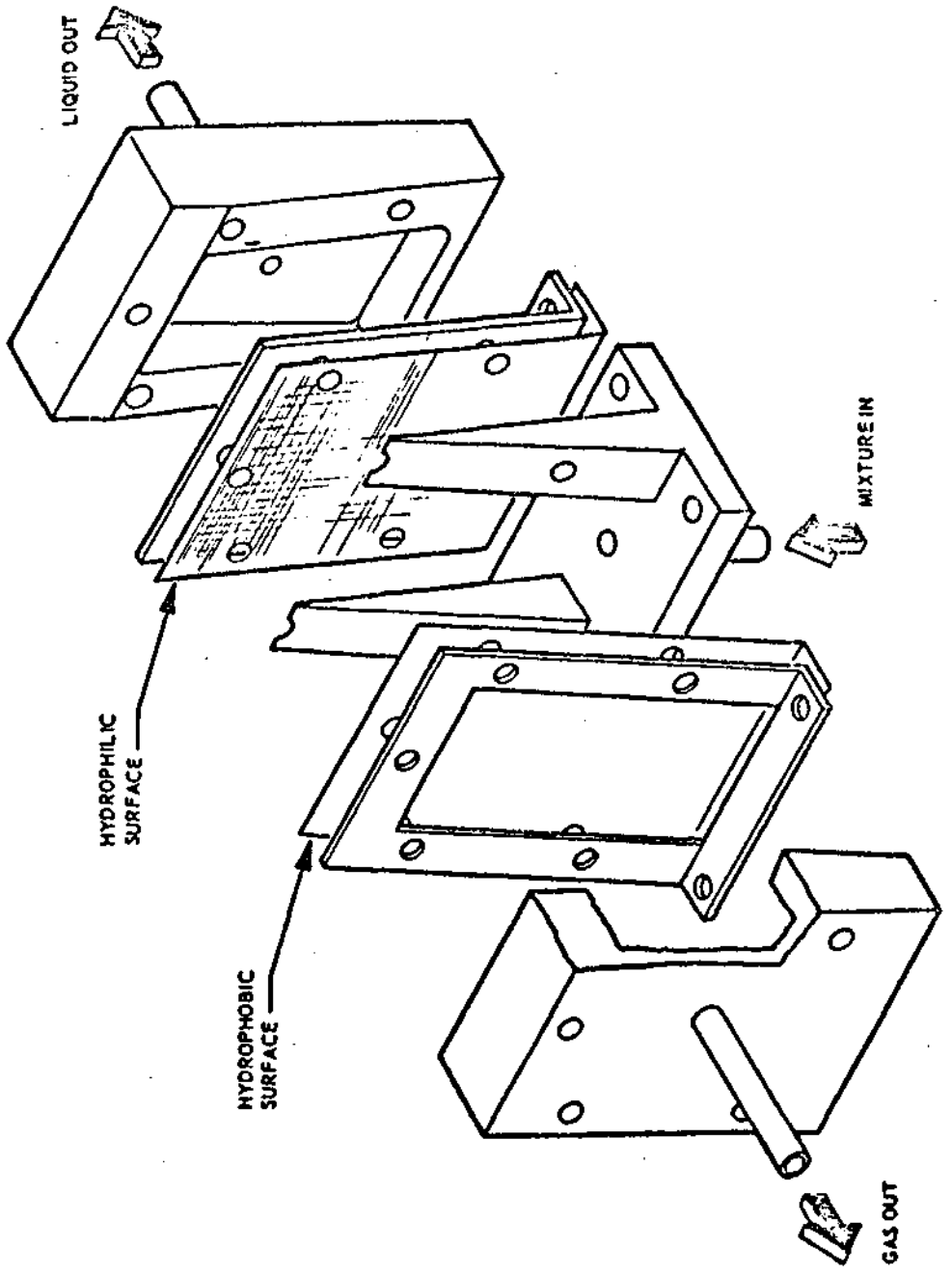

Fig. A-2 - Wedge Separator Configuration (from Ref. A.2)

is used throughout this discussion. The following discussion of the parameters critical to the hydrophobic/hydrophilic concept is repeated from Ref. A.2.

"The selection of materials for use in zero gravity bubble separators depends upon their properties of bubble point or water initiation pressure. These properties are related to the tendency of a surface to be wettable or non-wettable. For the purpose of this study, the bubble point is that gas pressure which is required to force liquid from the wettable material resulting in a gas flow. The liquid initiation pressure is that liquid pressure which is required to initiate liquid flow through a non-wettable material.

The extent to which any material is hydrophobic or hydrophilic can be inferred from the contact angle. As shown in Fig. A-3(a), the contact angle is the angle a drop of liquid makes with a surface. As a general rule, for angles less than 90 degrees, the lower the contact angle, the higher the degree of hydrophilicity. For angles greater than 90 degrees, the higher the contact angle, the higher the level of hydrophobicity. Thus, a contact angle of zero degrees indicates complete wettability, and a contact angle of 180 degrees suggests the ultimate in water repulsion.

An indication of the principles underlying the performance of bubble separator materials can be drawn from simple capillary theory. If we consider a round hole, or capillary, in a piece of material (See Fig. A-3(b), the pressure differential is given by the capillary pressure rise equation attributed to Laplace:

$$\Delta P = \frac{2\sigma \cos\theta}{r}$$

where:

ΔP = Pressure to force liquid from pore, psi
σ = Surface Tension, lb/in.
θ = Contact angle, deg
r = Capillary radius, in.

Returning to our criteria of hydrophilic materials in terms of the contact angle, we find that for θ less than 90 degrees the capillary rise, or bubble point, increases as θ decreases. For hydrophobic materials the

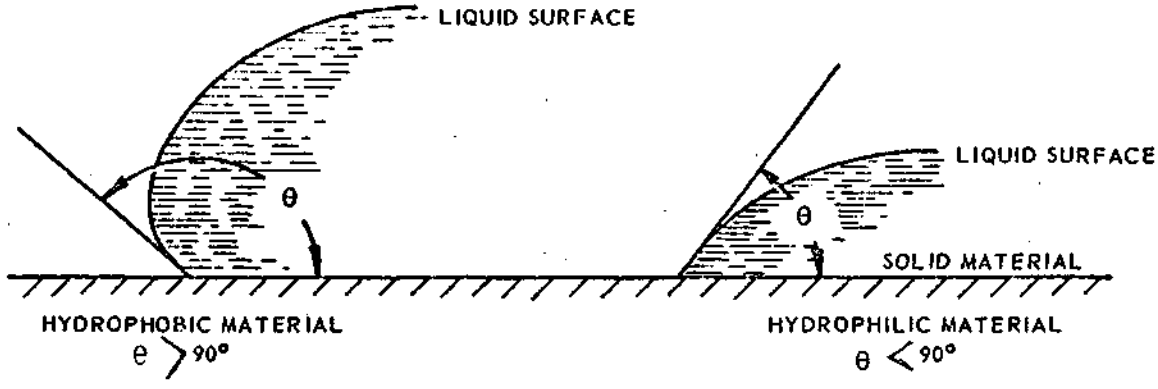

Fig. A-3(a) - Contact Angle (from Ref. A.2)

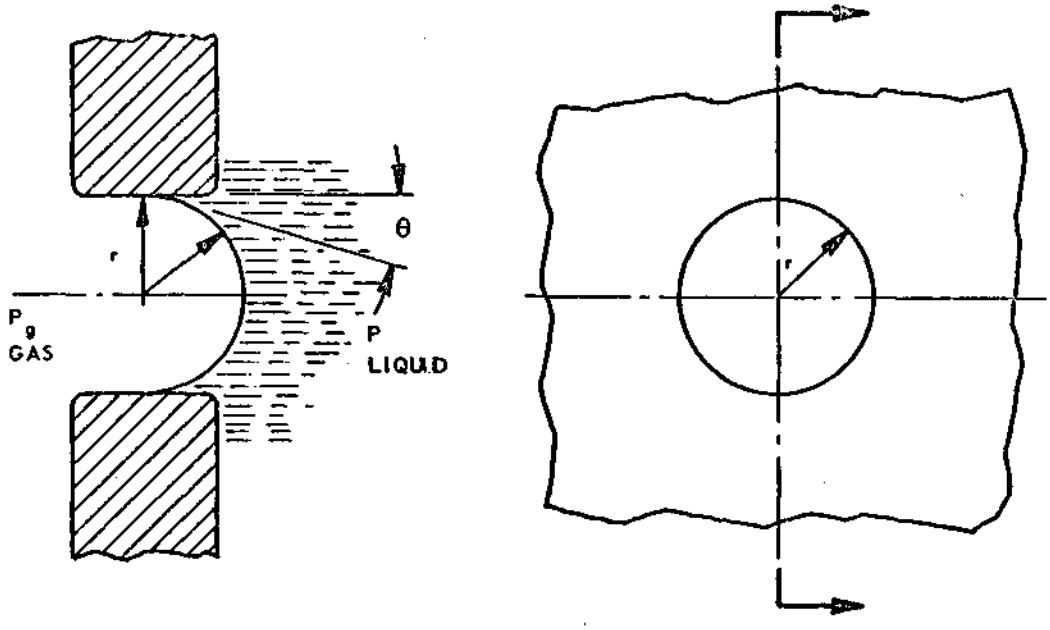

Fig. A-3(b) - Stability of a Liquid-Gas Interface (from Ref. A.2)

capillary depression, or water initiation pressure, increases with increasing 0. Further, in both cases, the ΔP increases with a decrease in pore size.

In the real world, the actual structures of separator materials are far from the round capillary hole model. However, the factors in the Laplace equation serve as a primary criterion for materials selection. The contact angle gives a direct indication of the extent of the hydrophilic or hydrophobic properties of the materials. The maximum pore size gives an indication of the bubble point or water initiation pressure which might be expected.

In the selection of materials, the surface finish also has an effect upon the properties. In general, surface roughness has the effect of enhancing the hydrophilic or the hydrophobic properties of a material."

The wedge separator shown in Fig. A-2 demonstrated 100% separation efficiency in both 1g laboratory tests and 0g flight tests. Separation surfaces successfully used were stainless steel screen mesh (hydrophilic) and porous teflon sheet (hydrophobic). During the zero g flight tests (KC-135), the aircraft was cycled in a parabolic flight path from 2g + 0g and back to 1g over a period of 70 seconds. The zero gravity portion lasted approximately 25 seconds. The wedge separator demonstrated 100% separation efficiency during all phases. After these tests, a prototype configuration was built and evaluated through more extensive laboratory tests. During these tests there were occasions of water or bubble breakthrough. However, in all cases the separation efficiency was in excess of 90%.

The conclusions drawn as to using this type separator for the absorption cycle refrigeration system were:

1. For one g tests these separators have a favored orientation for successful operation.
2. There were occasions of liquid and vapor breakthrough that were not clearly explained.

3. It may be difficult to find a hydrophobic material for the E-181 liquid.

Thus, this concept is not a clear favorite for our application.

Wick Separator

This separator concept (Fig. A-4) was developed by Dynatech Corp. and is reported in Ref. A.3. The separation mechanism is the surface tension forces holding liquid in the wick material and allowing it to be sucked out the liquid port. The gas or vapor is allowed to pass through the wick thickness. This mechanism is depicted in Figs. A-5(a) and A-5(b).

Laboratory tests on this concept indicated essentially 100% separation efficiency over a 40 hour operation period. The primary problem with this technique is that the liquid must be carefully degassed prior to use in order to remove non-condensable gases. These gases form vapor bubbles which become trapped in the wicking material and eventually block the flow passage. The saturated solution of R-22 vapor in the E-181 liquid may present problems in this regard. Otherwise, degassing is an extra precaution which is not desirable. Thus, this concept was not a clear favorite, either.

Conical Hydrophilic Separator

This concept (Fig. A-6) was considered for the whole body shower separator in Ref. 1 but was discarded because of contamination problems with the hydrophilic screen. It was built and tested by the NASA-MSFC Astronautics Laboratory. This concept utilized both centrifugal force and surface tension as the separation mechanisms. The results of tests on this concept (Ref. A.4) indicated very good separation performance. However, some tests showed liquid droplets adhering to the inner conical surface and eventually entering the vapor outlet. No estimate of separation efficiency was given but this presents a questionable area for the absorption cycle system. It is believed that further

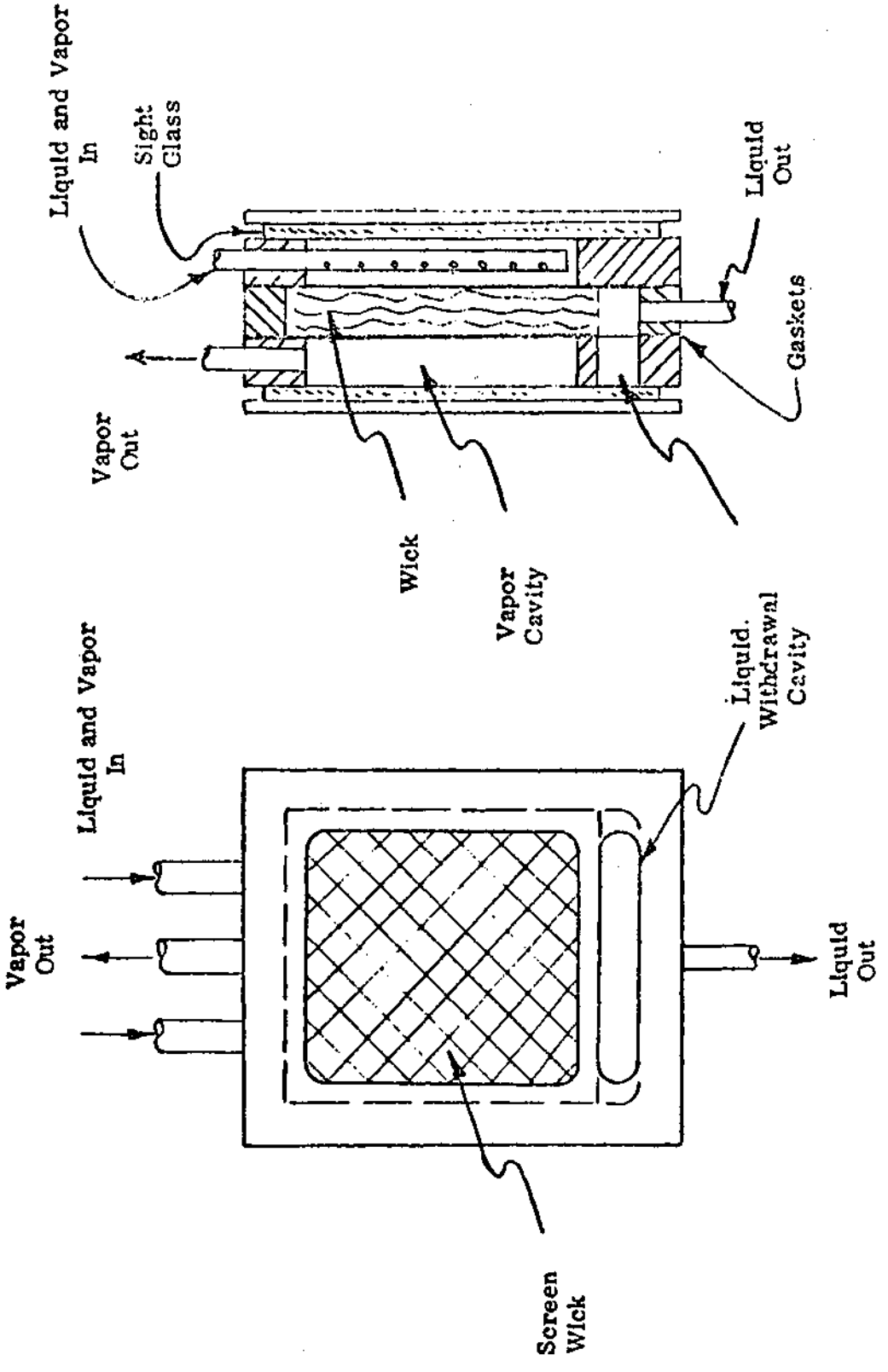

Fig. A-4 - Wick Separator Model Schematic (from Ref. A,3)

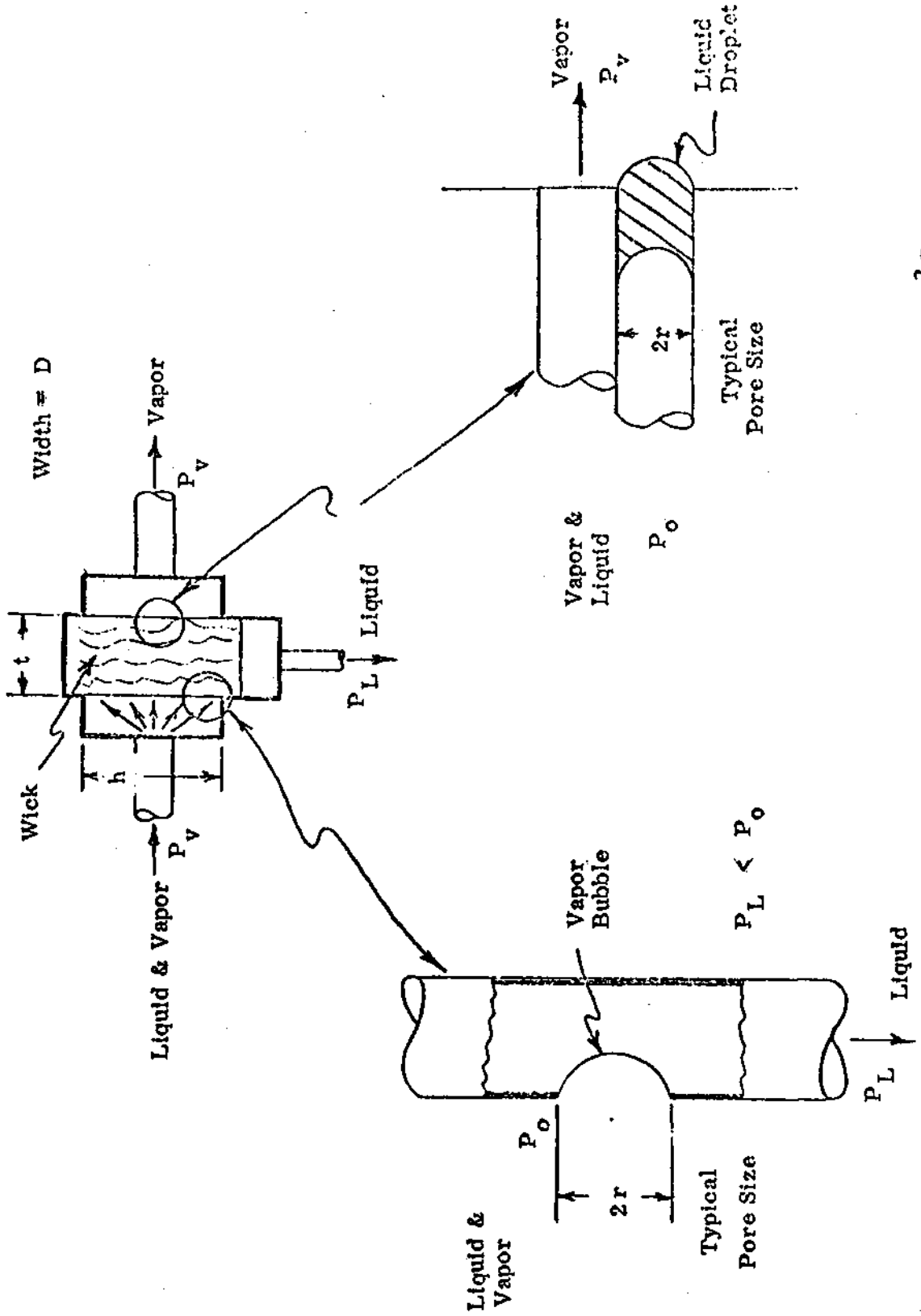

Fig. A-5 - Failure Modes for Wick Type Separator (from Ref. A.3)

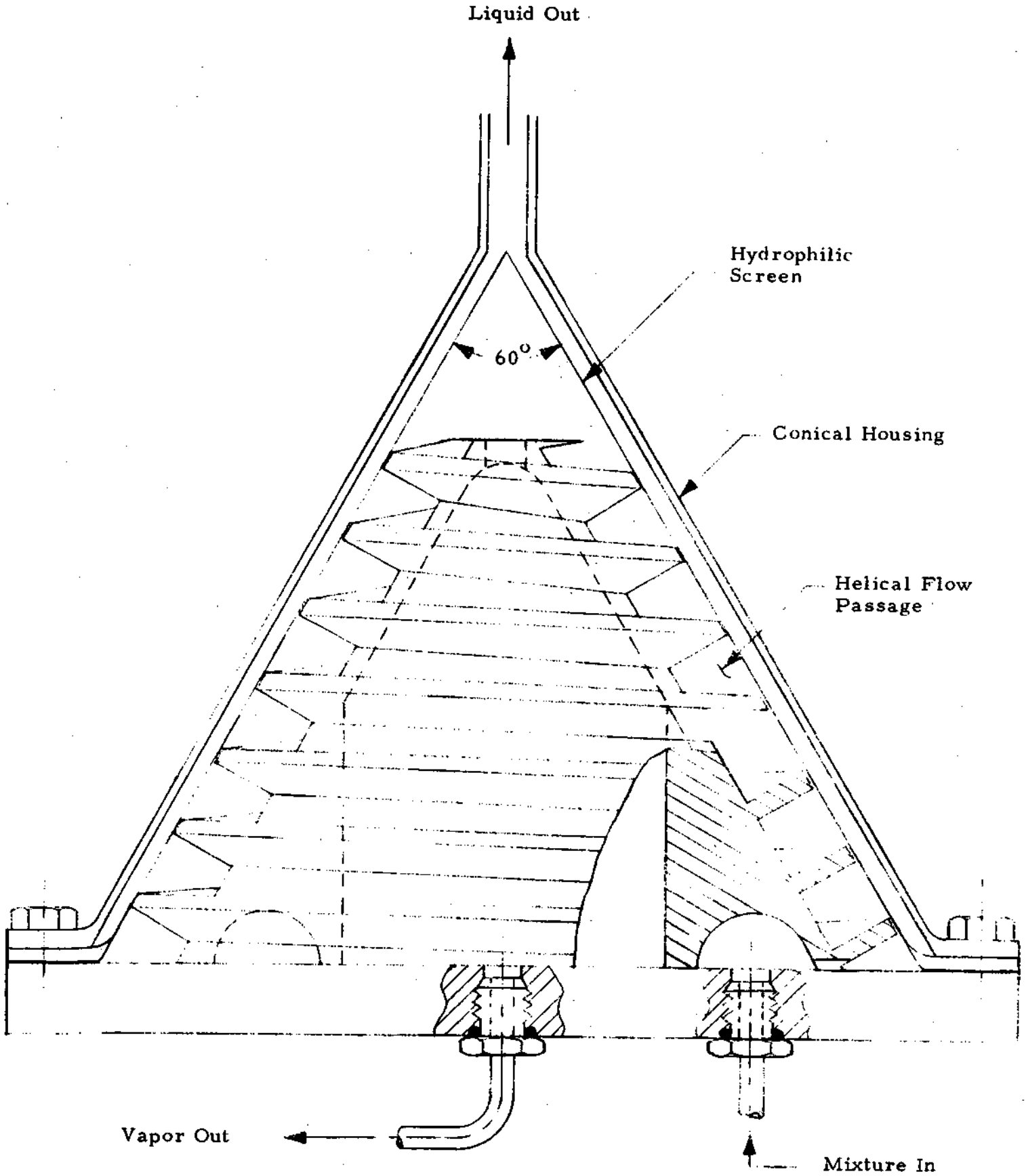

Fig. A-6 - Conical Hydrophilic Separator (data from Ref. A.4)

development could result in a successful product. However, the fabrication costs of this concept prompted investigation of other concepts which may be more suitable.

A.2 SEPARATOR CONCEPT SELECTION

After reviewing the concepts described in the previous section, it became obvious that no one concept clearly could meet the requirements of a simple, reliable separation system for the absorption cycle refrigeration system. It also became apparent that none of these concepts utilized all the separation mechanisms available and that further separation efficiency and reliability could be achieved in this manner. This resulted in the development of the concept shown in Fig. A-7.

This concept utilizes the basic principles of the vortex separator described in Ref. A.1 and the hydrophobic/hydrophilic separators described in Ref. A.2. Both principles work together to minimize the requirements of each other. For instance, separation from the vortex liquid motion minimizes the probability of vapor breakthrough in the hydrophilic screen, and liquid breqkthrough in the hydrophobic screen. Similarly, the hydrophilic screen tends to control the liquid outflow (as in the conical hydrophilic concept), and the hydrophobic screen prevents reentrainment of liquid through the vapor outlet. Both screens would be supported by a cage for structural stability. Other screen and liquid outlet configurations than the conical were considered. Hemispherical and cylindrical shapes offer higher screen area/unit length advantages but appear more costly for both screens and housings. The conical configuration is recommended for detailed analysis and design. The design should keep in consideration the flexibility to test various screen sizes (porosity, etc.) and other performance parameters which may appear critical during the design analysis.

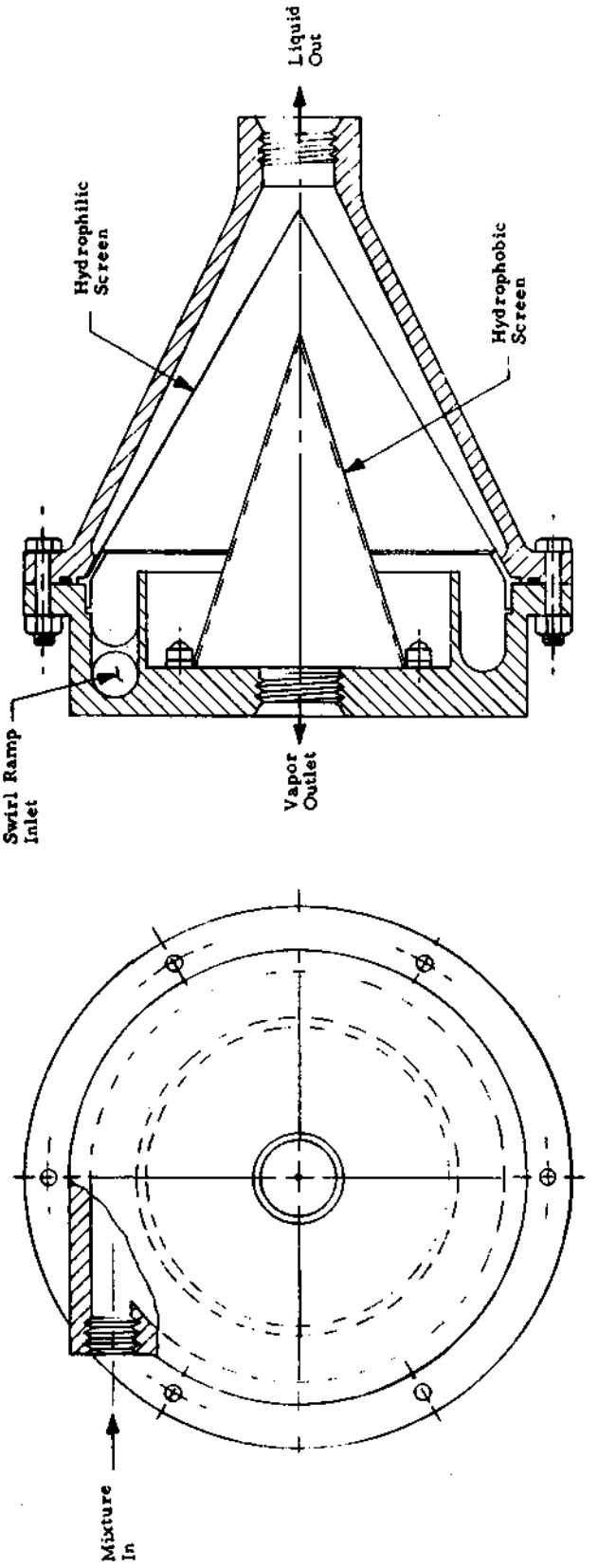

Fig. A-7 - Selected Separator Concept for Absorption Cycle Refrigeration System

A.3 SEPARATOR SCREENS ANALYSIS

After the separator concept was selected, the hydrophilic and hydrophobic screens were analyzed. The objective of the analysis was to determine the types of screen materials to be used in the separator.

The requirements of the screen materials can be summarized, with the aid of Fig. A-8, as listed below:

- $(P_1 - P_2)$ must be large enough to maintain the design liquid flow rate, $\dot{m}_L$.
- $(P_1 - P_3)$ must be large enough to maintain the required vapor flow rate, $\dot{m}_V$.
- $(P_1 - P_2)$ must be low enough to prevent vapor breakthrough at the hydrophilic screen.
- $(P_1 - P_3)$ must be low enough to prevent liquid breakthrough at the hydrophobic screen.

In Ref. A.2, an extensive survey of both types of screen materials was conducted, and data were presented regarding breakthrough ΔP's and flow rate/ΔP dependencies. Unfortunately, the data were restricted to air as the vapor and water as the liquid. Lack of data for the R-22/DME-TEG fluids forced the assumption that the air/water screen properties would closely approximate the R-22/DME-TEG screen properties. Therefore, the data given in Ref. A.2 were used in the screens analysis. Before presenting these data, the following symbols must be defined:

$\Delta P_L = P_1 - P_2$ (ΔP across hydrophilic screen)

$\Delta P_V = P_1 - P_3$ (ΔP across hydrophobic screen)

LBP = ΔP_V which allows liquid breakthrough at hydrophobic screen

VBP = ΔP_L which allows vapor breakthrough at hydrophilic screen

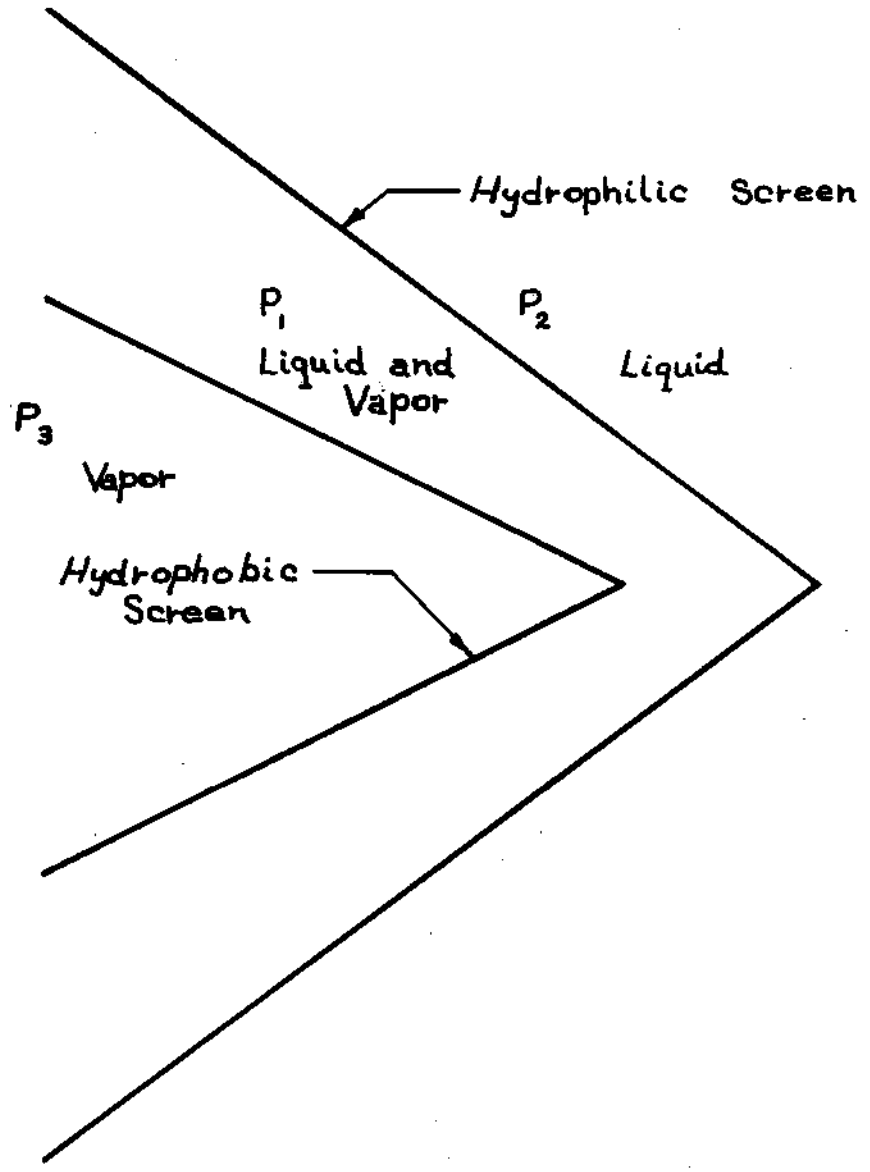

Figure A8 - Pressure Regions within Separator

Since volumetric flow rate per unit area for both hydrophilic and hydrophobic screens varies almost linearly with ΔP across the screen, the following screen constants can be defined:

$$C_V = \left(\frac{\dot{m}_V}{\rho_V}\right) \Big/ (A_V \Delta P_V) = \text{hydrophobic screen constant}$$

$$C_L = \left(\frac{\dot{m}_L}{\rho_L}\right) \Big/ (A_L \Delta P_L) = \text{hydrophilic screen constant} .$$

where

$\dot{m}_V$ = vapor mass flow rate
ρ_V = vapor density
A_V = hydrophobic screen area
$\dot{m}_L$ = liquid mass flow rate
ρ_L = liquid density
A_L = hydrophilic screen area.

The data in Ref. A.2 provide C_V and LBP for numerous hydrophobic materials, and these data are presented in Table A-1. The data in Ref. A.2 also provide C_L and VBP for numerous hydrophilic materials, and these data are presented in Table A-2.

With the nomenclature previously defined, the four governing relations for the screens can now be concisely written as:

- $\Delta P_V < \text{LBP}$
- $\Delta P_L < \text{VBP}$
- $\Delta P_V = \left(\frac{\dot{m}_V}{\rho_V}\right) \Big/ (A_V C_V)$
- $\Delta P_L = \left(\frac{\dot{m}_V}{\rho_L}\right) \Big/ (A_L C_L)$.

Table A-1
HYDROPHOBIC MATERIALS

No.	Type		C_V $\left(\frac{cc/cm^2\ min}{mm\ Hg}\right)$	LBP (mm Hg)
1	Zitex	K233-222	7.28*	25*
2	↓	H662-123	6.67	68
3	↓	H662-124	6.67	79
4	↓	E610-122	3.48	116
5	↓	E610-122+H662-123	2.00	267
6	↓	E610-122 (2 ply)	1.67	343
7	↓	E610-122 (3 ply)	0.89	432
8	↓	E610-122 (6 ply)	0.68	368
9	↓	E610-122 (12 ply)	0.75	279
10	↓	E610-122C	0.78	419
11	↓	E610-122C+E610-122 (6 ply)	0.18	483
12	↓	E610-122C 92 ply) + E610-122 (3 ply) + H662-123 (2 ply)	0.15	760
13	↓	12-104	0.21	760
14	Paulflex	TV20A40	5.00	62
15	↓	TV20A60	5.00	102
16	↓	TS. 1GC-32	0.30	419
17	↓	TX40H80	0.54	432
18	Saunders	S-20 Teflon Tape	0.22	1500
19	↓	S-22 Teflon Tape	0.13	1500

*Values were measured for air and water (Ref. A.2) and are assumed valid for R-22 and DME-TEG.

Table A-2

HYDROPHILIC MATERIALS

No.	Type	C_L $\left(\frac{cc/cm^2/min}{mm\ Hg}\right)$	VBP (mm Hg)
1	325 x 2300 SS Filler Cloth	8.10*	90*
2	250 x 1370 SS Filler Cloth	10.00	70
3	200 x 1400 SS Filler Cloth	16.00	51
4	Regimesh K	12.50	49
5	15 mil Synpore PVC	0.22	224
6	10 mil Synpore PVC	0.094	287
7	Manville Asbestos	0.003	762
8	Acco-1 Asbestos	0.045	254
9	Ultipore .1 Asbestos	0.020	533
10	Nylon Cloth - 10 micron	8.48	35
11	450 x 2750 SS Filler Cloth	7.80	101

*Values were measured for air and water (Ref. A.2) and are assumed valid for R-22 and DME-TEG.

For the test system operating at design conditions, the following flow rates are fixed:

$$\frac{\dot{m}_V}{\rho_V} = 4610 \text{ cc/min}$$

$$\frac{\dot{m}_L}{\rho_L} = 4175 \text{ cc/min.}$$

With the volumetric flow rates fixed, the ΔP_V is a function only of A_V for a given hydrophobic screen material and the ΔP_L is a function only of A_L for a given hydrophilic screen material. Therefore, curves of ΔP_V versus A_V can be plotted for each hydrophilic screen material. This has been done in Fig. A-9 and Fig. A-10. The curves each end at a maximum ΔP equal to LBP for the hydrophobic materials and VBP for the hydrophilic materials to satisfy the inequality requirements. Any point on any curve therefore represents a workable screen system, because none of the governing relations is violated by the plotted curves. From the figures it is apparent that a wide choice of workable screen materials is available which require small pressure drops across small screens to meet the separation requirements of the test assembly. The curves presented in Fig. A-9 and Fig. A-10 were used in sizing the separator, as discussed in the following section.

A.4 SEPARATOR SIZING

A.4.1 Screen Sizing

The screens were sized to prevent large pressure drops across the screens and to fit within a reasonably small separator housing. The conical hydrophilic screen was sized to be about 200 cm^2 in area and the conical hydrophobic screen was sized to be about 90 cm^2 in area. Five different screens of each type were selected for fabrication. Table A-3 shows the pressure drops predicted for each material.

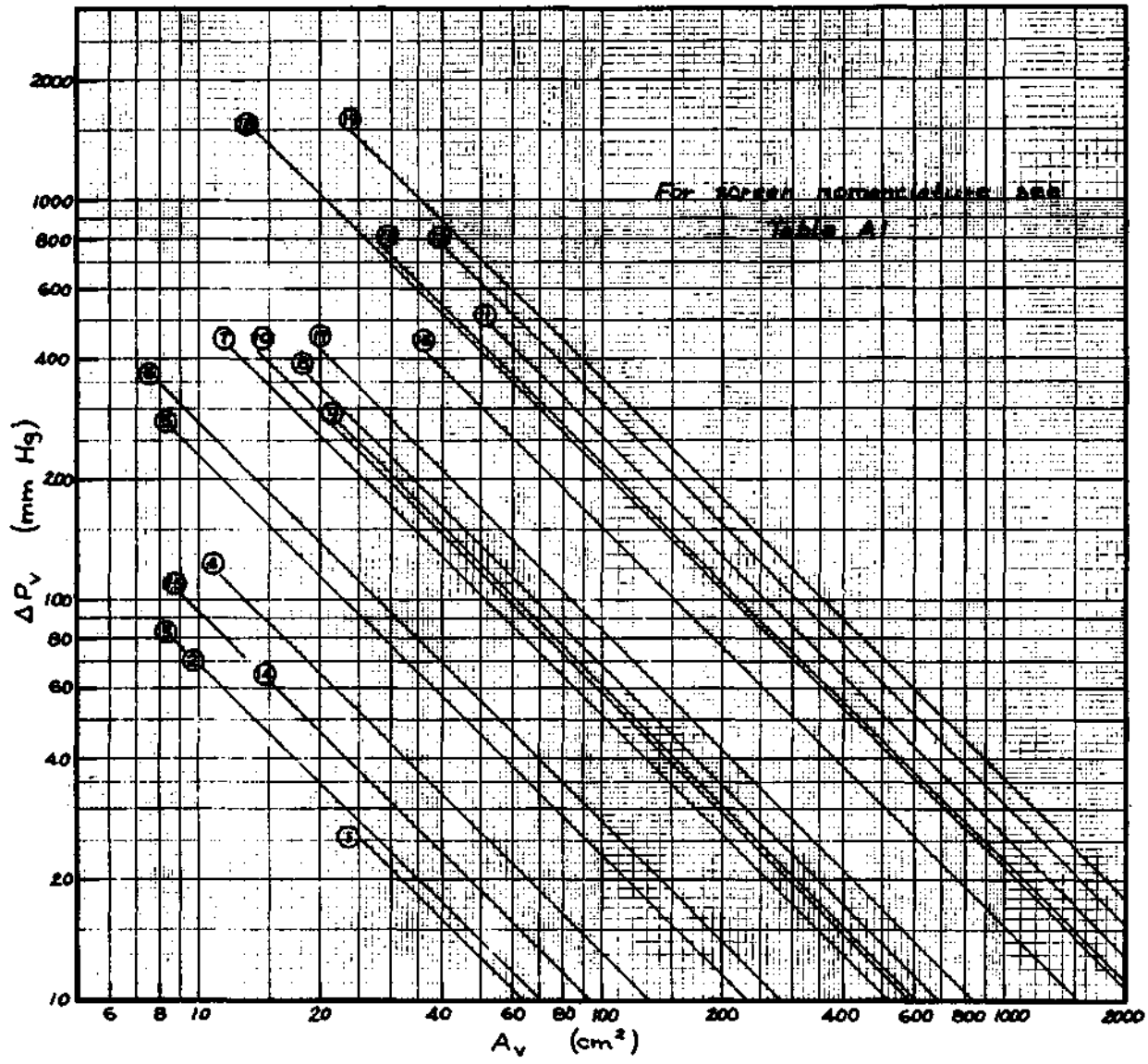

Fig. A9 - Pressure Drop-Area Relations for Hydrophobic Materials

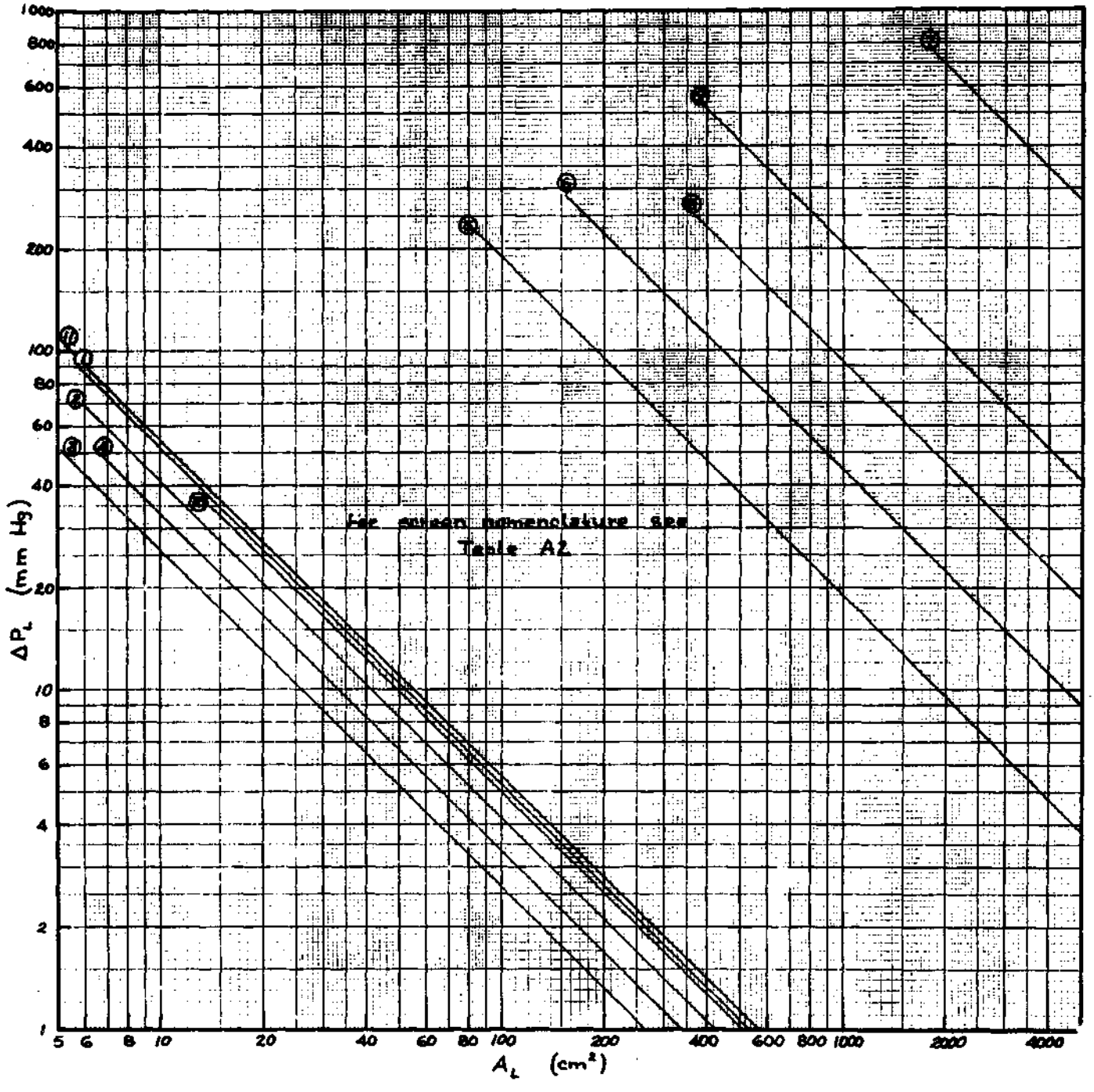

Fig. A10 - Pressure Drop-Area Relations for Hydrophilic Materials

TABLE A-3

Screen Pressure Drop Data

Hydrophobic Screen No.	Material	ΔP_v mm Hg
2	Zitex H622 - 123	7.0
4	Zitex E610 - 122	13.6
6	Zitex E610 - 122 (2 Ply)	28.8
10	Zitex E610 - 122C	59.6
14	Paulflex TV20A40	9.6

Hydrophilic Screen No.	Material	ΔP_L mm Hg
1	325 x 2300 SS Filler Cloth	2.45
2	250 x 1370 SS Filler Cloth	1.93
3	200 x 1400 SS Filler Cloth	1.22
4	Regimesh K	1.54
11	450 x 2750 SS Filler Cloth	2.57

A.4.2 Inlet Pipe Sizing

The inlet pipe was sized to provide a large inlet liquid velocity so that centrifugal acceleration would overshadow gravitational acceleration. A minimum ratio of centrifugal to gravitational accelerations of 5.0 was considered adequate. Therefore, the following relation must hold:

$$(V_L^2/R)_{inlet} = 5g .$$

Since the relative cross-sectional areas filled by the liquid and vapor are not easily calculable, a conservative assumption is to consider the liquid as filling the entire cross-section. Then, for the design flow rate in the test assembly, the inlet diameter must be 0.295 in. for a 5g centrifugal acceleration. This value was rounded down to 0.25 in. for convenience.

A.4.3 Exit Pipe Sizing

To minimize flow constrictions and associated pressure losses, both the vapor exit and the liquid exit pipes were sized at 0.50 in. diameter.

A.4.4 Inlet Ramp Sizing

To stabilize the liquid flow and to provide a longitudinal velocity component in addition to the tangential velocity, a 360 deg spiral ramp was included in the design with a 75 deg inclination to the centerline.

The complete design of the separator is given in Fig. 2-1 in Section 2 of this document.

A.5 REFERENCES FOR APPENDIX A

A.1. Rosener, A.A., and others, "Development of a Zero Gravity Whole Body Shower," Interim Report MCR-71-97, March 1971, NASA Contract NAS1-9819, Martin-Marietta Corporation, Denver Division, Denver, Colorado.

A.2. Lamparter, Richard A., "Development of Zero Gravity Hydrophilic/Hydrophobic Bubble Separators," NASA CR-66922, 18 May 1970, NASA Contract NAS1-08228, Biotechnology Organization, Lockheed Missiles & Space Company, Sunnyvale, Calif.

A.3. Blutt, J. R., and S. E. Sadek, "A Gravity Independent Vapor Absorption Refrigerator," NASA CR-836, July 1967, NASA Contract NASW-1372, Dynatech Corporation, Cambridge, Mass.

A.4. Clark, Dave, Bob Middleton and Joe Morris, NASA-MSFC Astronautics Laboratory, Informal Discussions on Conical Hydrophilic Separator.

Appendix B

B.1 MATHEMATICAL MODEL OF GENERATOR

An accurate mathematical model of the generator must necessarily be complex in order to treat the two-component, two-phase flow in conjunction with simultaneous heat transfer, mass transfer, momentum transfer and phase change. This inherent complexity dictated a numerical approach to the generator analysis. The basic model is shown schematically in Fig. B-1. The generator was assumed to be a cylindrical tube with a constant wall temperature. The thermal energy required to maintain this constant wall temperature was assumed available as waste heat from an unspecified source. Initial calculations revealed that the flow regime would be homogeneous, bubbly flow for optimum heat and mass transfer. Therefore, a one-dimensional treatment of the flow field was justified. The entire flow field was considered to be in a steady-state, steady-flow condition.

The inner volume of the generator tube was divided into numerous, small control volumes, or nodes. The inlet conditions were taken to be the design conditions for the space station optimized cycle with an exit generator temperature of 350°F (as discussed in Section 5). A computer program was written to determine the exit conditions for each small control volume from the inlet conditions and governing equations. To illustrate the calculation procedure, the following example is given.

The conditions at location 1 (Fig. B-1) are known and it is desired to determine the conditions at location 2. The governing equations are:

B.1.1 Momentum Equation

$$P_2 = P_1 - \frac{2L\tau_w}{R} - \left(\frac{\dot{m}_T}{\pi R^2}\right)^2 \left[\frac{\bar{\rho}_1 - \bar{\rho}_2}{\rho_1 \rho_2}\right]$$

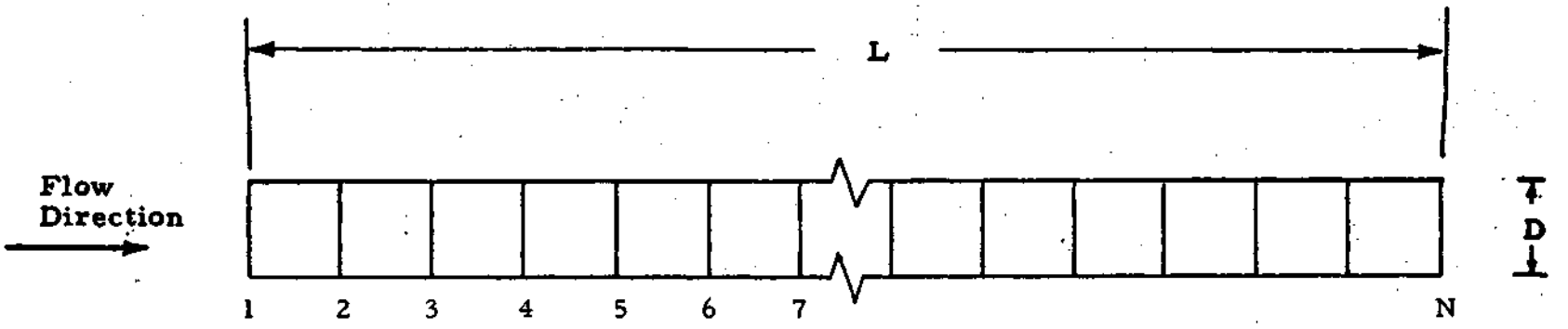

Given Inlet Conditions:	To Determine:
1. Pressure, P_1	1. $P(x)$
2. Temperature, T_1	2. $T(x)$
3. Liquid mass flow rate, $\dot{m}_{L_1}$	3. $\dot{m}_L(x)$
4. Vapor mass flow rate, $\dot{m}_{V_1}$	4. $\dot{m}_V(x)$
5. Refrigerant mole fraction of liquid, X_1	5. $X(x)$

Fig. B1 - Mathematical Model of Generator

where $\tau_w = \frac{1}{2} \bar{\rho} \bar{V}^2 \bar{f}$

where $\frac{1}{\sqrt{4\bar{f}}} = -0.8 + 0.87 \ln \left(\overline{Re}_D \sqrt{4\bar{f}} \right)$.

(The third relation above is the Karman-Nikuradse equation for turbulent flow friction factors.)

B.1.2 Energy Equation

$$\dot{m}_{L_1} h_{L_1} + \dot{m}_{V_1} h_{V_1} + \frac{\dot{m}_T^3}{2(\bar{\rho}_1 \pi R^2)} + Q$$

$$= \dot{m}_{L_2} h_{L_2} + \dot{m}_{V_2} h_{V_2} + \frac{\dot{m}_T^3}{2(\bar{\rho}_2 \pi R^2)}$$

where $Q = 2\pi R L \bar{h} \left[T_W - \frac{1}{2} (T_1 + T_2) \right]$

where $\bar{h} = \dfrac{\bar{\rho} \bar{V} \bar{c}_p \sqrt{\bar{f}/2}}{0.9 \left[5 \overline{Pr} + 5 \ln (5 \overline{Pr} + 1) + 2.5 \ln \left(\dfrac{\overline{Re}_D \sqrt{\bar{f}/2}}{60} \right) \right]}$.

(The third relation above is from the Karman-Boelter-Martinelli analogy for turbulent flow with $Re_D \approx 10^6$.)

B.1.3 Continuity Equations

- Total Continuity Equation:

$$\dot{m}_{L_1} + \dot{m}_{V_1} = \dot{m}_{L_2} + \dot{m}_{V_2}$$

- Absorbent Continuity Equation:

$$\frac{\dot{m}_{L_1} X_{A_1} M_A}{X_{R_1} M_R + X_{A_1} M_A} = \frac{\dot{m}_{L_2} X_{A_2} M_A}{X_{R_2} M_R + X_{A_2} M_A} .$$

B.1.4 Equations of State

Accurate curve fits of the following nature were used:

$$X_{R_{eq}} = \text{function } (P, T)$$

$$\tilde{\rho} = \text{function } (P, T, X_R, \dot{m}_v/\dot{m}_T)$$

$$h_L = \text{function } (P, T, X_R)$$

$$h_v = \text{function } (P, T) .$$

B.1.5 Mass Transfer Efficiency Relation

$$\eta = \frac{X_{R_2} - X_{R_1}}{X_{R_{2_{eq}}} - X_{R_1}} \quad .$$

B.1.6 Transport Property Relations

$$\bar{c}_p = \text{function}\left(P, T, X_R, \dot{m}_v/\dot{m}_T\right)$$

$$\bar{\mu} = \text{function}\left(P, T, X_R, \dot{m}_v/\dot{m}_T\right)$$

$$\bar{k} = \text{function}\left(P, T, X_R, \dot{m}_v/\dot{m}_T\right)$$

$$\bar{P}_r = \frac{\bar{\mu}\bar{c}_p}{\bar{k}}$$

$$\overline{Re}_D = \frac{\bar{\rho}\bar{V}D}{\bar{\mu}}$$

where $$\bar{V} = \frac{\dot{m}_T}{\bar{\rho}\left(\pi D^2/4\right)} \quad .$$

The computer program solves all of the above equations through an iterative calculation process to yield P_2, T_2, X_{R_2}, $\dot{m}_{L_2}$, $\dot{m}_{V_2}$, etc., for a given input set of the following parameters:

- D,
- $\dot{m}_T$ ($\dot{m}_T = \dfrac{278\ lb_m/min}{number\ of\ tubes}$),
- η
- T_W.

Now that the conditions at location 2 are known, these conditions can be taken as inlet conditions for the next small control volume and conditions at location 3 can be determined. This is precisely the manner in which the computer program proceeds. Thus, by moving down the generator tube one small control volume at a time, the program yields the complete distribution of P, T, X_r, etc., as functions of location.

B.2 PARAMETRIC GENERATOR ANALYSIS

The computer program described in the previous section was used to analyze the generator parametrically. The primary parameter of interest was the generator weight, which is a function of number of tubes, η, T_W, D, and L_t. The weight calculation for each parametric case was based upon using stainless steel as the generator tube material; tube wall thickness was sized to withstand the pressure forces with a safety factor of 2.0, and the weight was calculated as

$$\text{Weight} = (\text{No. of tubes})\,\rho_{ss}\,\pi D L_T t .$$

The number of independent variables can be significantly reduced by considering the following points:

- The generator weight was found to be virtually independent of η when $\eta > 0.20$. Since the experimental studies

indicated that η would be larger than 0.20, this variable was eliminated from further consideration by assuming $\eta = 0.80$.

- A reasonable value for T_w was selected arbitrarily, namely $T_w = 380^\circ F$.
- A value of 1.6×10^6 for the $Re_{d_{exit}}$ was found to be large enough for good heat transfer and small enough to prevent excessive pressure drop through the generator. Therefore, this value was selected as optimum and, for any given number of tubes, the diameter required to maintain this proper Reynold's number was fixed. Thus, diameter (D) was eliminated as an independent variable.
- For a given number of tubes, η, T_w, and D, there is a certain length required to attain the proper generator exit concentration level, $X_{R_{gen}}$. Making the tubes longer will result in an improper concentration at the generator exit. Thus, L_T is the value which corresponds to the proper $X_{R_{gen}}$ and can therefore be eliminated as an independent variable.

After the previous points are considered, only one independent variable of interest remains, the number of tubes (N). Figure B-2 presents generator length, diameter, and weight as functions of number of tubes for the space station optimized cycle conditions for $T_G = 350^\circ F$. Although the total generator weight decreases with increasing number of tubes, the simplicity of a single-tube generator overshadows the weight savings because the single tube generator weighs only 17.2 lb_m itself. Therefore, the single-tube generator was selected as the best prototype design for the space station environmental control system. The pertinent facts for this design are summarized below:

- D = 2.0 in.
- L_T = 17.4 ft
- Weight = 17.2 lb_m.

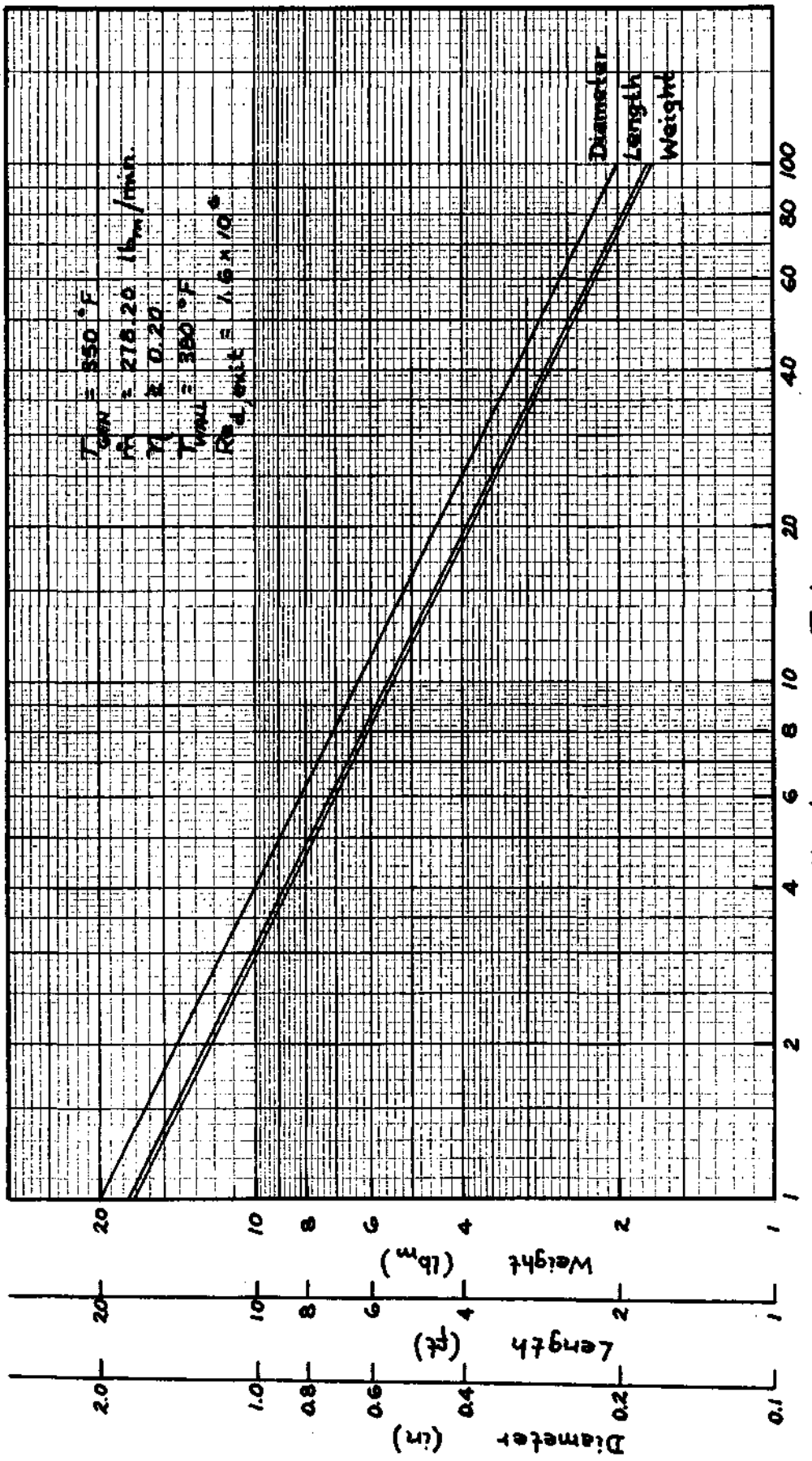

Figure B2 - Results of Parametric Generator Analysis

The temperature, pressure, and concentration distribution for this chosen generator design are presented in Fig. B-3. The figure shows that the exit temperature and concentration are at their design values, while the pressure drop through the generator is only 0.3 psia. Therefore, this design represents a simple, light-weight, efficient generator for use in the space station environmental control system.

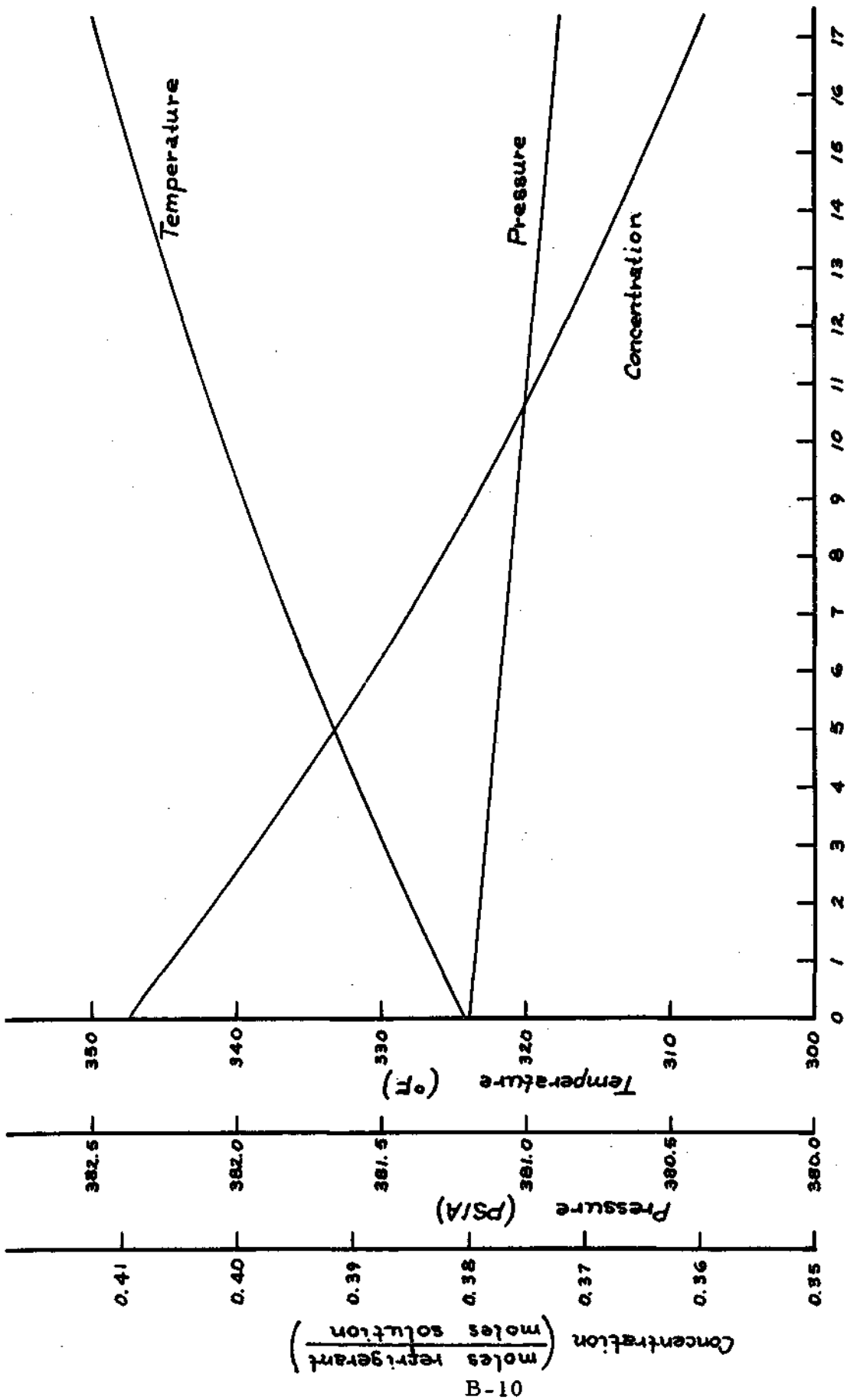

Figure B3 - Temperature, Pressure and Concentration Distribution Within Generator

Appendix C

C.1 MATHEMATICAL MODEL OF ABSORBER

The absorber performs essentially the same process as the generator in the opposite direction. Therefore, the mathematical model of the absorber is the same as the mathematical model of the generator (described in Appendix B) with different inlet conditions and wall temperature. The absorber heat rate must be dumped to space by a radiator; therefore, multiple small cylindrical tubes were assumed to make up the absorber, with the tubes integrally bonded to the space radiator. The flow regime inside the tubes was again homogeneous, bubbly flow, and steady-state, steady-flow conditions were assumed for the analysis.

The inner volume of each tube was again divided into small control volumes and the governing equations remained the same as those for the generator. The most important dependent variable was the total absorber weight, which is a function of N, η, T_w, D, and L_t. The same computer program used in the generator analysis was used in the absorber analysis to determine the solution to the flow field and to calculate the absorber weight for different input design parameters.

C.2 PARAMETRIC ABSORBER ANALYSIS

The number of independent variables affecting absorber weight can be significantly reduced by considering the following points:

- As for the generator, the absorber weight was found to be virtually independent of η when $\eta > 0.20$. Therefore, since the experimental studies indicated that η would be greater than 0.20, this variable was eliminated from further consideration by setting $\eta = 0.80$.

- Since a large ΔT from absorber fluid to tube wall would result in an excessive absorber radiator area, the tube wall temperature was set at $1^{\circ}F$ below the design absorber exit fluid temperature. Thus, $T_w = 158^{\circ}$ was the only wall temperature considered.

- Since a contraction from large plumbing to the small absorber tubes would require a pressure drop, the diameter (D) of such tubes has a lower limit for any value of $\Delta P_{contraction}$. Since the principal portion of $(P_{H1} - P_{L0})$ must be used to produce power in the hydraulic motor, $\Delta P_{contraction}$ must be kept small. Arbitrarily, $\Delta P_{contraction}$ was set equal to $\frac{1}{64}$ $(P_{H1} - P_{L0})$. Therefore, for any given number of tubes, the diameter (D) of each tube was fixed at the value which would yield the proper $\Delta P_{contraction}$. This eliminated D as an independent variable.

- For a given N, η, T_w, and D, there is a certain length at which complete absorption is attained. Making the tubes longer than this length increases weight without appreciably changing exit conditions. Thus, L_T was set at the value which corresponded to complete absorption, and this variable was eliminated as an independent parameter.

After considering the previous points, there remains only one independent variable of interest, the number of tubes (N). Figure C-1 presents absorber length, diameter, and weight as functions of N for the space station optimized cycle conditions for $T_G = 350^{\circ}F$. The figure shows that total absorber weight decreases with increasing N. For 100 tubes, the total weight is only 1.87 lb_m* for all the tubes. Decreasing the weight below this value is unnecessary; therefore, this value of N was chosen for the prototype design. The pertinent facts for this design are:

- N = 100 tubes
- L_T = 12.5 ft
- D = 0.264 in.
- Weight = 1.87 lb_m*.

* The reason this weight is so small for 1250 ft of tubing is that the required tube wall thickness to withstand the pressure forces (with a safety margin of 2.0) is less than 1 mil. The point to be understood is that the tubing weight will be negligible, even by comparison with the weight of the fluid within the tubes which itself will result in a radiator weight well below 0.1 lb_m/ft^2.

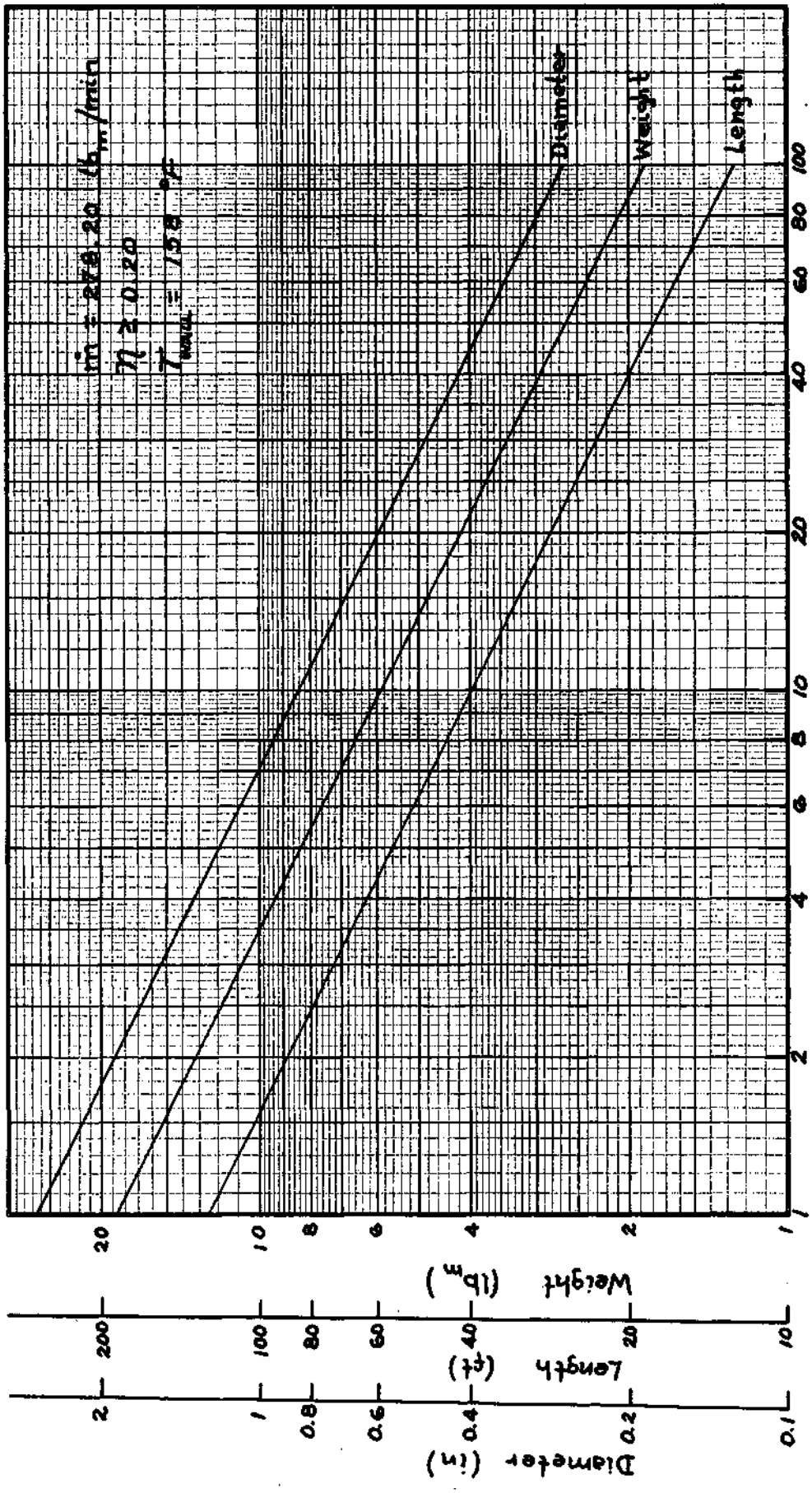

Figure C1 - Results of Parametric Absorber Analysis

The temperature, pressure, and concentration distribution for this chosen absorber design are presented in Fig. C-2. This figure shows that the exit temperature and concentration are at their design values, while the pressure drop through the absorber is only 0.3 psia. Therefore, this design represents a simple, light-weight, efficient absorber for use in the space station environmental control system.

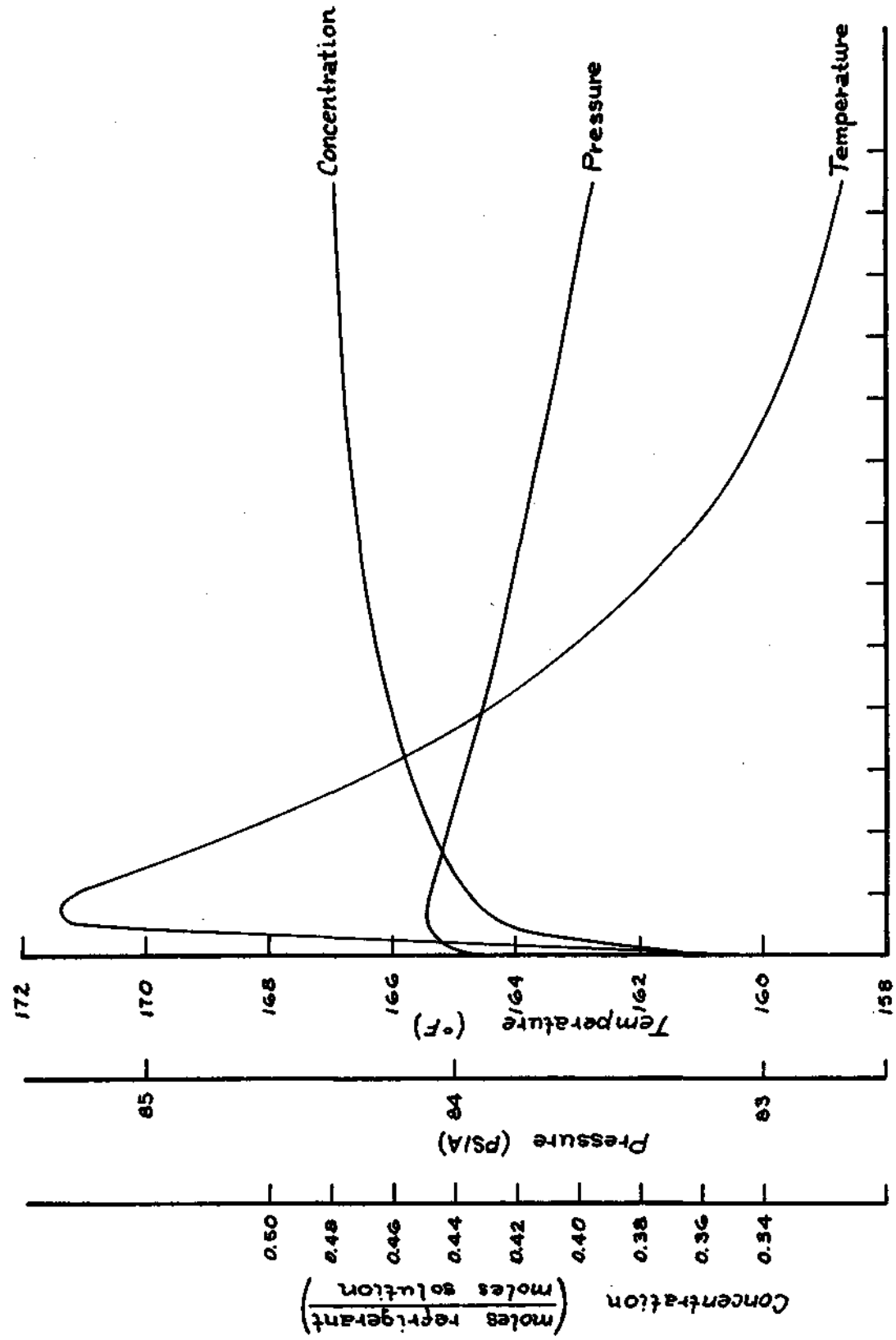

Figure C2 - Temperature, Pressure and Concentration Distribution Within Absorber

Appendix D

SYSTEMATIC INVESTIGATIONS TO SYNTHESIZE NEW REFRIGERANT-ABSORBENT FLUID COMBINATIONS

SYSTEMATIC INVESTIGATIONS TO SYNTHESIZE NEW REFRIGERANT-ABSORBENT FLUID COMBINATIONS

Final Report

June 25, 1972

Contract H60-37007

by

R.L. McNeely
T.M. Carney
L.D. Russell

University of Tennessee at Chattanooga

CONTENTS

Abstract

Systemmatic investigations have been undertaken to synthesize refrigerant-absorbent combinations which exhibit a high degree of refrigeration efficiency and that conform to high standards of safety. On the basis of heat of vaporization, hydrogen bonding capability, and safety, refrigerants have been narrowed to Freon-22, Freon-11, and water, with Freon-22 generally preferred for space application. On the basis of solubility, hydrogen bonding capability, and safety, potential absorbent solvents chosen for testing are polyethers, polyether-alcohols, aliphatic and aromatic polyethers, and fluorinated hydrocarbons. Solubility was measured to determine pressure-temperature-mole fraction data for all combinations. From those data and from calculated heats of mixing, computer evaluations of efficiency have been run to show minimum radiator areas and system weights necessary if the given refrigerant-absorbent combination is utilized.

Section 1 Introduction

The necessity of a heat rejection system in space vehicles is well established. The results of the Lockheed Missile and Space Company Report on a Parametric Study of Heat Rejection Concepts (LMSC-A742093, 12 April 1965) demonstrates advantages of absorption refrigeration over other alternatives such as the standard vapor compression refrigeration system of heat rejection for many applications. Absorption refrigeration is operated by thermal energy rather than by mechanical compression of a vapor. Instead of mechanically compressing a refrigerant gas into its liquid state, a second fluid is used to absorb or dissolve the refrigerant gas to form a solution.

The absorption cycle of absorption refrigeration has been evaluated (Lockheed Interim Report LMSC-HREC D162909), and based on fluid properties available in the literature the most acceptable fluid combination was tentatively determined to be: R-22 (DuPont Freon 22, monochlorodifluoromethane) as the refrigerant gas and DME-TEG (Ansul E-181, dimethylether of tetraethyleneglycol) as the absorbent liquid. However, literature data on pure components is unsatisfactory for predicting properties of non-ideal solutions. It was recommended, therefore, that systematic investigations be conducted to synthesize new refrigerant-absorbent combinations, to determine experimentally their properties, and to evaluate the usefullness of the combinations by computer analysis. The purpose of this paper is to report the results of such a study.

Section 2 Criteria for Selection of Fluids

In choosing potential refrigerant gases and absorbent liquids there are two overriding criteria for selection: efficiency and safety.

Efficiency must be judged not on any single set of properties but rather on an overall system analysis. The present computer program is set up to judge overall system efficiency by the mass of the system and by the area of the radiator necessary for the refrigeration system using the refrigerant-absorbent combination being evaluated. The principal parameters contributing to overall efficiency are:

1. A refrigerant with a high heat of vaporization at the evaporator temperature, a property needed to minimize the quantity of refrigerant circulated and to maximize the quantity of heat absorbed per unit mass of refrigerant.
2. An absorbent exhibiting a high degree of solubility for the refrigerant, a property which minimizes the quantity of absorbent circulated and permits the heat absorbing and heat emitting changes of state between gas and liquid for a larger proportion of refrigerant.
3. The refrigerant must have a sufficiently high vapor pressure and the absorbent a sufficiently low vapor pressure to allow effective separation of the components in the generator. However, too great a difference in vapor pressures decreases solubility. Too high a refrigerant vapor pressure would require use of excessively high pressures within the system.
4. Within the operational temperature ranges the absorbent must remain a liquid and the refrigerant must remain in a fluid state.
5. All fluids should have low viscosity.

6. Heat capacities of both components should be high.
7. A high rate of solution is desirable.

The principal parameters contributing to safety are:

1. Both components should be non-toxic.
2. Both components should be reasonably non-flammable and should exhibit no explosion hazard when contacted with oxygen.
3. Both components should be chemically stable, unreactive, and non-corrosive.

The approach taken to systematically investigate potential new refrigerant-absorbent mixtures has been as follows:

1. To select potential refrigerants on the basis of high heats of vaporaization.
2. To narrow the selection of potential refrigerants on the basis of safety considerations.
3. To select potential absorbent liquids on the basis of potential solubility for given refrigerants judged on potential intermolecular attraction, particularly hydrogen bonding potential.
4. To narrow the selection of potential absorbents on the basis of safety considerations.
5. To further narrow the selection of potential absorbents on the basis of other desirable properties such as low vapor pressure, high heat capacity, low freezing point, low viscosity, and particularly high chemical stability.
6. To experimentally determine for the selected potential combinations the properties which are not completely predictable such as solubility and heat of mixing.

7. To judge overall efficiency by computer analysis by comparison to the R-22 and DME-TEG (E-181) combination now being tested.

Section 3 Selection of Potential Refrigerants

From literature surveys of chemically stable, inert, non-toxic, non-corrosive, non-flammable gases, summaries of potential refrigerants have been made and the best ones are listed below in decreasing order of heats of vaporization.

R		H_{vap} at 40°F	
Water	H_2O	1070	(Btu/lb)
R-21	$CHCl_2F$	106	
Carbon Dioxide	CO_2	94	
R-22	$CHClF_2$	87	
R-11	CCl_3F	80	
R-113	$CCl_2F\text{-}CClF_2$	69	
R-12	CCl_2F_2	64	

Anticipating that high solubility of the refrigerant in any typical solvent will require strong hydrogen bonding characteristics, the superior refrigerant will have at least one electron deficient hydrogen atom in its molecular structure. Of the refrigerants considered only water, R-21, and R-22 are hydrogen donors having this capability for hydrogen bonding to typical solvents such as high molecular weight ethers. Earlier studies (Mastrangelo, J. Phys. Chem. 1959, 608) have demonstrated that comparing the solubility of R-21, R-22, R-11, and R-12 in DME-TEG that indeed only R-21 and R-22 show a strong negative deviation from Raoult's Law of Ideal Solutions indicating the increased solubility of these compounds due to their hydrogen bonding characteristics.

Water is by far the superior choice except that as both a potential hydrogen donor and potential hydrogen acceptor in hydrogen bonding it forms

bonds with itself lowering its vapor pressure and raising its freezing point. Water is soluble in typical solvents such as glycols or salt brines and could be ideal for heat rejection systems not requiring operation below 32°F and should be further investigated for selected uses. However for space vehicle refrigeration use water must be discounted for this one deficiency.

R-22 has been selected over R-21 for this present study because its vapor pressure is sufficiently higher than that of R-21 to allow desirable refrigerant-absorbent separations but this is not too high to require excessive pressures in the refrigeration system. In a direct comparison of R-22 and R-21 specifically with DME-TEG (E-181) a previous study has shown that the R-22 is superior, under many operating conditions. Therefore the list of potential refrigerants based on criteria of safety, high heat of vaporization, moderately high vapor pressures, freezing point, and capability for hydrogen bonding has narrowed to only two real possibilities: R-22 (Freon 22, monochlorodifluoromethane, $CHCIF_2$) or alternatively R-21 (dichloromonofluoromethame, $CHCI_2F$). This study then narrows to a selection of potential absorbents for R-22 or R-21 which would produce an overall superior system. R-22 has been selected for all laboratory measurements, but R-21 is expected to behave similarly chemically but with slightly reduced solubility.

Section 4 Potential Solvents

In systematically selecting potential solvents first consideration was given to solubility potential. In dealing with liquid-liquid mixtures greatest mutual solubility occurs when the components are very similar in chemical characteristics: polar compounds dissolve in polar compounds, alcohols dissolve in alcohols, etc. An extension of this idea is that Freons (fluorinated hydrocarbons) should be excellent solvents for other Freons. The principle is that the Van der Waal's forces of attraction between molecules A and B should be similar to those between A and A or between B and B if A and B are similar compounds. There are two Freons of sufficiently low vapor pressure and freezing point to be considered: Freon 11 and Freon 113.

However, when dealing with mixtures of gases and liquids in the absence of specific interactions between molecules other than Van der Waal's forces a maximum solubility is defined by Raoult's Law.

$$P_M = X_R P^\circ_R$$

where P_M = vapor pressure of the mixture

P°_R = vapor pressure of the pure refrigerant

X_R = mole fraction of refrigerant in the mixture (the solubility of the refrigerant gas)

Restated, the law states that the solubility (expressed as mole fraction) cannot exceed the value $\frac{P_M}{P^\circ_R}$ in the ideal (no specific interaction) case

$$X_R = \frac{P_M}{P^\circ_R}$$

Operational pressures in the system should be low keeping P_M low. The vapor pressure of the refrigerant P°_R must be relatively high for good separation. Therefore solubility X_R is too low for high efficiency refrigeration. For example, at an operational pressure of 1 atmosphere and working at 30°C

C-2

solubility of Freon-22 in a solvent forming an ideal solution would not exceed .09 mole fraction.

The specific interaction that must be designed into the system is hydrogen bonding. The solvent must have a high electron density site capable of being a hydrogen acceptor in hydrogen bonding. It must have the following chemical structure

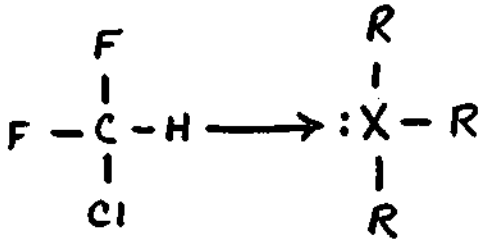

Where X is a highly electronegative atom containing at least one pair of unbonded electrons. Atoms generally capable of hydrogen bonding are oxygen and nitrogen. Potential nitrogen compounds are amines and amides.

Amines 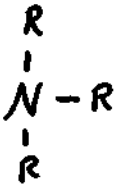

Amides 

The amines can generally be discounted due to low boiling points, high vapor pressures, and high degrees of reactivity. Amides are generally more stable and less reactive. Possible solvents could be:

N,N-dimethyl formamide $CH_3CON(CH_3)_2$
N,N-diethyl formamide
N,N-dimethyl acetamide
and other dialkylated amides

Although probably acceptable as solvents for Freon-22, the amides in general do not show the long range stability of ideal solvents, and the potential decomposition products, amines and acids, are quite reactive and corrosive.

Of the potential oxygen containing solvents by far the most unreactive and stable are the high molecular weight ethers and esters.

ether $R-\ddot{O}-R$

ester $R-\ddot{O}-C-R$

High molecular weight ethers being generally the more stable and less reactive of the two types. Many potential ether and ester solvents are available.

Those representing typical classes or groups of solvents are listed as follows:

A. Polyethers of type $R-O-CH_2CH_2-(O-CH_2CH_2)_n-O-R$

1. Dimethylether of tetraethyleneglycol (E-181)
2. Dibutylether of diethyleneglycol (Dibutyl Carbitol)
3. Dimethylether of triethyleneglycol (E-161)

B. Polyether-alcohols of type $R-O-CH_2CH_2-(O-CH_2CH_2)_n-O-H$

1. Monomethyl ether of tripropylene glycol (Dowanol TPM)

C. Ethers of the type R-O-R

1. Diphenyl ether

D. Aliphatic Esters of the type

1. Dioctyl Sebacate

E. Aromatic Esters of the type

1. Dioctyl phthalate

Section 5 Experimental Determination of Solubility

Solubility measurements were attempted initially by saturating a measured quantity of solvent with refrigerant gas at controlled temperatures and pressures and then extracting the gas at low pressures to finally calculate the mass of refrigerant dissolved from the volume extracted. This method was long and tedious and suitable only for low solubility cases. The method finally adopted for use consists of simply weighing the fluid before and after saturation with gas at controlled temperatures and pressures. The method was checked for accuracy by comparison of results with the method developed by Mastrangelo (J. Phys. Chem. 1959, 64) in which temperature and weights of solvent and gas were controlled and final equilibrium pressures were measured. Results were identical.

Resulting pressure-temperature-mole fraction data are presented in the following graphs of P versus X at given T for the solvents measured. The straight line represents the pressure if Raoult's Law were obeyed and if there were no hydrogen bonding contribution to solubility.

The results for Dowanol TPM and Dioctyl Phthalate are nearly identical and are shown on the same graph. Similarly the results for the three solvents E-161, Dibutyl Carbitol, and Dioctyl Sebacate are nearly identical and are shown on the same graph. Freon 11 and presumably Freon 113 (though not experimentally verified) form an ideal solution with R-22 and are represented by the straight line Raoult's Law graphs. Diphenyl ether showed slight positive deviation from Raoult's Law and is not further considered.

The final graph in this P versus X series shows a comparison of the results all shown at 30°C. E-181 shows the greatest solubility, the Dibutyl Carbitol group second, the Dowanol TPM group third, and the Freon 11 group least soluble of the solvents shown.

The graphs ln p versus 1/T for given values of X allow extrapolation of P-X data to any temperature.

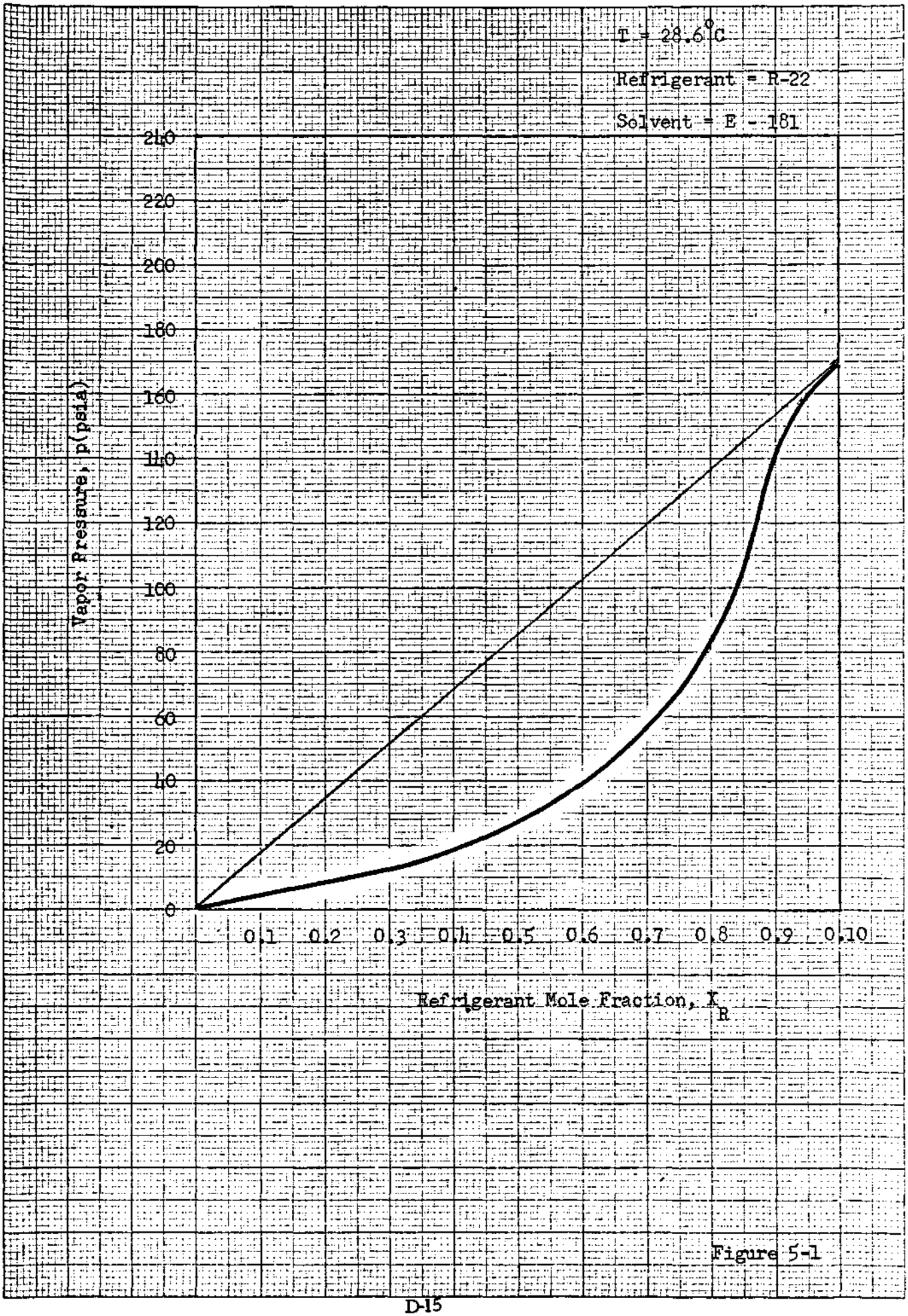

Figure 5-1

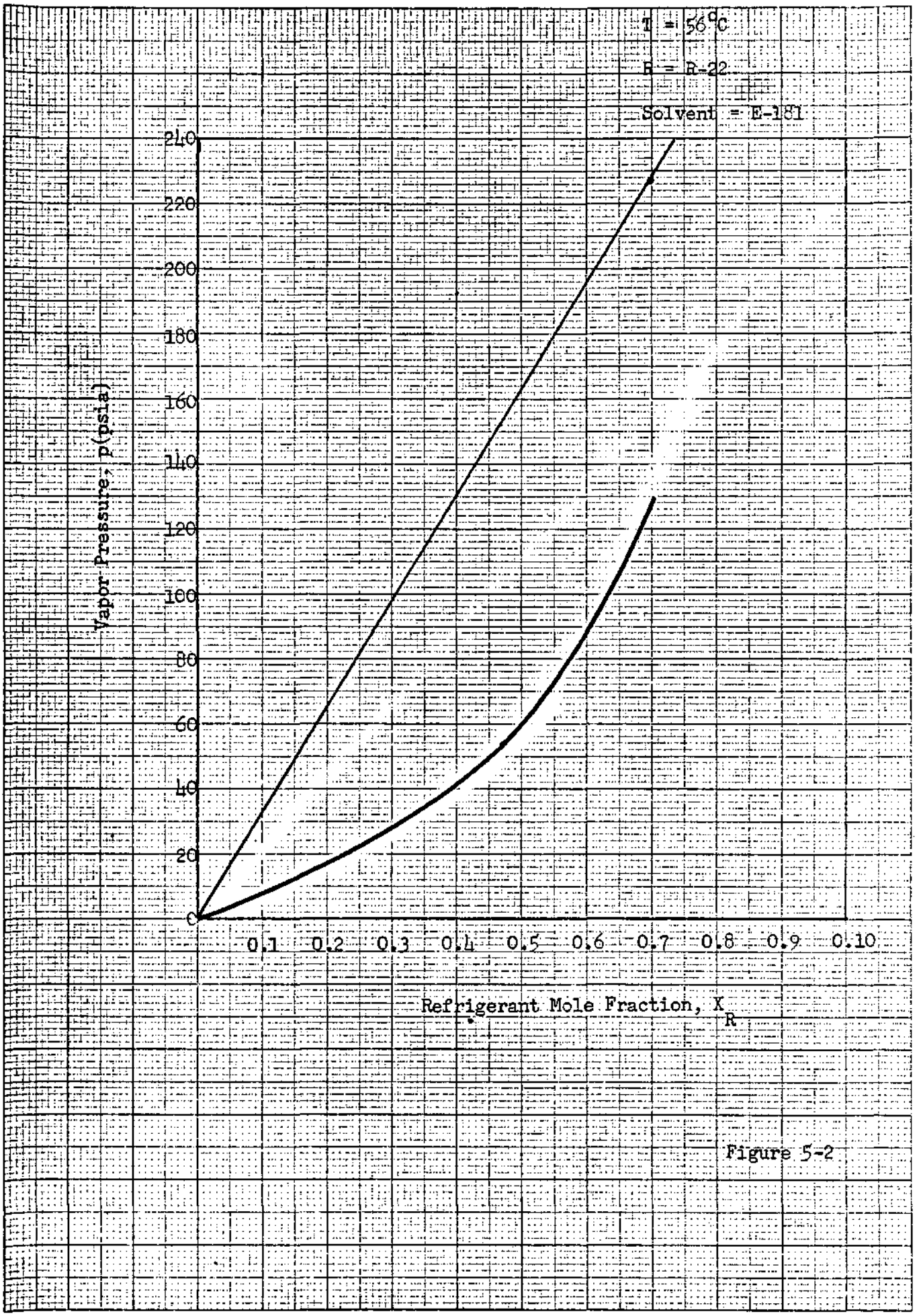
T = 56°C
R = R-22
Solvent = E-181
Vapor Pressure, p (psia)
240
220
200
180
160
140
120
100
80
60
40
20
0
0.1
0.2
0.3
0.4
0.5
0.6
0.7
0.8
0.9
0.10
Refrigerant Mole Fraction, X_R

Figure 5-2

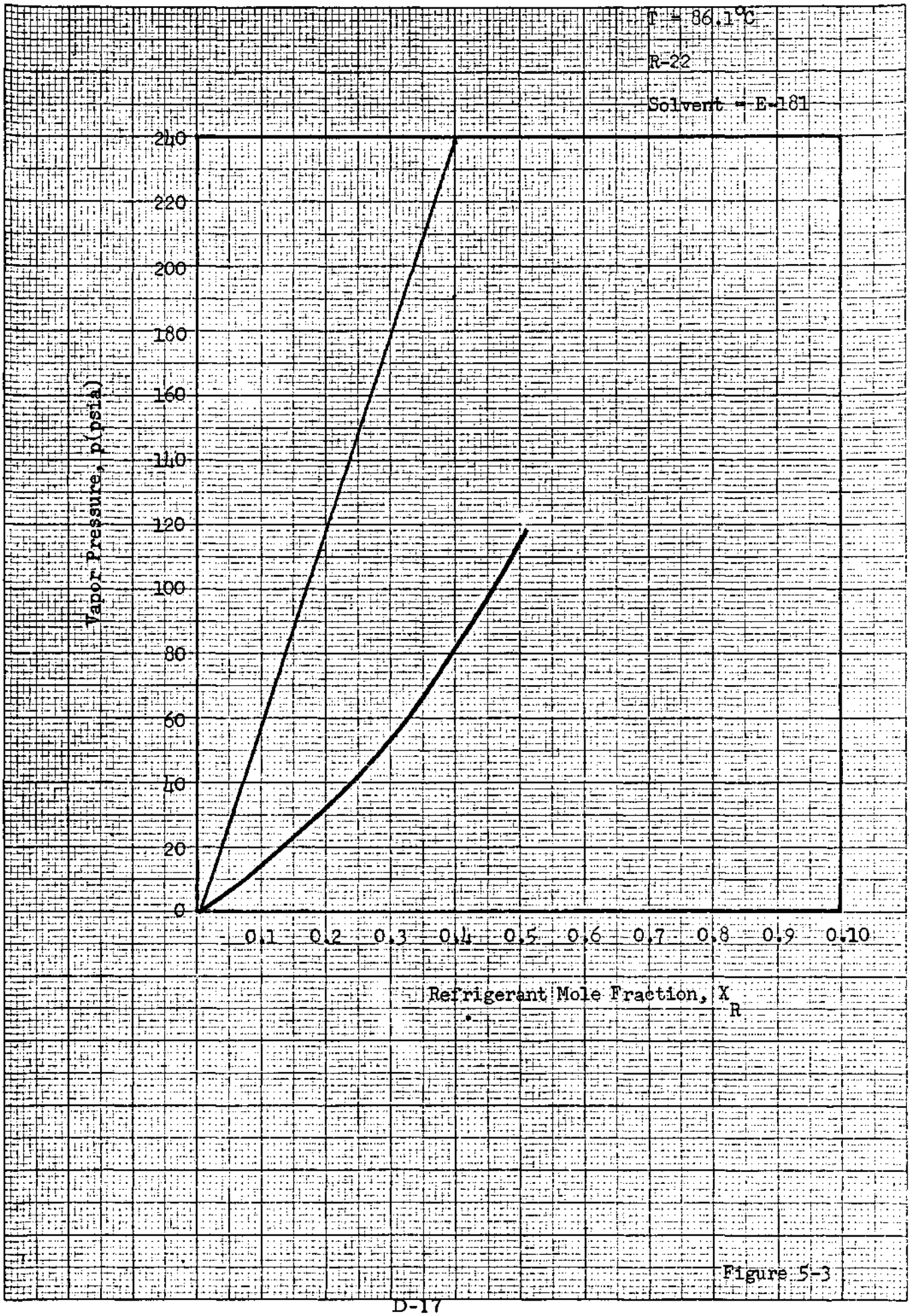
T = 86.1°C
R-22
Solvent = E-181
Vapor Pressure, p(psia)
240
220
200
180
160
140
120
100
80
60
40
20
0
0.1
0.2
0.3
0.4
0.5
0.6
0.7
0.8
0.9
0.10
Refrigerant Mole Fraction, X
R

Figure 5-3

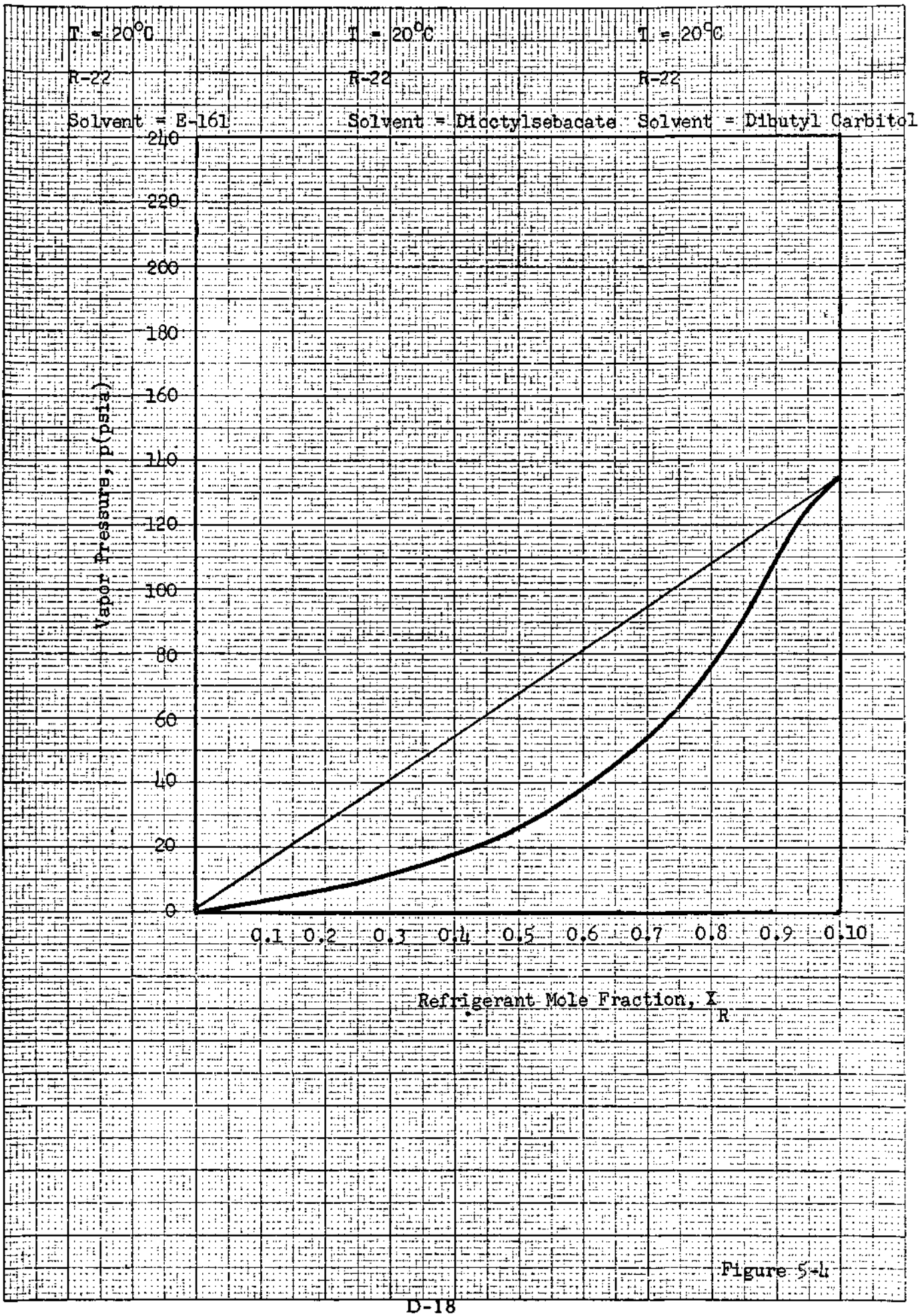
T = 20°C
R-22
Solvent = E-161
T = 20°C
R-22
Solvent = Dioctylsebacate
T = 20°C
R-22
Solvent = Dibutyl Carbitol
Vapor Pressure, p(psia)
240
220
200
180
160
140
120
100
80
60
40
20
0
0.1
0.2
0.3
0.4
0.5
0.6
0.7
0.8
0.9
0.10
Refrigerant Mole Fraction, X
R

Figure 5-4

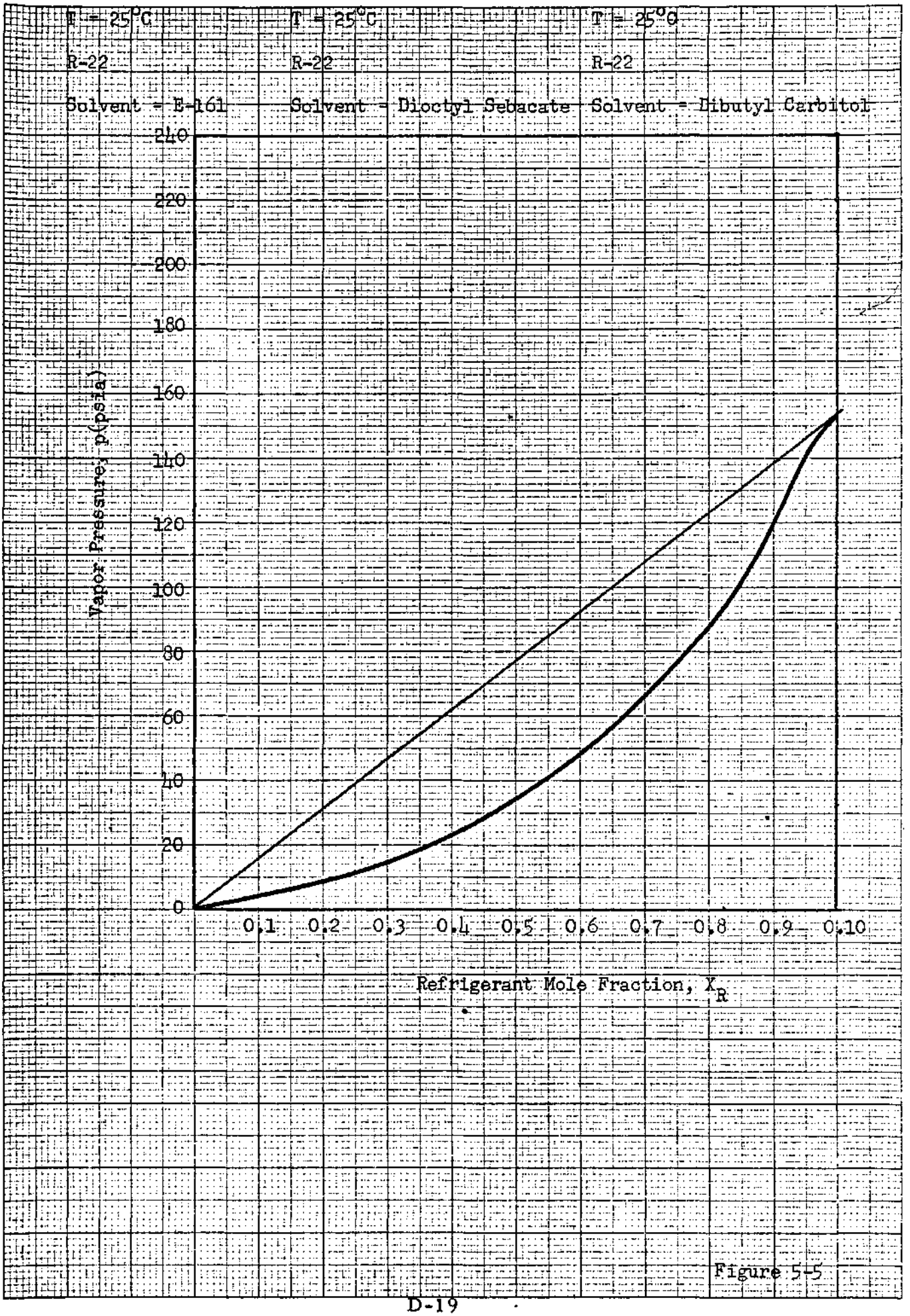

12-282
20 SQUARES TO THE INCH

Figure 5-5

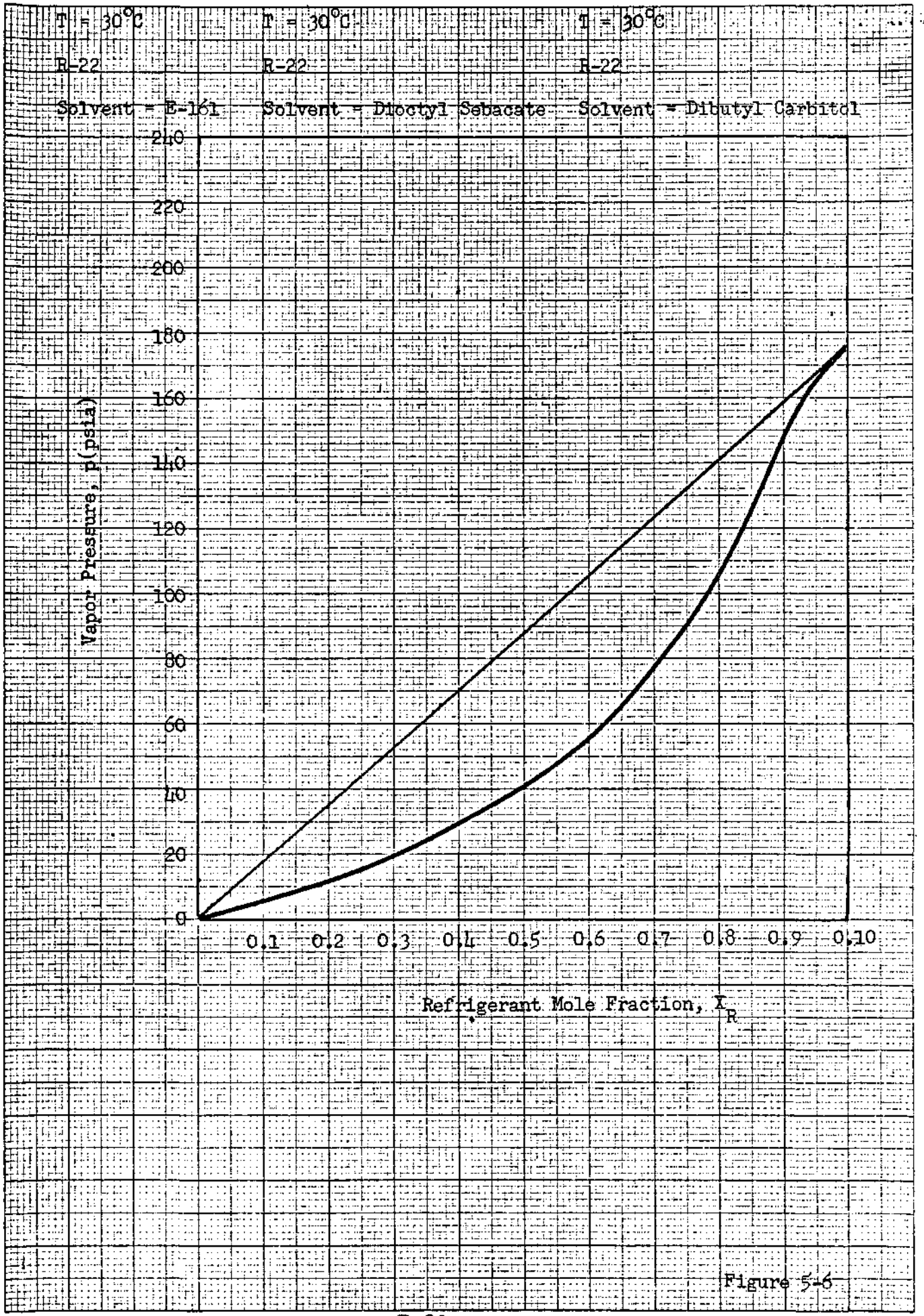

Figure 5-6

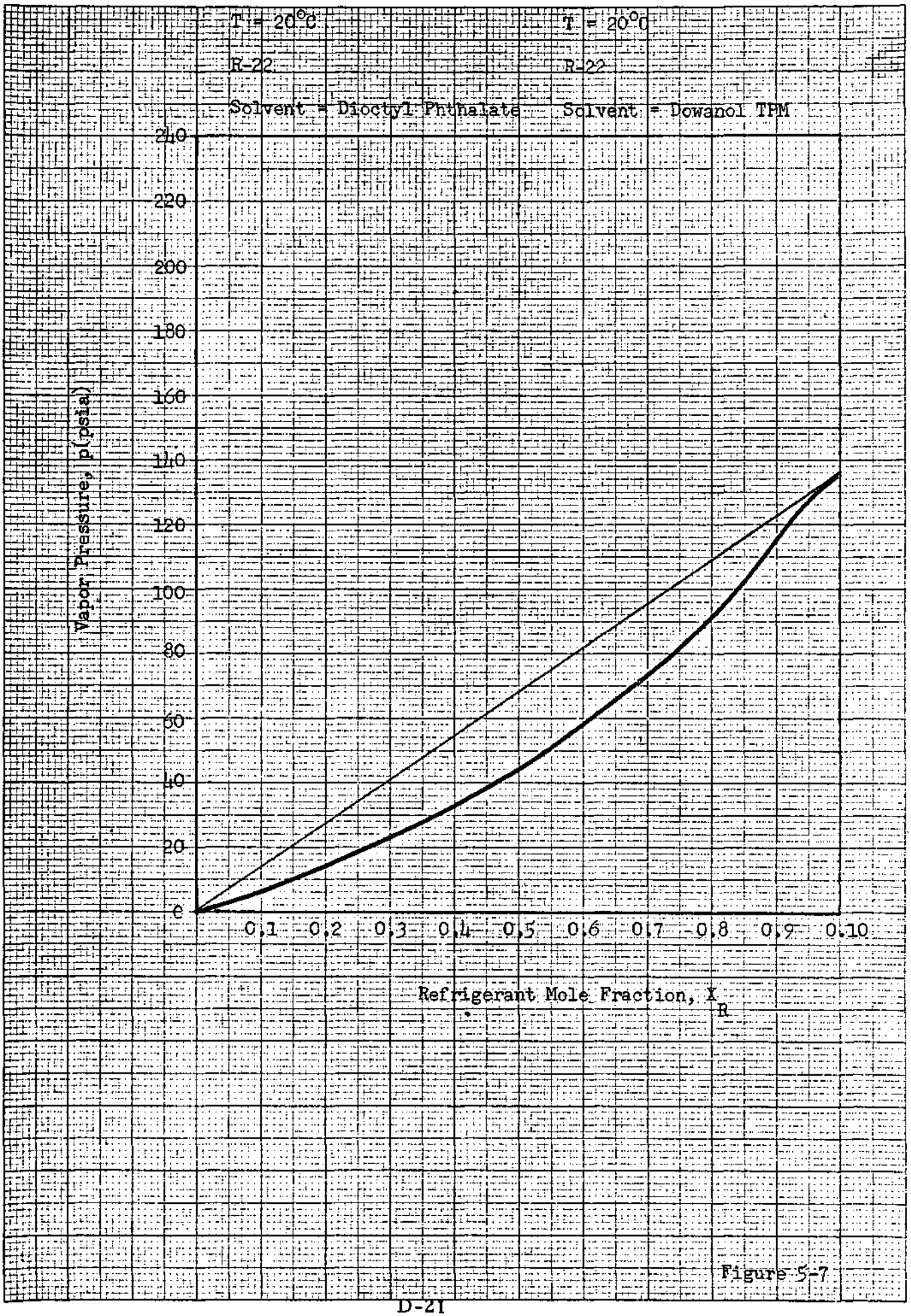
T = 20°C
R-22
Solvent = Dioctyl Phthalate
T = 20°C
R-22
Solvent = Dowanol TPM
Vapor Pressure, p (psia)
240
220
200
180
160
140
120
100
80
60
40
20
0
0.1
0.2
0.3
0.4
0.5
0.6
0.7
0.8
0.9
1.0
Refrigerant Mole Fraction, X_R

Figure 5-7

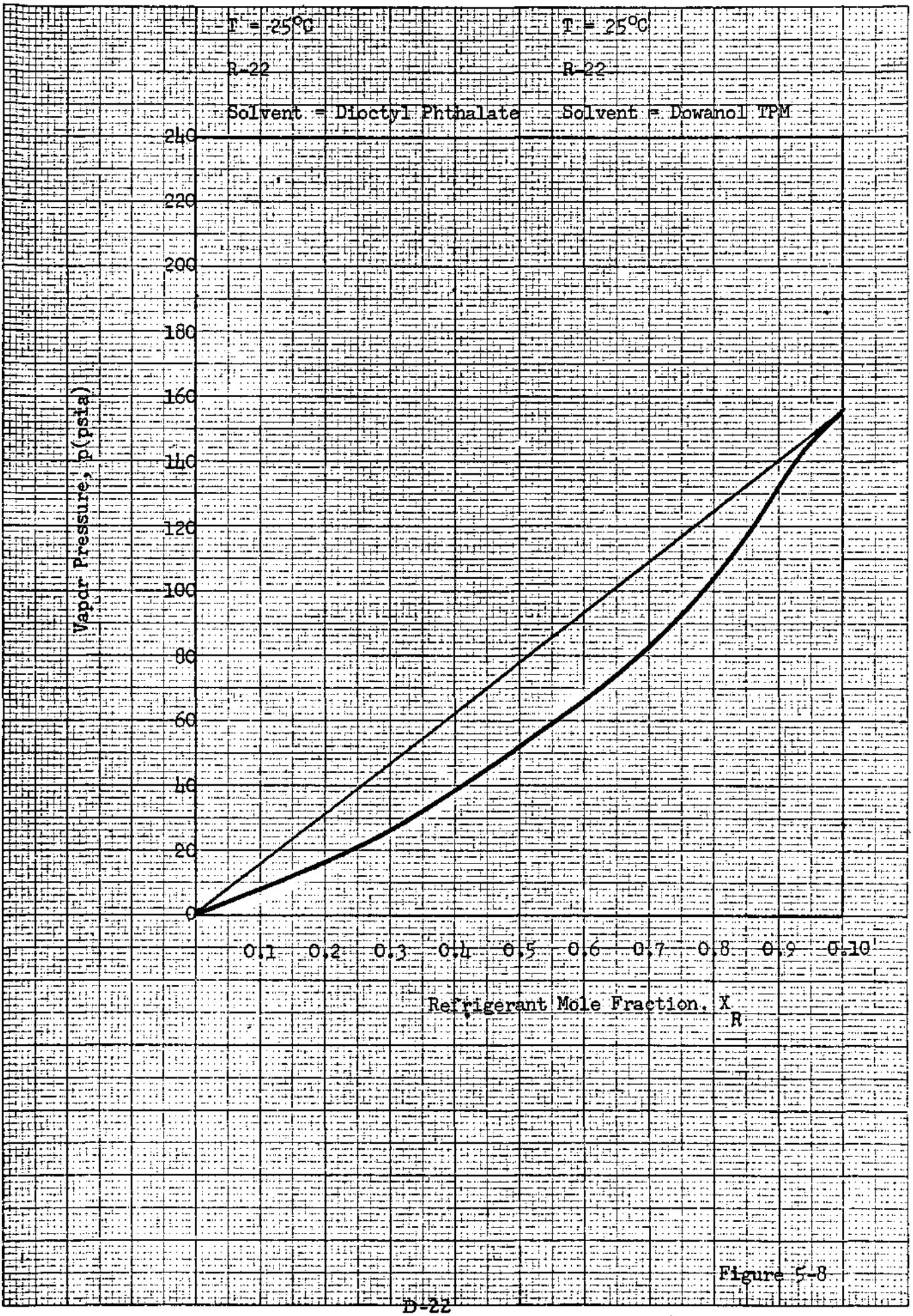
T = 25°C
R-22
Solvent = Dioctyl Phthalate
T = 25°C
R-22
Solvent = Dowanol TPM
Vapor Pressure, p(psia)
240
220
200
180
160
140
120
100
80
60
40
20
0
0.1
0.2
0.3
0.4
0.5
0.6
0.7
0.8
0.9
0.10
Refrigerant Mole Fraction, X_R

Figure 5-8

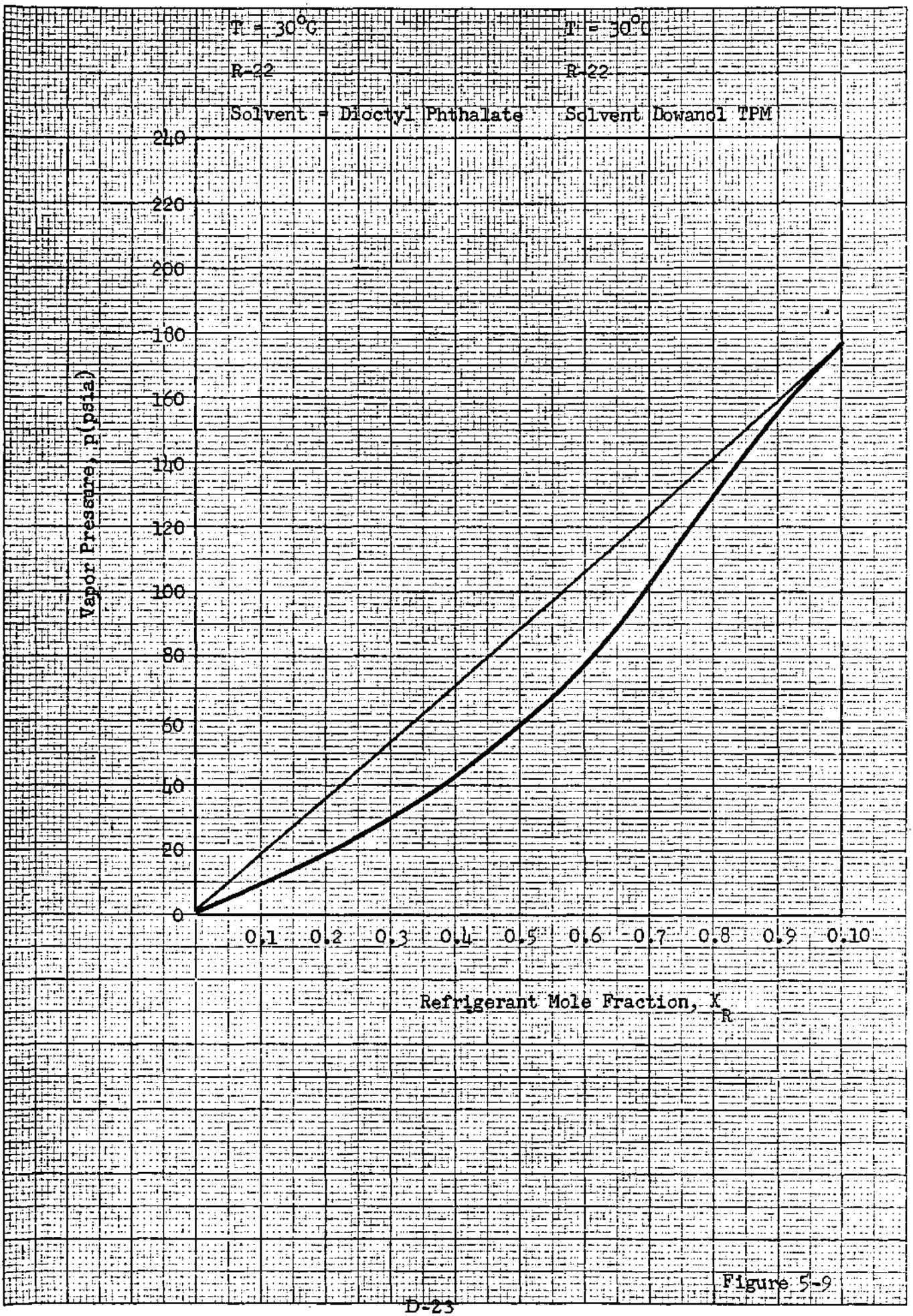

12-282
20 SQUARES TO THE INCH

Figure 5-9

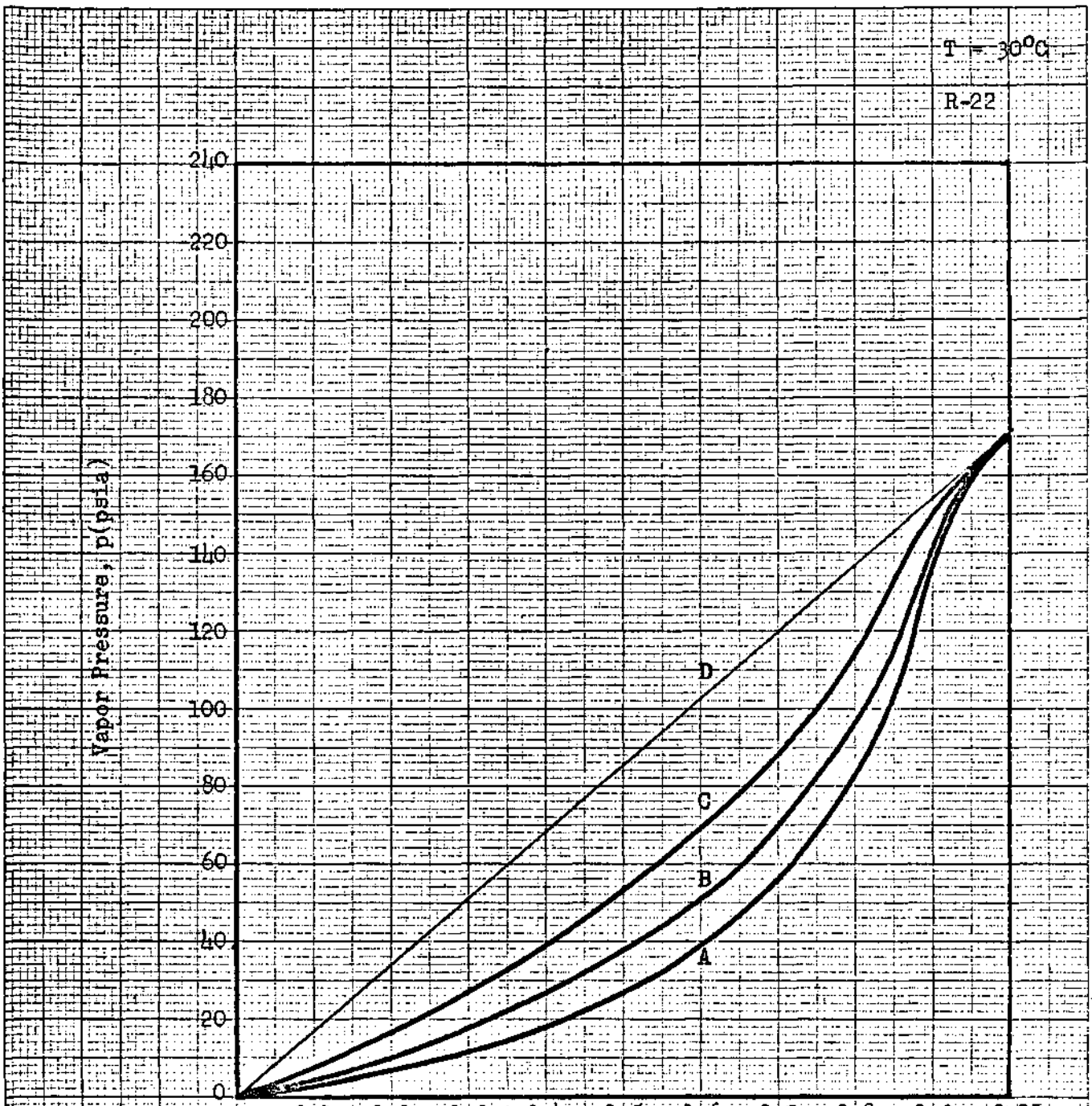

Figure 5-10

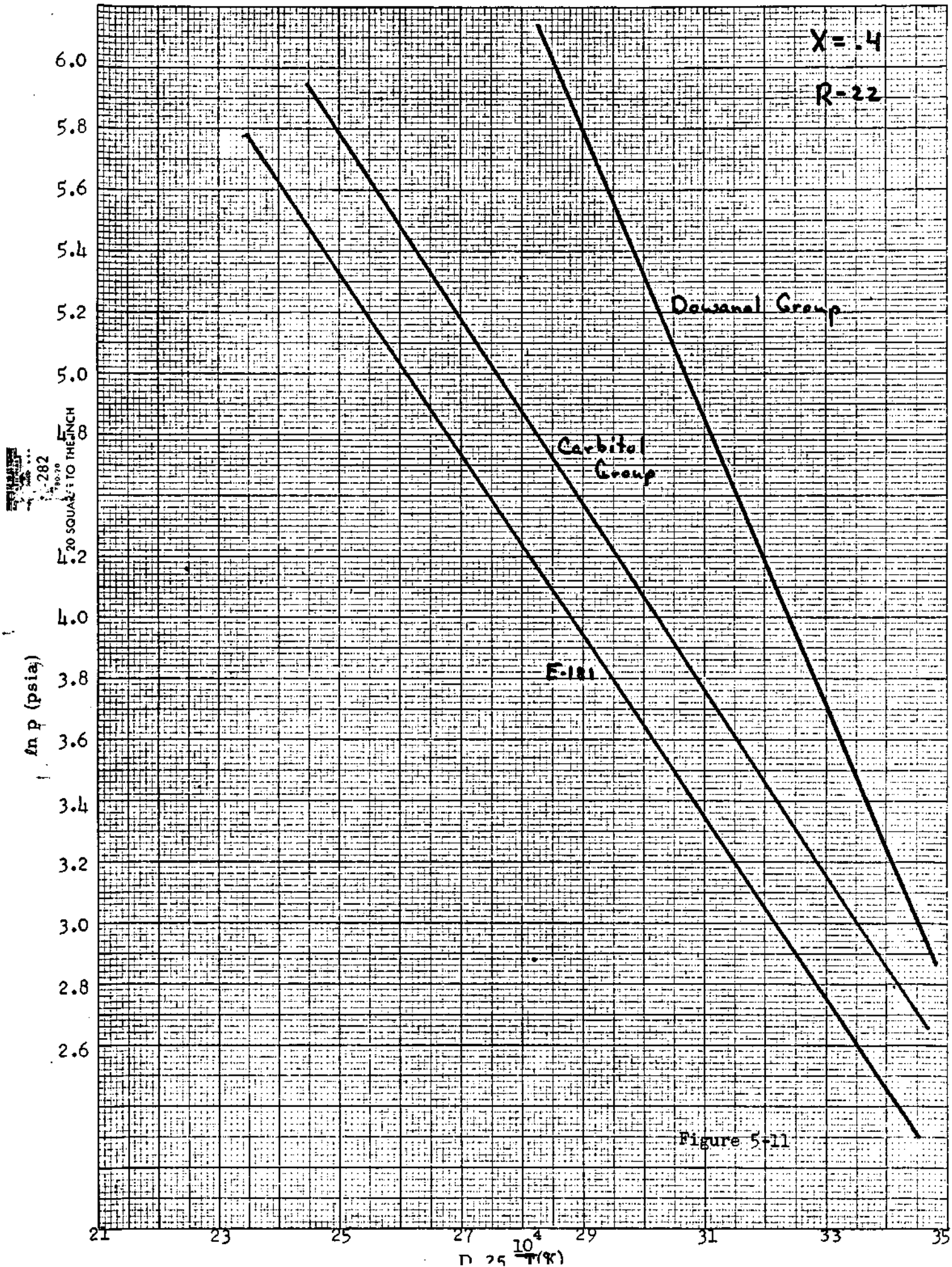
X = .4
R-22
Dowanol Group
Carbitol Group
E-181
ln p (psia)
6.0
5.8
5.6
5.4
5.2
5.0
4.8
4.6
4.4
4.2
4.0
3.8
3.6
3.4
3.2
3.0
2.8
2.6
21
23
25
27
29
31
33
35
$D_{25}\frac{10^4}{T(°K)}$

Figure 5-11

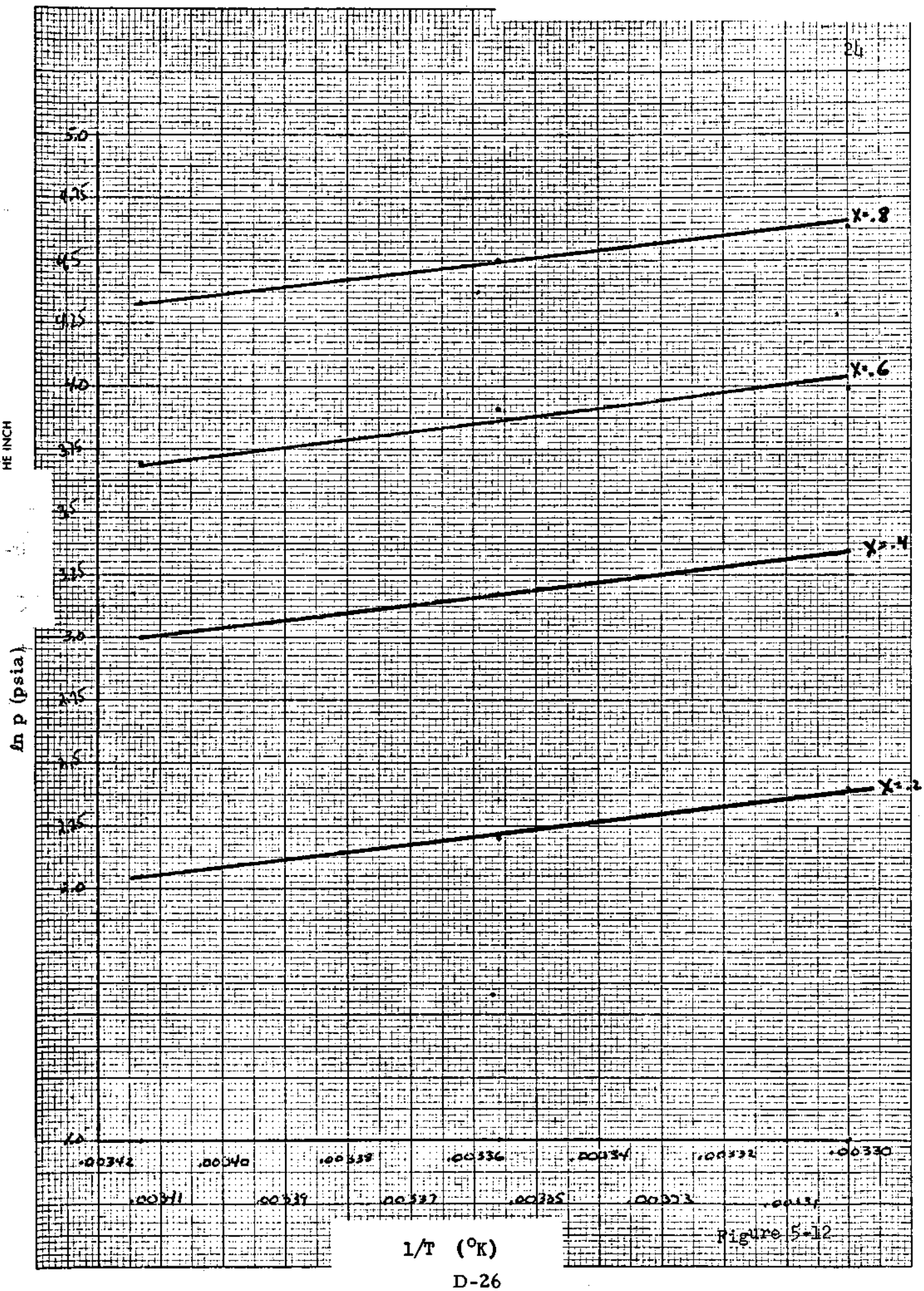

Figure 5-12

Freon-22 in Dowanol TPM Group

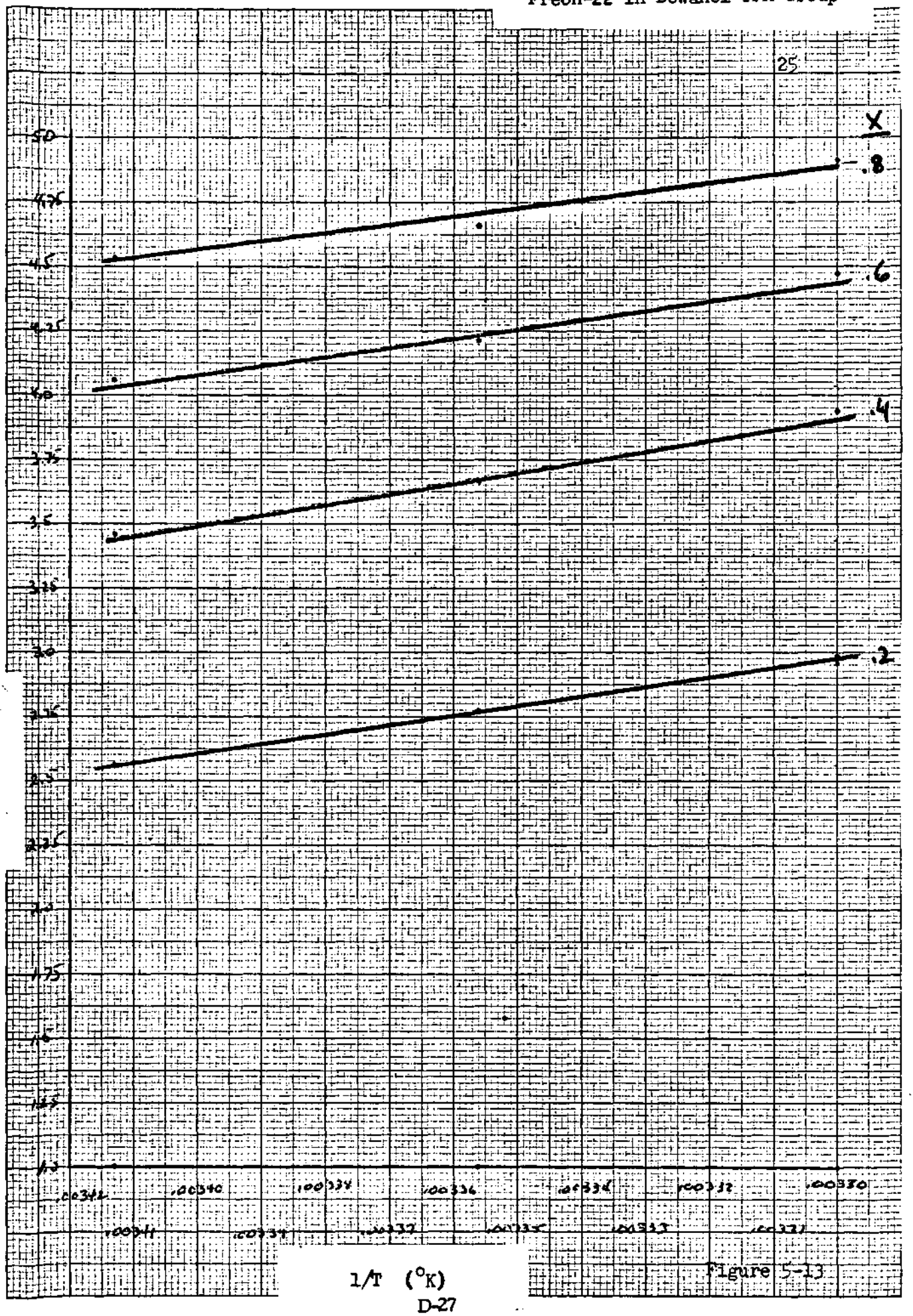

12.282
1"=0.20
20 SQUARES TO THE INCH

Figure 5-13

The following two graphs restate the solubility results in terms of solubility versus temperature for constant one atmosphere pressure. The first graph shows the solubility in units of moles of R-22 per mole of solution. The second graph shows solubility in terms grams of R-22 per gram of solution. The plots appear linear over the short range of temperatures shown, but are not truly linear.

Note that no single solvent measured exhibits greater solubility for R-22 than the solvent E-181. However all the solvents tested have sufficient solubility to be considered if other properties are superior to those of E-181.

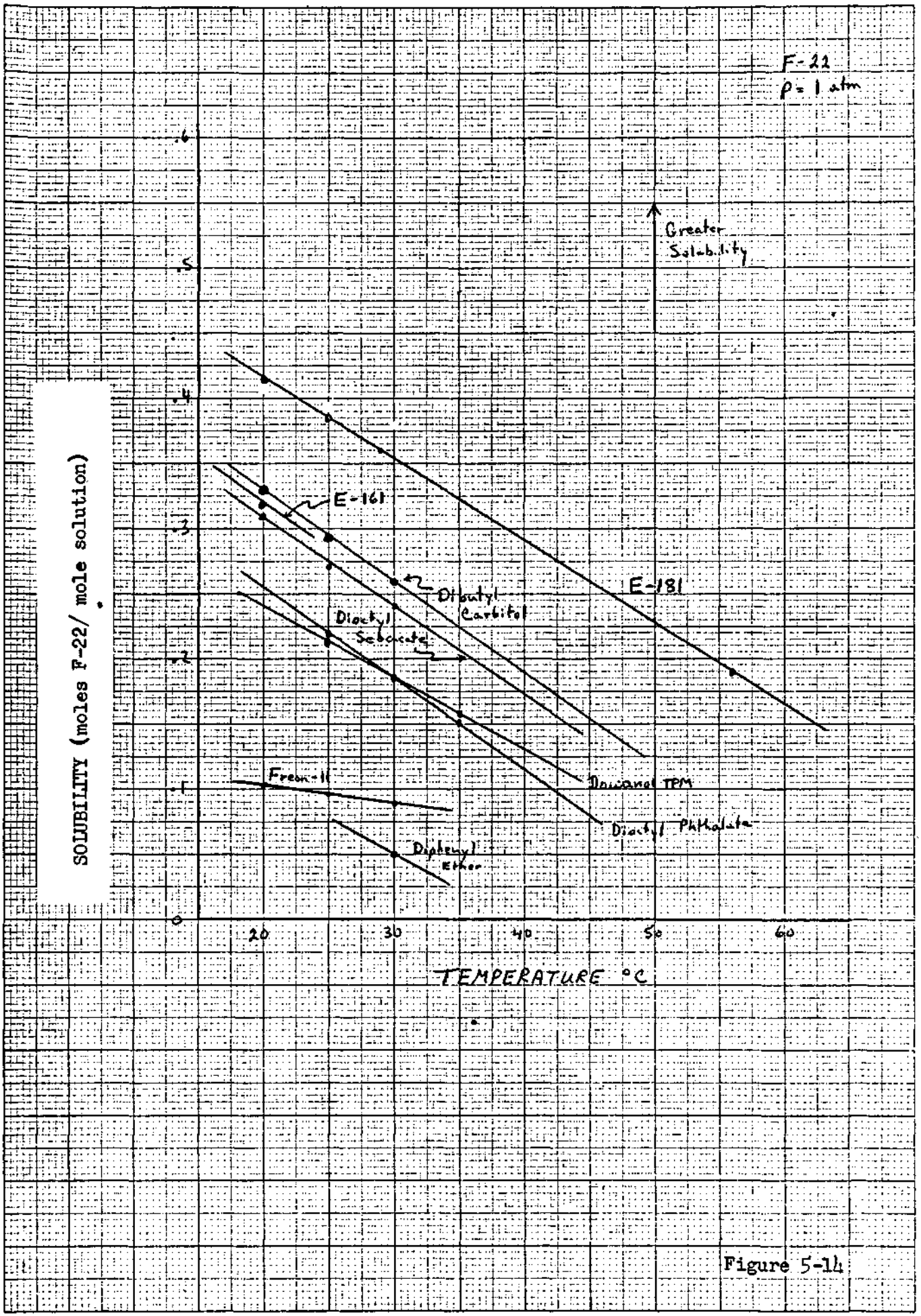

Figure 5-14

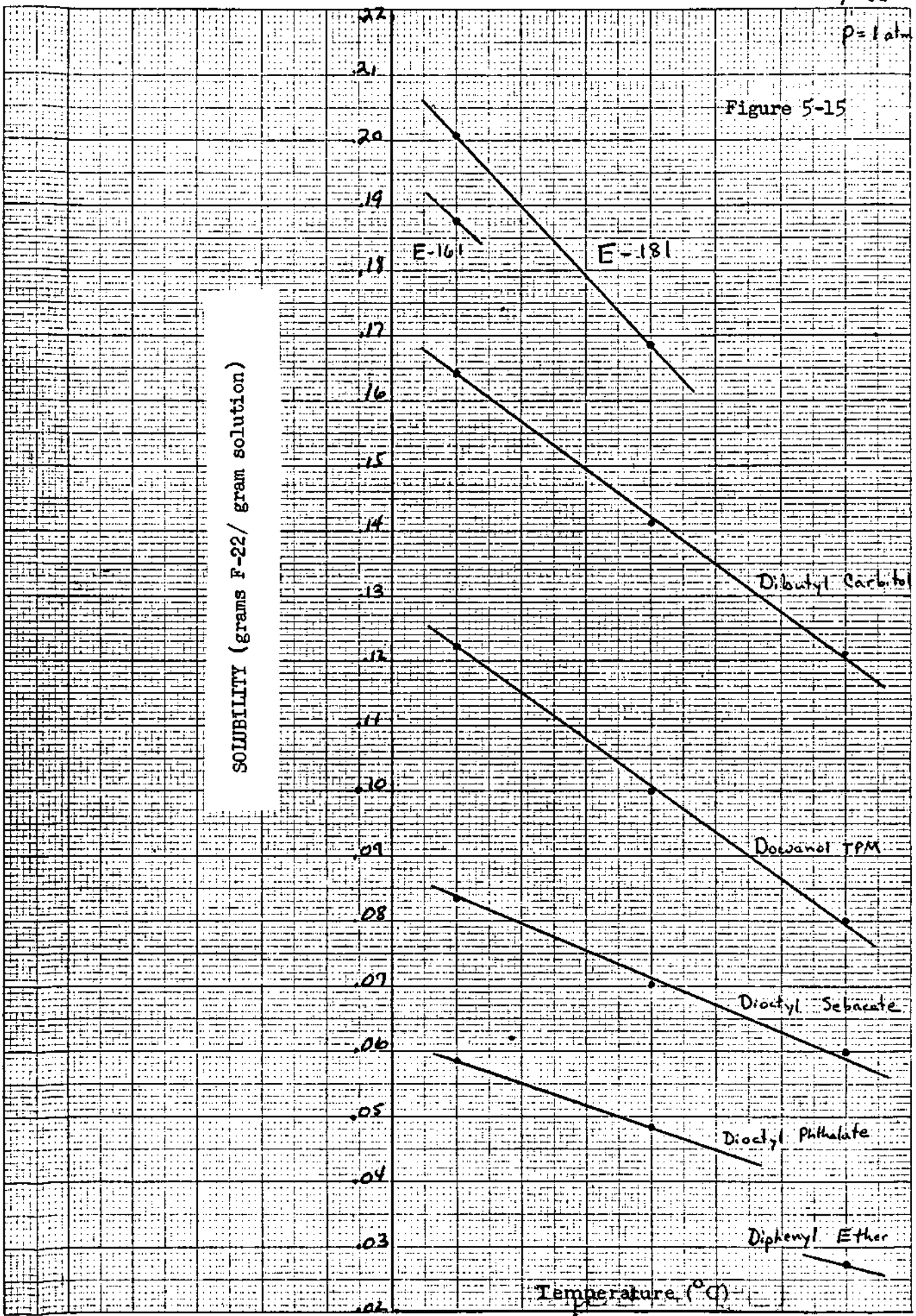
P = 1 atm
SOLUBILITY (grams F-22/ gram solution)
.22
.21
.20
.19
.18
.17
.16
.15
.14
.13
.12
.11
.10
.09
.08
.07
.06
.05
.04
.03
.02
E-161
E-181
Dibutyl Carbitol
Dowanol TPM
Dioctyl Sebacate
Dioctyl Phthalate
Diphenyl Ether
Temperature (°C)
20
25
30

Figure 5-15

Section 6 Calculation of Heats of Mixing

The total heat of reaction when a gas is dissolved in a liquid is the sum of the heat vaporization of the given quantity of gas and the heat of mixing which is due to the specific interactions of gas and solvent molecules. Heat of vaporization per mole of solution can be calculated directly from the heat of vaporization per mole of gas.

$$(\Delta H_{vap})_{Solution} = X_R (\Delta H_{vap})_{Gas}$$

Where (ΔHvap) gas is a function of temperature and X_R is the measured solubility and is a function of temperature and pressure. Total heat of reaction can perhaps be measured calorimetrically and heat of mixing calculated by difference ΔHreaction - ΔHvap, but heat of mixing is usually calculated from direct analysis of p-T-X measurements.

If solutions are ideal then activity a (effective concentration) is equal to concentration X

$$A_R = X_R$$

However, when nonideal (specific interaction generates a heat of mixing) then

$$A_R = \gamma_R X_R$$

where γ_R (the activity coefficient) is a measure of deviation from ideality. Heats of mixing can be calculated from measured deviations from ideality by the following method:

1. p is measured as a function of X as in the previous solubility studies.
2. $a_R = \frac{p}{p^\circ}$ Raoult's Law
3. $\gamma_R = \frac{a_R}{X_R}$ by definition
4. $\gamma_R = K_1 + K_2 a_R$ experimental observation where K_1 and K_2 are intercept and shape of a plot of γ_R versus a_R

5. By theoretical relationships derived by Mastrangelo (J. Phys. Chem., 1959, 63,608.)

$$\Delta H_m = \Delta H_r \left(\frac{fK}{1 + K} \right) \left(\frac{X_R X_S}{X_R + fX_S - Z} \right)$$

where $Z = \frac{\Delta Hm}{\Delta Hr}$

$$\Delta H_r = -R \left[\frac{d \ln K}{[d\ (1/T)]} \right] f$$

$$K = \frac{1}{fK_1} - 1$$

(Note that this equation is stated incorrectly in LMSC-HREC D162909.

From the above detailed data treatment the following results were produced:

A. R-22 in E181	T=28.6°C	K_1 = 0.172	K_2 = 0.920	K = .938
	T=56.0°C	K_1 = 0.200	K_2 = 0.907	K = .667
f=3.0	T=86.1°C	K_1 = 0.234	K_2 = 0.870	K = .425

B. R-22 in Dibutyl Carbitol, Dioctyl Sebacate, E-161

	T= 20°C	K_1 = 0.222	K_2 = 1.027	K = .877
f= 2.4	T= 30°C	K_1 = 0.240	K_2 = 0.983	K = .736

C. R-22 in Dowanol TPM, Dioctyl Phthalate

	T= 20°C	K_1 = 0.422	K_2 = 0.743	K = .185
f= 2.0	T = 30°C	K_1 = 0.446	K_2 = 0.720	K = .121

12-282

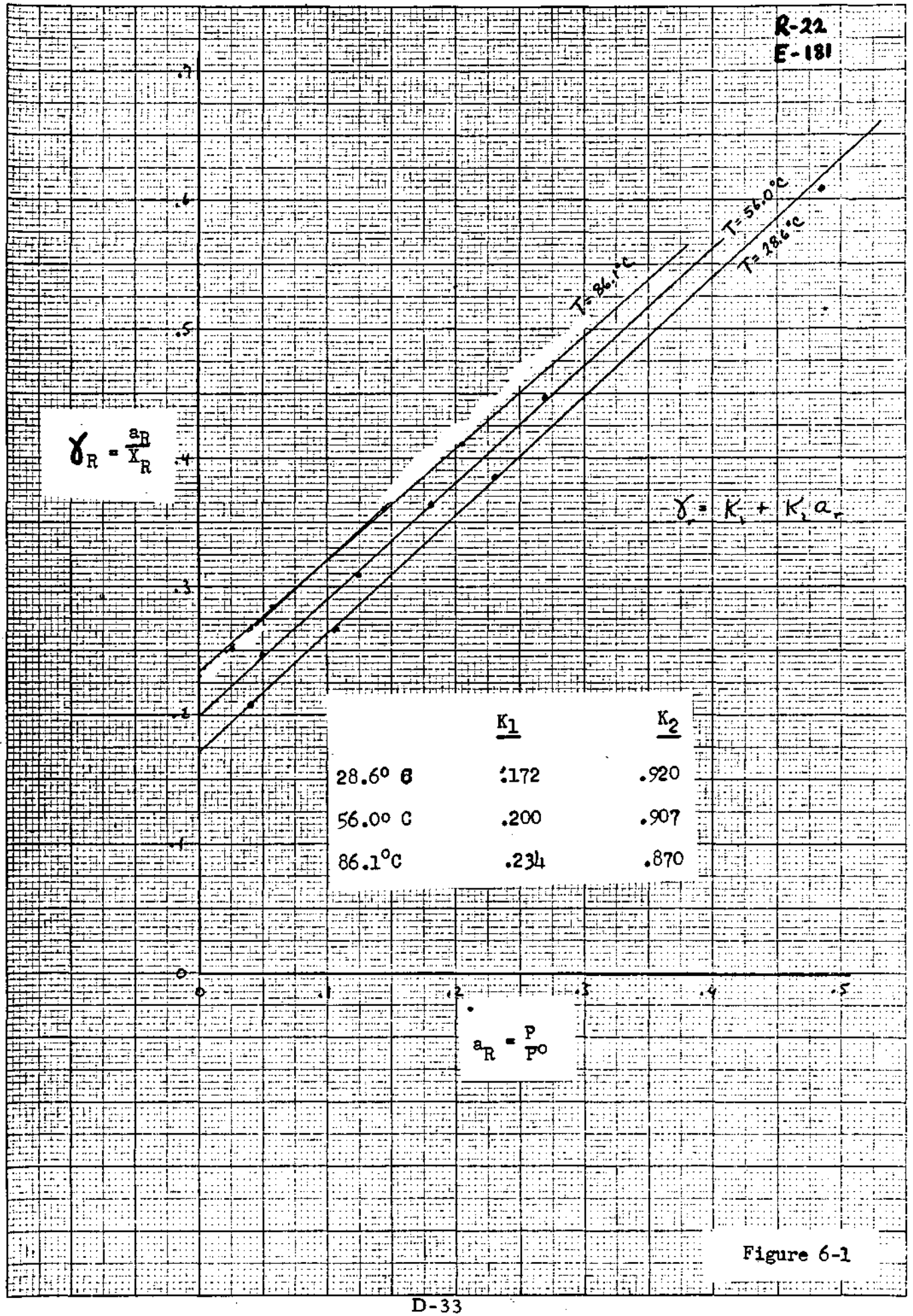

	K_1	K_2
28.6° C	.172	.920
56.00 C	.200	.907
86.1°C	.234	.870

Figure 6-1

to the inch

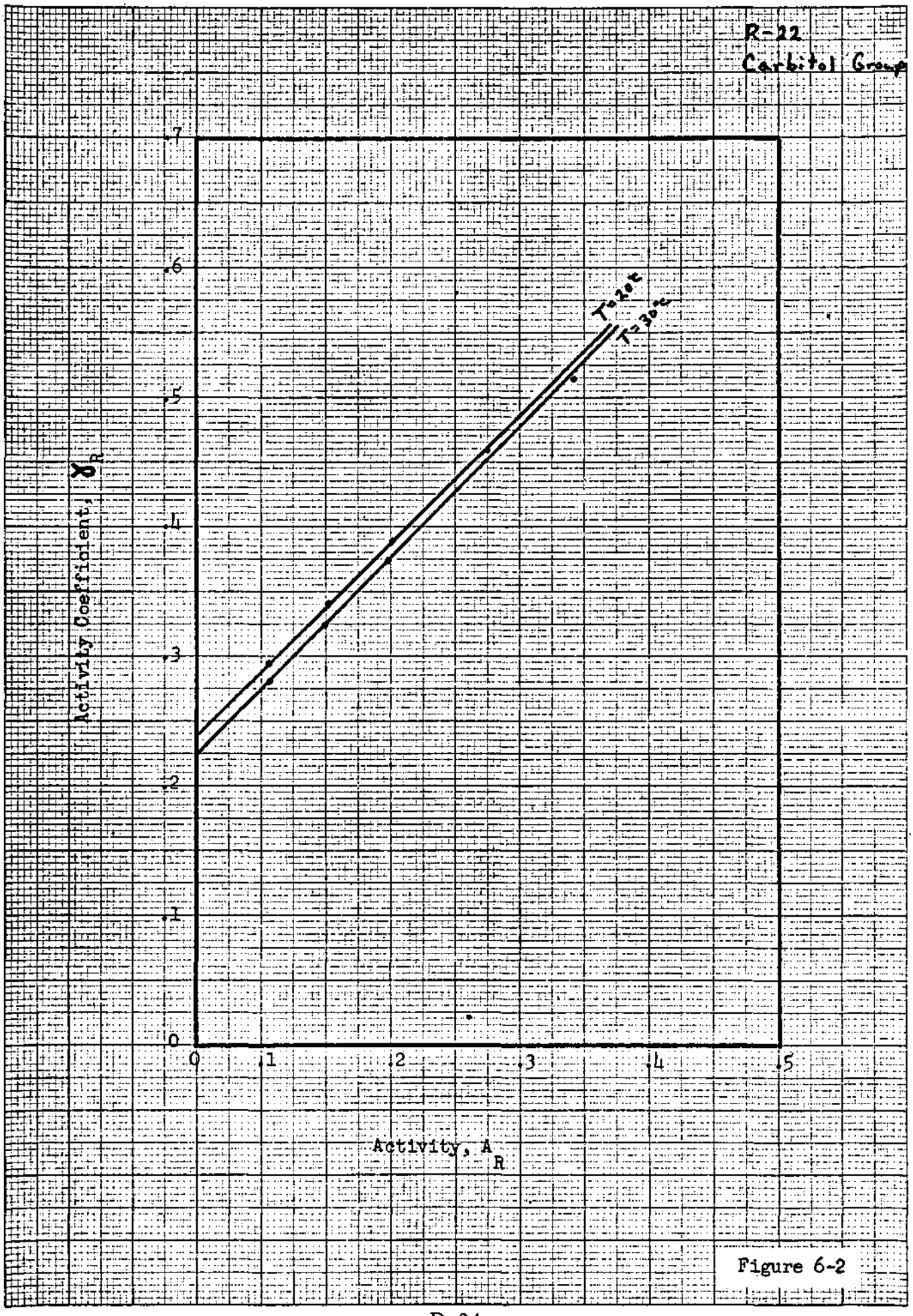

Figure 6-2

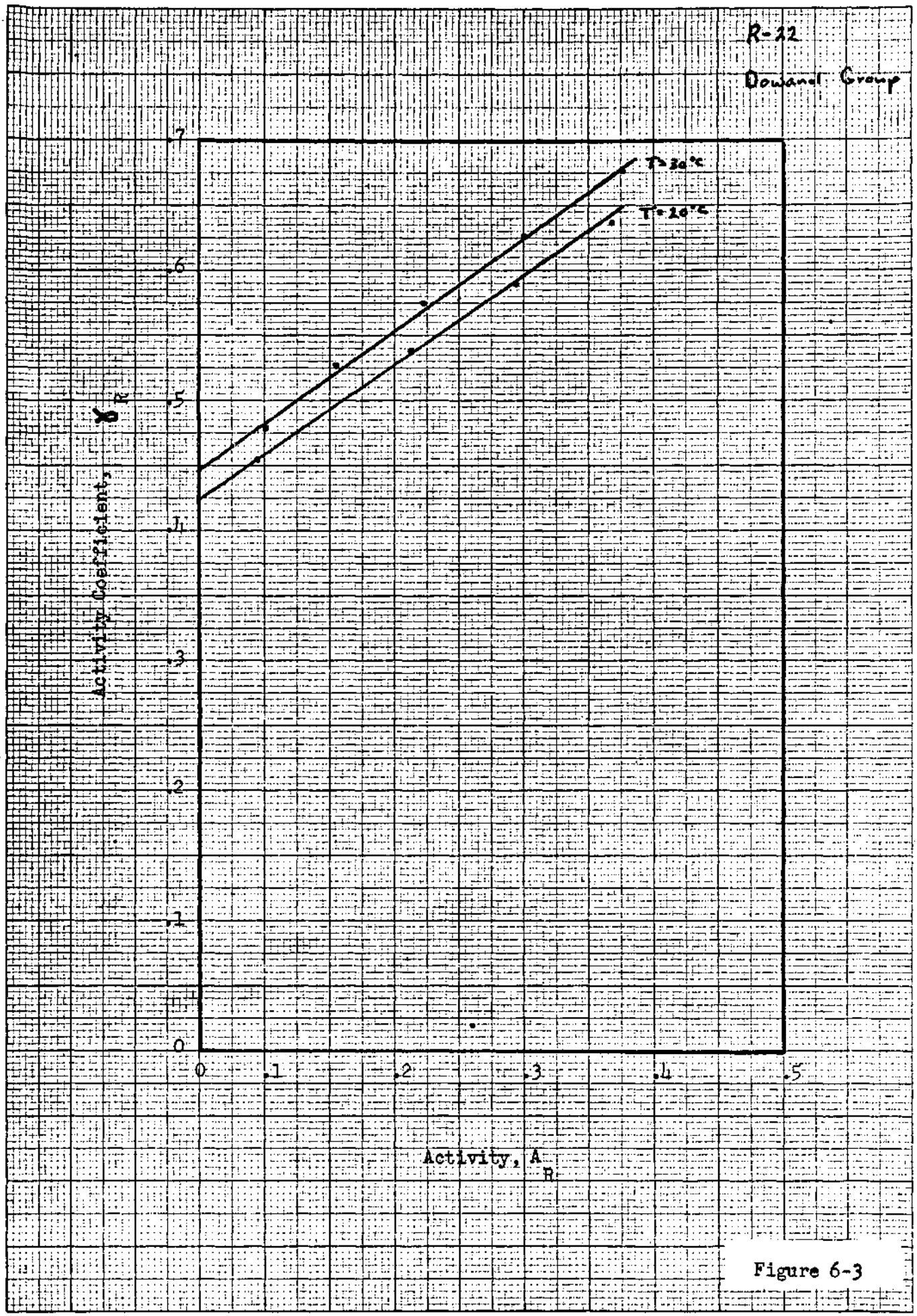
R-22
Dowanol Group
T = 20°C
T = 10°C
Activity Coefficient, γ_R
.7
.6
.5
.4
.3
.2
.1
0
0
.1
.2
.3
.4
.5
Activity, A_R

Figure 6-3

Section 7 Computer Study

Lockheed's weight optimization and area optimization programs were used to make a preliminary evaluation of the relative merits of the various fluids studied. These programs were altered in four ways to suit the requirements of this study;

i) The input was altered to read in all fluid properties.

ii) Thermodynamic and P-T-X calculations were done by means of function subroutines or statement functions to facilitate alterations.

iii) Certain changes were made in iteration procedures to speed the operation of the program.

iv) Based on experience with the data properties during the experimental work, an improved P-T-X data fitting procedure was developed and used.

The study consisted of first comparing results to prior Lockheed results for R-22, DME-TEG. Thereafter, weight optimization cases were run for a representative heat load and a range of generator temperature from 250°F to 500°F. Using temperature differentials from these cases, the same range of generator temperatures was investigated with the area optimization program. A discussion of the program alterations, the results and some suggestions for future program improvements follows.

PROGRAM ALTERATIONS

The first changes consisted of adding to the program inputs to accept the names of the fluid combination, the molecular weight, density and specific heat of each fluid, and applicable constants for the heat of mixing and P-T-X routines. At the same time, all statements involving these

quantities were changed to use symbolic rather than numerical constants.

Calculations of vapor pressure, specific enthalpy and concentration were moved into statement functions because they were used more than once and to facilitate alterations. Since R-22 was used as the refrigerant in every case, alteration proved to be unnecessary. In addition the ideal concentration calculation was moved to a function subroutine, and special routines were used for the Raoult's Law cases (R-22, R-113) and the remainder of the cases.

Three iterative calculations from the original program were improved to cut the time required to run the program, which proved to be a consideration on UTC's IBM 360-30 machine. T(8) is calculated via a bounded Newton-Raphson technique rather than a stepping technique. This proved to converge so rapidly that an error criterion of .01° was used rather than the prior criterion of .05° expected error. A direct solution for T(4) was used rather than the prior method. In the heat of mixing routine, it was found that Mastrangelo's equation was a quadratic. To be consistent with the result of his iteration technique, the smaller root is used. A final change was to calculate the heat of mixing (a scalar quantity) in a function routine rather than a subroutine in order to speed up the linkages.

Finally, in inspecting the P-T-X data it was observed that ln(p) vs. (1/T) for various concentrations was very nearly linear with a consistent slope for all concentrations. Accordingly, to calculate concentrations it is easy to correct an input pressure to a standard inverse temperature, and then to use a cubic fit of concentration vs. ln(p) to find the concentration. When compared to the prior method, this amounts to adding (significant) terms in $\ln(p)^2$, and (1/T) ln(p). For the Raoult's Law case, Lockheed's fit for the vapor pressure of R-22 and a similar fit for R-113 were used together with

an assumed linear variation between them. All the input data used for the various fluids are tabulated in Table 7-1.

STUDY RESULTS

The initial stage of the study was to verify the operation of the program and to ascertain the changes due to the new P-T-X data fits. Using the Lockheed data and R-22; DME-TEG input, the program reproduced the Lockheed IBM 7094 results with very small discrepancies due to the 32 bit word length of the UTC 360-30 as opposed to the 36 bit 7094 and due to changes in the iteration scheme. The UTC data fit for R-22, E-181 (our nomenclature for DME-TEG) gave greater negative deviations from Raoult's Law than the Lockheed data fit. Using our data and the improved P-T-X representation, a comparison was run with weight optimal results from Lockheed. For this comparison and all subsequent runs a single representative case was selected except for the generator temperature, which was varied. The representative case consisted of Q_{in} = 50, WD = 2.0 and $\eta_g = \eta_A$ = 0.8. The generator temperature, which has a strong influence on radiator area and weight, was allowed to range from 250°F to 500°F in 50°F increments. This comparison appears in Fig. 7-1, where it can be seen that the same general type of variation holds except that the minima are shifted to higher temperatures.

The R-22, Carbitol; R-22, Dowanol and R-22, R-113 fluid combinations were run in the weight optimization program, and the resulting optimal weights and associated areas appear in Fig.7-2. Using the temperature differentials at locations 2 and 7 which were optimal for the weight program, the same fluid combinations were run in the area optimization program and the results appear in Fig. 7-3, where the optimal areas are plotted together with the associated weights. These results are presented without further interpretation, since evaluation of the relative merits of the fluid combinations involves material properties as well as area and weight considerations.

TABLE 7-1

R-22, E-181

Refrigerant: Mol. Wt. = 86.5
Density = 74.53 $LB_m/Ft.^3$
Spec. Ht. = 0.3 $Cal_m (°K)g^{-1}$

Absorbent: Mol. Wt. = 222.3
Density = 63.313
Spec. Ht. = 0.46

P-T-X Data ($p^1 = p\ (1/T = .0034\ °K^{-1})$)

$\ln p^1 = \ln p + 5310.\ (1/T) - 10.03$
$X = -.0832 + .1332\ \ln p + .0185\ (\ln p)^2$

Heat of Mixing Data

$f = 3.0$
$\ln K = (1625./T) - 5.375$
Heat of Reaction = 3230.

R-22, Carbitol

Absorbent: Mol. Wt. = 218.3
Density = 55.313
Spec. Ht. = 0.43

P-T-X Data

$\ln p^1 = \ln p + 5490.\ (1/T) - 10.37$
$X = -.0199 + .0132\ \ln p + .0358\ (\ln p)^2$

Heat of Mixing Data

$f = 2.4$

$\ln K = (1513/T) - 5.385$
Heat of Reaction = 3005.

R-22, Dowanol

Absorbent: Mol. Wt. = 206.3
Density = 60.438
Spec. Ht. = 0.51

R-22, Dowanol (continued)

P-T-X Data

$\ln p^1 = \ln p + 6660.\ (1/T) - 12.58$

$X = .2422 - .1989\ \ln p + .0704\ (\ln p)^2$

Heat of Mixing Data

$f = 2.0$

$\ln K = (3450/T) - 13.465$

Heat of Reaction = 6855.

R-22, R-113

Absorbent: Mol. Wt. = 187.4
Density = 97.7
Spec. Ht. = 0.218

P-T-X Data

$$p_{ref} = EXP\ (12.531 - 3.676 \times 10^3/T - 1.87 \times 10^5/T^2)$$

$$p_{abs} = EXP\ (11.594 - 8.6153 \times 10^3/T - 5.952 \times 10^5/T^2)$$

$$X = (p - p_{abs})/(p_{ref} - p_{abs})$$

No Heat of Mixing

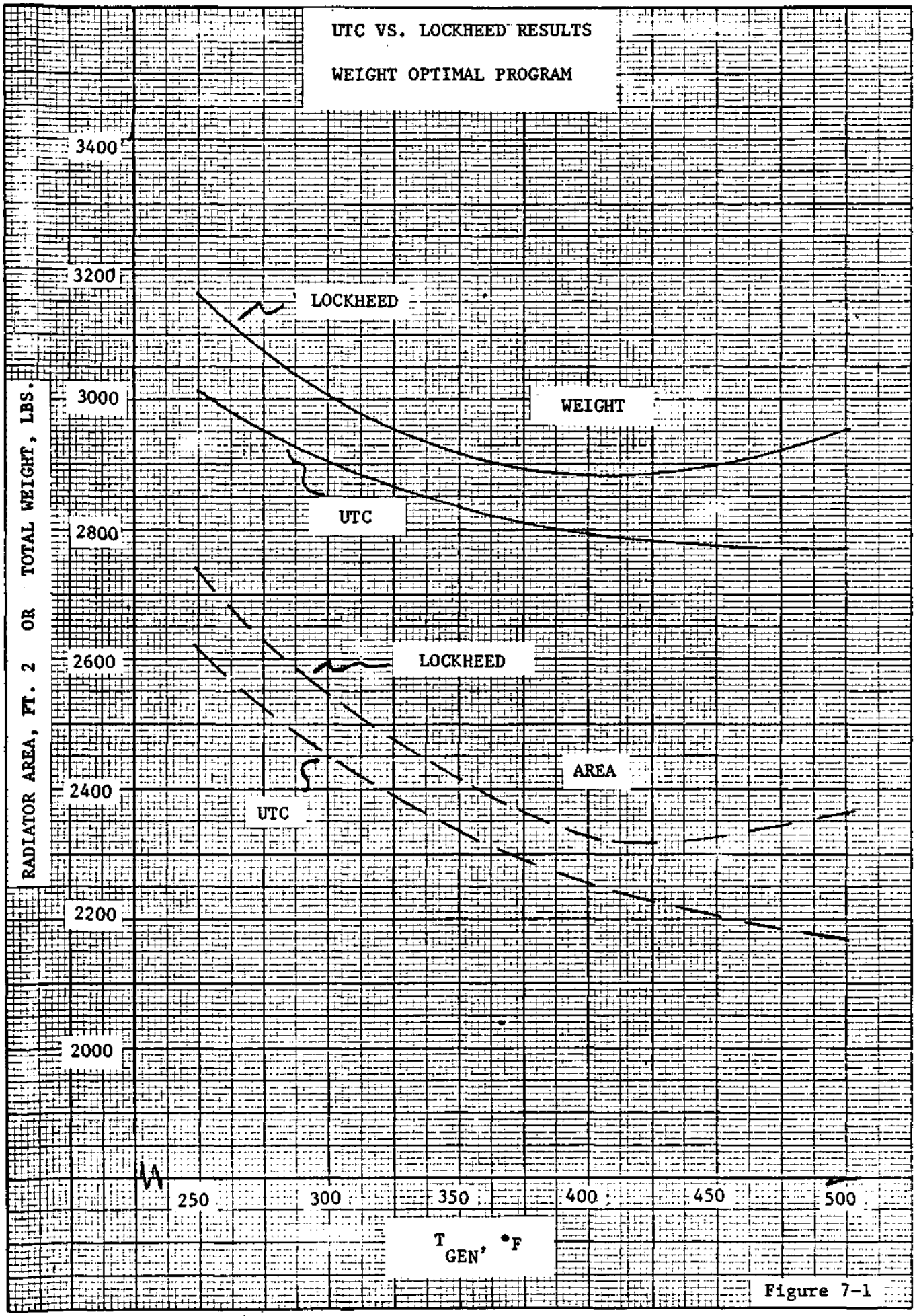
UTC VS. LOCKHEED RESULTS
WEIGHT OPTIMAL PROGRAM
RADIATOR AREA, FT. 2 OR TOTAL WEIGHT, LBS.
3400
3200
3000
2800
2600
2400
2200
2000
LOCKHEED
WEIGHT
UTC
LOCKHEED
AREA
UTC
250
300
350
400
450
500
T GEN, °F

Figure 7-1

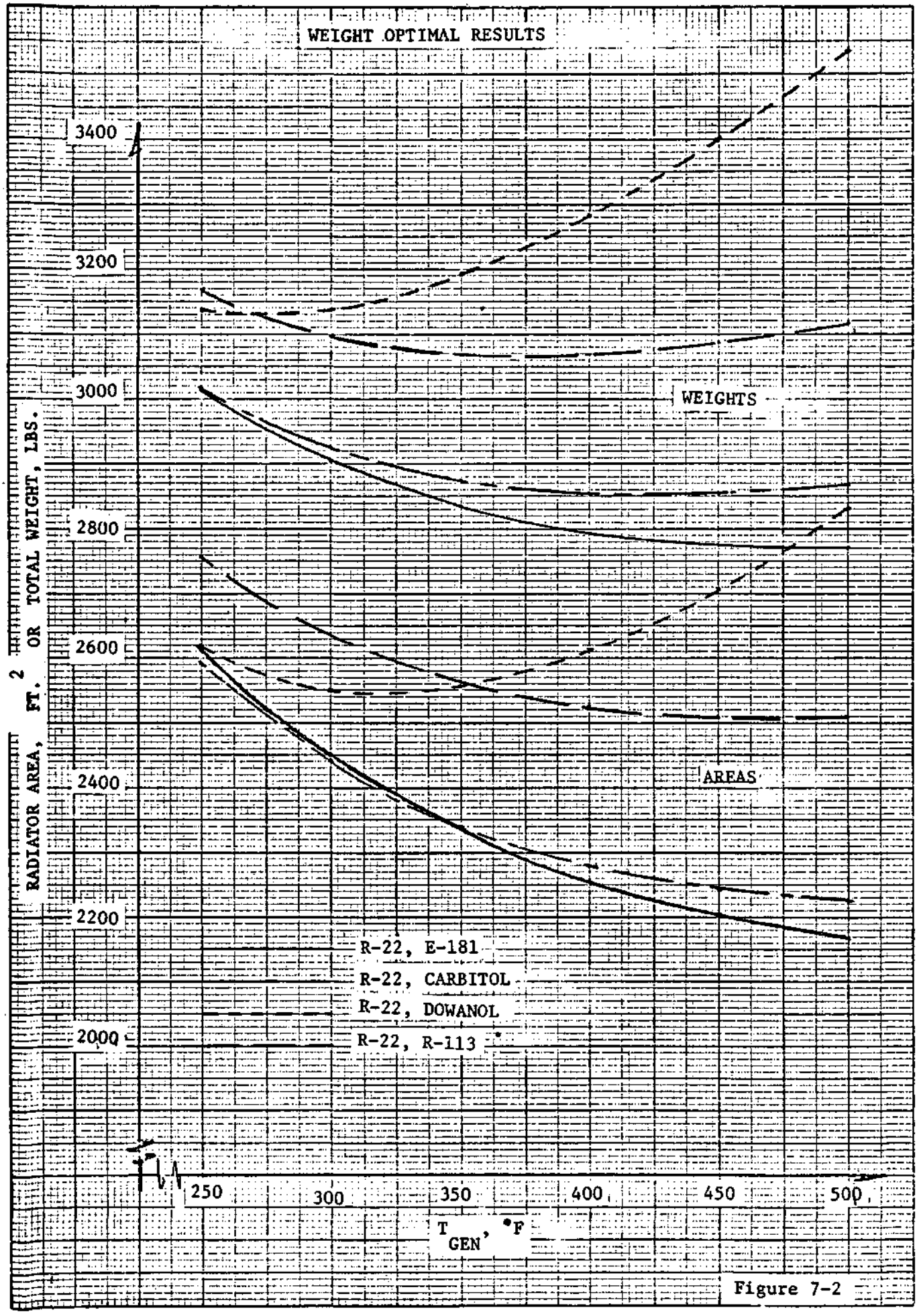
WEIGHT OPTIMAL RESULTS
3400
3200
3000
2800
2600
2400
2200
2000
RADIATOR AREA, FT.2 OR TOTAL WEIGHT, LBS.
WEIGHTS
AREAS
R-22, E-181
R-22, CARBITOL
R-22, DOWANOL
R-22, R-113
250
300
350
400
450
500
T GEN, °F

Figure 7-2

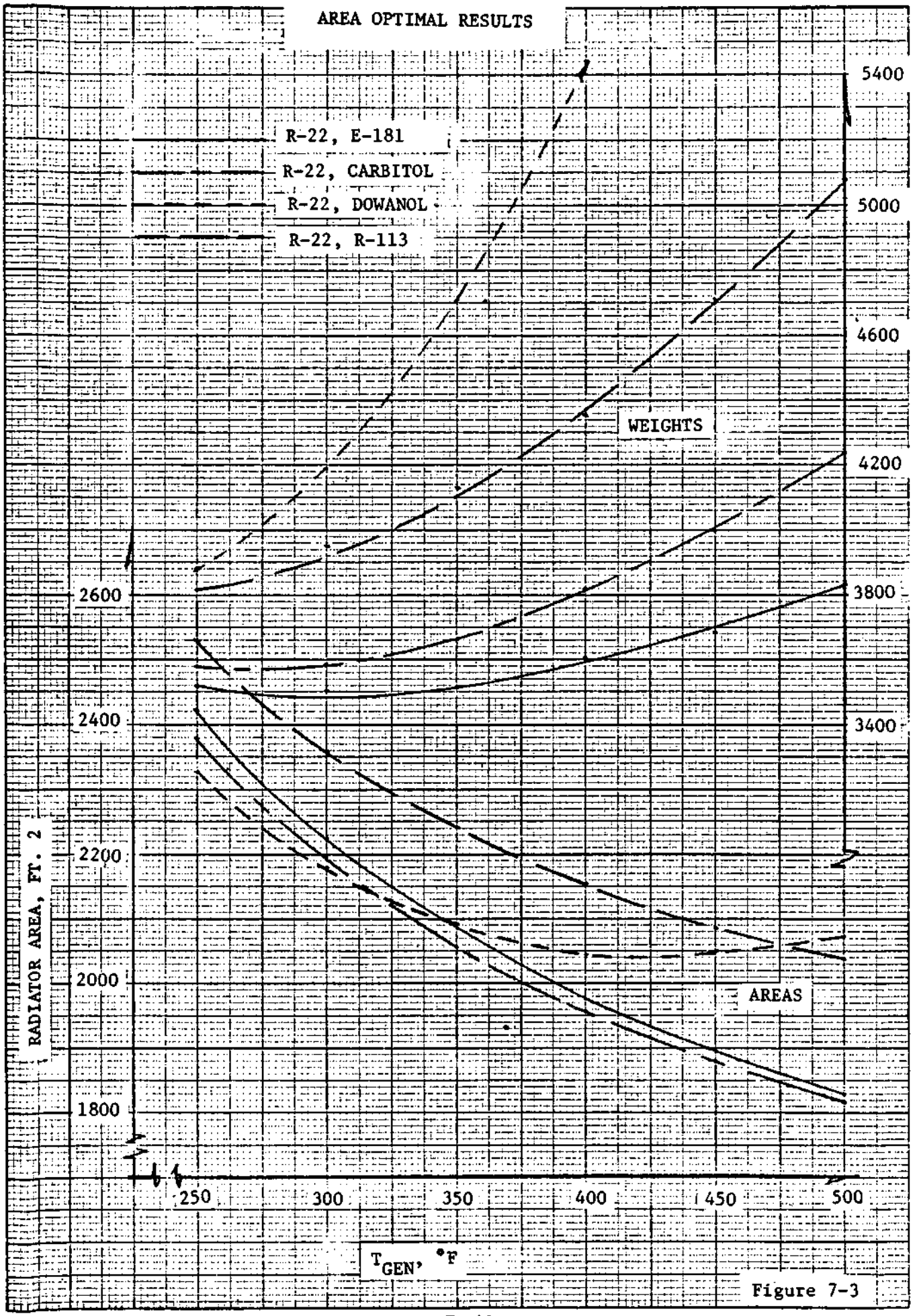
AREA OPTIMAL RESULTS
R-22, E-181
R-22, CARBITOL
R-22, DOWANOL
R-22, R-113
WEIGHTS
AREAS
RADIATOR AREA, FT. 2
TOTAL WEIGHT, LBS.
2600
2400
2200
2000
1800
5400
5000
4600
4200
3800
3400
250
300
350
400
450
500
T_{GEN}, °F

Figure 7-3

AREAS FOR ADDITIONAL WORK

The computer program for optimizing radiator weight and area could be greatly improved by going to a method such as conjugate gradients for locating the minimum point. This would be rather simple to implement, but the present study was too limited to provide for such development. Also, the temperature differentials appear from Lockheed's studies to be an important influence on the area, and it would seem to be natural to free them in the area optimization program. This may not be practical from a sensitivity standpoint using the current optimization technique, but would probably be handled easily by a gradient approach.

Section 8 Summary

As can be seen from the computation of radiator areas and system weights, there is no refrigerant-absorbent combination tested that is clearly superior to R-22 and E-181, however, there are some operating conditions under which some of the new combinations offer acceptable alternatives. In the final determination several additional factors must be considered in addition to the parameters programed. Those additional factors are principally safety factors such as low flammability and long range chemical stability. No organic solvent will be completely non-flammable but flash points give a measure of flammability. No high molecular weight organic solvent suitable as an absorbent will exhibit complete stability over a long range period of time at high temperature. All the solvents tested in this study exhibit a high degree of stability but need to be tested over a long period of time at operating temperatures and in the presence of typical construction materials before a final judgment can be made. The following table includes some of the additional factors that must be considered in determing the best overall refrigerant-absorbent combination.

	Solubility at 20°C gm solute gm solution	Specific Heat Cal/°C-gm	Flash Point °C	Viscosity at 20°C Centipoise	Comments
E-181	20.1%	.46	141	4.0	High solubility. Decomposes in presence of oxygen.
E-161	18.7%		111	3.8	Higher vapor pressure. Decomposes in presence of oxygen.
Dibutyl Carbitol	16.4%	.43 (13°C)	118		Decomposes in presenc of oxygen.
Dowanol TPM	12.2%	.51	127	6.1	High chemical stability. High specific heat.
Dioctyl Secacate	8.3%		227	24	Vinyl plasticizer synthetic lubricant low flammibility
Dioctyl Phthalate	5.8%		218	83	Vinyl plasticizer low flammability
Freon 11	1.0%	.21	very high	.42	Highest chemical stability. Low solubility. Low viscos. Very low flammability
Freon 113	0.8%		very high		Highest chemical stability. Low solubility. Very low flammability.
Diphenyl ether	0.5%	.40	115	3.9	High freezing point. Very low solubility. Extremely high thermal stability to 400°C Very non-corrosive. Chemically inert.